Sede Amministrativa: Università degli Studi di Padova

Dipartimento di Biologia

CORSO DI DOTTORATO DI RICERCA IN: Bioscienze e Biotecnologie
CURRICOLO: Biotecnologie
CICLO XXIX

Unveiling salt-tolerance mechanisms in Italian rice varieties

Coordinatore: Ch.mo Prof. Paolo Bernardi
Supervisore: Ch.mo Prof. Fiorella Lo Schiavo
Co-Supervisore: Dott.ssa Elide Formentin

Dottorando: Cristina Sudiro

Table of contents

Riassunto

Il fenomeno della salinizzazione dei suoli colpisce più di un quarto dell'intera superficie coltivata. Nelle piante, la capacità di tollerare alti livelli di salinità varia da specie a specie. Il riso (*Oryza sativa*) è uno dei cereali più coltivati al mondo, ma è anche il più sensibile al sale. Tuttavia, definire il riso solamente come una specie sensibile allo stress salino è limitativo, poiché esiste una grande variabilità di risposta tra le diverse varietà. Ciò è dovuto al fatto che la tolleranza allo stress salino è determinata da un sistema complesso di tratti fisiologici, vie metaboliche, e complesse reti geniche e molecolari. Mentre tutte le piante presentano alcuni meccanismi di tolleranza allo stress salino, nessuna specie o varietà presenta contemporaneamente tutti questi tratti. Pertanto, è necessaria una comprensione completa a diversi livelli di complessità di come le piante rispondono allo stress salino, combinando strumenti molecolari con tecniche fisiologiche e biochimiche, per lo sviluppo di nuove varietà più resistenti al sale.

Sulla base di queste premesse, sono state selezionate due varietà di riso italiano, Vialone Nano (VN) e Baldo (B), che presentano la maggior differenza di risposta allo stress salino. In particolare, abbiamo dimostrato, attraverso un'approfondita analisi morfologica e fisiologica, che VN è più sensibile allo stress salino di B. B, infatti, è in grado di reagire rapidamente ad entrambe le componenti dello stress salino: risponde allo stress osmotico arrestando rapidamente la sua crescita e chiudendo gli stomi nelle prime 24 ore, mentre reagisce allo stress ionico escludendo almeno inizialmente il sodio dalla parte aerea. Ciò consente alla pianta di mettere in atto un programma di adattamento che porta alla ripresa della crescita. VN, invece, risponde più lentamente allo stress, e come conseguenza si induce un processo di senescenza precoce. L'analisi a livello di espressione genica evidenzia ulteriormente questo diverso comportamento tra le due varietà. Infatti, B aumenta più rapidamente di VN l'espressione di geni coinvolti nella regolazione osmotica e nella regolazione della concentrazione citosolica di potassio e sodio. Questa differente risposta allo stress salino è ulteriormente confermata dall'analisi dell'espressione di alcuni geni noti per essere coinvolti nella percezione e trasduzione del segnale di stress salino e che sono espressi più tardi nella varietà sensibile. Inoltre, B aumenta l'espressione di geni che codificano per enzimi coinvolti nella detossificazione da specie reattive dell'ossigeno. In questo modo, B è in grado di mantenere bassi i livelli di queste specie reattive potenzialmente dannose, che quindi possono potenzialmente acquisire la funzione di molecole segnale.

Questi risultati dimostrano una differente risposta allo stress salino nelle due varietà, che infatti portano a due diversi esiti: una risposta adattativa nella varietà tollerante e alla morte cellulare in quella sensibile.
L'analisi a livello cellulare delle componenti delle vie di trasduzione del segnale indotte da stress salino, parte principale del mio lavoro di tesi, è stata effettuata su colture cellulari in sospensione derivate da entrambe le varietà. Queste linee cellulari conservano la stessa differenza in sensibilità al sale mostrate dalle piante da cui derivano. Infatti, le cellule di B sono in grado di attivare un programma di adattamento alla nuova condizione, mentre le cellule di VN vanno incontro a morte cellulare programmata. Quindi, abbiamo ulteriormente caratterizzato queste linee cellulari analizzando il ruolo di H_2O_2 e NO nella risposta allo stress salino. I risultati ottenuti dalle due linee cellulari mostrano differenze nell'ordine del tempo e della quantità nella produzione di H_2O_2 e NO in risposta al sale, dimostrando che queste due molecole hanno un diverso ruolo nelle due varietà. Infatti nella linea cellulare sensibile, portano all'induzione di morte cellulare programmata, mentre in quella tollerante, portano all'attivazione di meccanismi che conferiscono tolleranza. Le analisi molecolare e biochimica condotte su queste linee cellulari, confermano questa ipotesi. Abbiamo inoltre osservato la presenza di un innato sistema antiossidante più forte nelle cellule di B, che può spiegare il mantenimento di un livello di H_2O_2 basale più basso in questa varietà. Questa è una condizione necessaria per l'utilizzo di H_2O_2 come molecola segnale coinvolta nell'attivazione di meccanismi di tolleranza allo stress salino invece di indurre morte cellulare programmata.
Una caratteristica importante per la tolleranza al sale è il mantenimento di un alto rapporto $[K^+]/[Na^+]$ nel citosol. Pertanto il contenuto di K^+ e Na^+ è stato analizzato nelle colture cellulari sottoposte a stress salino. Le cellule di B sono in grado di mantenere una rapporto $[K^+]/[Na^+]$ più alto rispetto alle cellule di VN. In accordo con questo, le colture cellulari di B aumentano l'espressione di geni che codificano per canali e trasportatori del potassio più velocemente rispetto alla varietà sensibile.
In conclusione, in questo studio abbiamo individuato delle strategie adottate dalla varietà di riso Italiano B, sia a livello cellulare che a livello di intera pianta, che sono coinvolte nella tolleranza a condizioni di alta salinità. Inoltre, le linee transgeniche esprimenti la sonda per il Ca^{2+} Cameleon, prodotte nella parte finale del mio progetto di dottorato, verranno utilizzate per studiare le dinamiche di questa molecola segnale in risposta allo stress salino.

Summary

Soil salinity affects crop production on over a quarter of all agricultural land on Earth. Plants differ greatly in their tolerance to salinity, and among cereals, rice (*Oryza sativa*) is the most salt-sensitive one. However, genetic variations exist, and thus degrees of salt tolerance may vary among varieties. Plant adaptation to salinity stress involves complex physiological traits, metabolic pathways, and molecular or gene networks. Some salt-tolerance mechanisms may be present in all varieties at least to some extent, but not all of them can be found simultaneously in a single variety. Therefore, a comprehensive understanding on how plants respond to salt stress at different levels by combining molecular tools with physiological and biochemical techniques is mandatory for the development of new salt-tolerant varieties.

Based on these premises, we performed a physiological characterization on plants of Vialone Nano (VN) and Baldo (B), two Italian rice varieties showing the most contrasting salt sensitivity. We demonstrated, through morphological and physiological analyses analyses, that VN is more salt sensitive than B. B, in fact, seems to be able to rapidly respond to both the osmotic and the ionic components of salt stress, by arresting its growth and closing stomata in the first 24 h and by initial exclusion of Na^+ from the aerial part of the plant. This permits the development of an adaptive programme that allowed growth to resume. VN, instead, seems to be slower in the salt-stress response and as consequence early senescence is induced. Molecular analyses confirm these results. In fact, B upregulates genes involved in osmotic adjustment, increases of cytosolic K^+ concentration and promotes Na^+ sequestration much earlier than VN. The absence in the sensitive variety of a prompt initial response is also confirmed by the expression analysis of some genes known for being involved in early events as salt stress perception and signal transduction. These genes are, in fact, downregulated in VN. Moreover, B plants up-regulate genes encoding for enzymes involved in ROS scavenging. By doing so, harmful ROS levels are maintained low in the tolerant variety and, as a consequence of that, they can function as signalling molecules.

These results suggest the presence of differences in the salt-induced signals evoked in the two varieties, either in timing or in quality of responses. In fact, different outcomes are leading to an adaptive response or to cell death in the tolerant and sensitive variety, respectively.

The analysis of salt-stress signalling components and ROS responses induced by salt stress at cellular level, main part of my work thesis, was performed on suspension cell cultures derived from both varieties. These cell lines showed the same salt-sensitivity as in plants, with B cells activating

an adaptive response and VN cells undergoing PCD. The role of H_2O_2 and NO in stress response was analysed. Differences in timing and in the amount of salt-induced H_2O_2 and NO production in the two cell lines show these two molecules having different signalling roles, i.e., the induction of PCD in VN and the activation of tolerant mechanisms in B, as confirmed by molecular and biochemical analyses. In the tolerant variety, a basal stronger antioxidant system was found that may explain the maintenance of the low basal level of H_2O_2 in B cells, condition required for its use as a signalling molecule in activating salt-tolerance mechanisms.

In addition, being a high $[K^+]/[Na^+]$ ratio a trait required for salt tolerance at cellular level, the content of K^+ and Na^+ was investigated in salt-treated suspension cell cultures. The results showed B cells be more able to maintain a higher $[K^+]/[Na^+]$ ratio when compared to VN cells during salt stress. Consistent with this, genes encoding for K^+ channels and transporters resulted to be rapidly upregulated in the tolerant cells.

In conclusion, the mechanisms identified in this study unveiled the strategies adopted both at cellular and at whole-plant level by the Italian rice variety B that can be responsible for its tolerance and adaptation to salty conditions. Moreover, the production of transgenic lines expressing the Ca^{2+} sensor Cameleon will be a useful tool to study Ca^{2+} dynamics in response to salt in these varieties.

Aim of the project

Salinity affects at least 20% of world arable lands, seriously impairing crop growth and productivity. Although few plants can withstand high concentrations of salt, the majority of crop species cannot tolerate high salinity. Plants developed a plethora of biochemical and molecular responses to cope with salt stress. All these mechanisms have different time-scales: immediately upon stress reception, a signal transduction pathway is induced, resulting in the regulation of gene expression and eventually in metabolic changes. Rice is the most salt-sensitive among cereals, but the existence of salt tolerant varieties have been reported. However, not all traits for salt-tolerance were simultaneously present in one variety. Therefore, in spite of the progress made in studying these processes, the complexity of salt tolerance mechanisms requires deeper analyses.

The aim of my thesis was the set-up of new tools to be used in the development of new rice varieties tolerant to the salinity.

The goal was pursued by studying salt-tolerance mechanisms in Italian rice varieties at different levels of complexity. The analysis of the different behavior in response to salt stress of two Italian rice varieties contrasting in salinity tolerance gave the basis for the start of the main part of my project. The generation of suspension cell cultures from both varieties allowed the study of tolerance mechanisms at cellular level, eliminating the complexity of the presence of multiple tissue types. Therefore, my main project focused on the identification of salt tolerant mechanisms in these cell lines. To achieve this goal, components of the signalling transduction pathway induced by salt stress have been investigated: biochemical and molecular approaches were applied to identify peculiar mechanisms leading to salt tolerance.

In the frame of this thesis, new protocols and tools were set-up to investigate the role of H_2O_2, NO and Ca^{2+} as signalling molecules in salt stress response. In particular, in the final part of this project, plants encoding the calcium sensor Cameleon were obtained, that in the future will be exploited for the characterization of Ca^{2+} signalling in stress conditions.

Chapter 1:

Main Introduction

Plants growth and productivity is adversely affected by nature's wrath in the form of different stress factors, that are accentuated by various anthropogenic activities. In general, plants face two main types of stresses during their life cycle, biotic and abiotic, both of which can be deleterious. The first type of stress includes a wide spectrum of bacteria, fungi, and viruses that can attack plants at various stages of their development, while the latter includes high salinity, water deprivation, extreme temperatures, excessive light, high concentrations of heavy metals, poor soil nutrition, and so on. Moreover, the severity of these stresses may be altered by the simultaneous presence of other stress acting in parallel on the plant (Pandey *et al*., 2015). All these factors prevent plants from reaching their full genetic potential and limit crop productivity. In particular, the importance of abiotic stress to world agriculture is demonstrated by the fact that altogether abiotic factors are the principal cause of crop failure worldwide. For instance, Bray *et al*. (2000) estimates that more than 50% of the potential yield of annual crops is lost due to abiotic stress. Salt stress in particular is one of the major constraints for agriculture, severely impacting crop production worldwide.

1.1 Salinity and salt stress

According to the FAO Land and Plant Nutrition Management Service, over 6% of world's land is affected by salinity. But considering only the cultivated land, this percentage exceeds 20% and in irrigated lands also the 30%. Irrigated land represents only 15% of total cultivated land, but as irrigated land has at least twice the productivity of rain fed land, it may produce one-third of the world's food (FAO, http://www.fao.org/worldfoodsummit/english/newsroom/focus/focus1.htm).
Moreover, salinization is expected to deteriorate even more areas in the coming years due to global climate changes (FAO, http://www.fao.org/3/a-i4373e.pdf), posing a serious threat for food security.

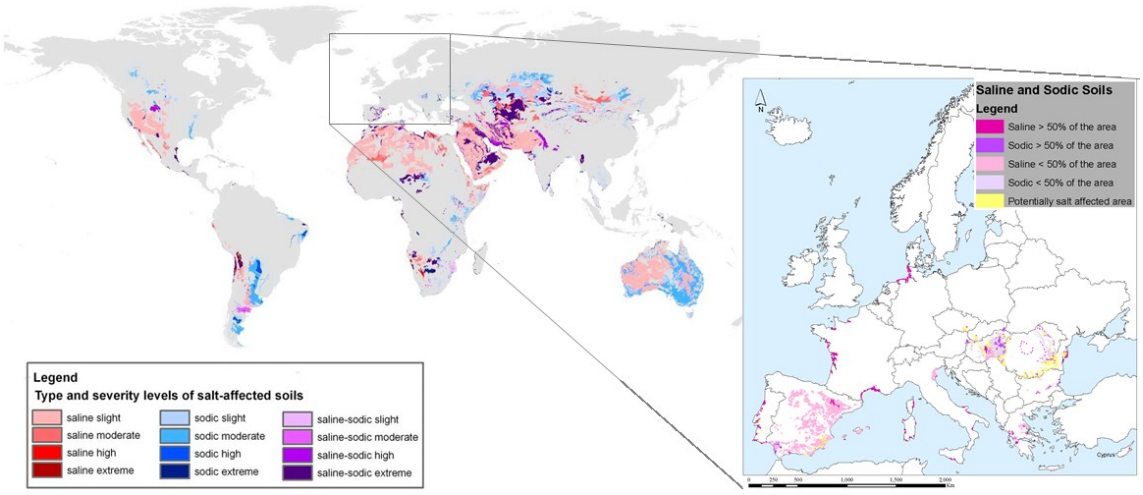

Figure 1. Distribution of saline and/or sodic soils. Salinity is a measure of the content of salts in soil or water. Soils are often considered sodic when the amount of sodium impacts soil structure. Modified from https://globusgreen.files.wordpress.com/2014/12/biosaline-agroforestry-and-forestry-world.jpg and Tóth *et al*., (2008): Updated Map of Salt Affected Soils in the European Union.

Salinity can occur through natural or human-induced processes that result in the accumulation of dissolved salts in the soil water. Natural causes of salinization, also called primary salinization, are the weathering of parent materials containing soluble salts (sodium chloride is the most soluble) and the deposition of oceanic salt carried in wind and rain. Secondary salinization results from human activities that change the hydrologic balance of the soil between water applied (irrigation or rainfall) and water used by crops (transpiration). The most common causes are (i) land clearing and the replacement of perennial vegetation with annual crops, and (ii) irrigation schemes using salt-rich irrigation water or having insufficient drainage.

The USDA Salinity Laboratory defines a saline soil as having an ECe of 4 dS/m (around 40 mM NaCl) or more. However, many crops are affected by soil with an ECe less than 4 dS/m.

Plants are exposed to two major stresses under high salt conditions. First, the presence of salt in the soil reduces the ability of the plant to take up water, and this leads to reductions in the growth rate. This is referred to as the osmotic effect of salinity, or the osmotic stress. Second, if excessive amounts of salt, and in particular the toxic Na^+, enter the plant this may cause further reductions in growth, and even death. This is called the ionic stress. Moreover, plant exposure to salinity induces formation of reactive oxygen species (ROS) that disturb the metabolic balance of the cells and cause oxidative stress (Dionisio-Sese and Tobita, 1998; Hernández *et al*., 1993; Gill and Tuteja, 2010; Gupta and Huang, 2014).

Plants differ greatly in their tolerance to salinity, as reflected in their different growth responses. Thus they are commonly distinguished as halophytes or glycophytes. Glycophytes ("sweet" plants) are able to withstand only low concentrations of salt, while halophytes (halas = salt, salt plants) can tolerate relatively high concentrations of salt (Flowers and Yeo, 1988). Unfortunately, the majority of crop species belong to the first category.

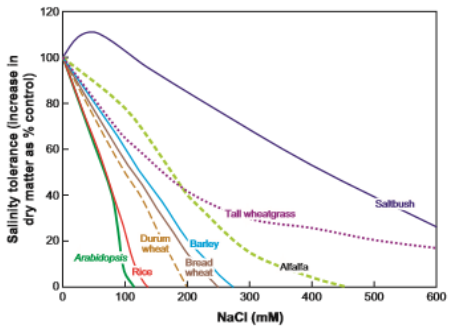

Figure 2. Diversity in the salt tolerance of various species, shown as increases in shoot dry matter after growth in solution or sand culture containing NaCl for at least 3 weeks, relative to plant growth in the absence of NaCl (Munns and Tester, 2008).

Nevertheless, it is not surprising that, because salinity is a common feature of many lands, both glycophytes and halophytes have evolved mechanisms to try to cope with it, even if often not with the same success. To cope with this adverse condition, plants have in fact evolved a multi-faceted range of physiological and metabolic responses by activation of many of stress-responsive genes and synthesis of diverse functional proteins through a complex signal transduction network (Hirayama and Shinozaki, 2010).

In the following paragraphs, the effects of the different faces of salt stress, and the mechanisms plants try to put in act to cope with them are discussed in more detail. Whereas all of them are indeed important, their relative contribution may differ, depending on plant species, stress severity and duration, and experimental conditions.

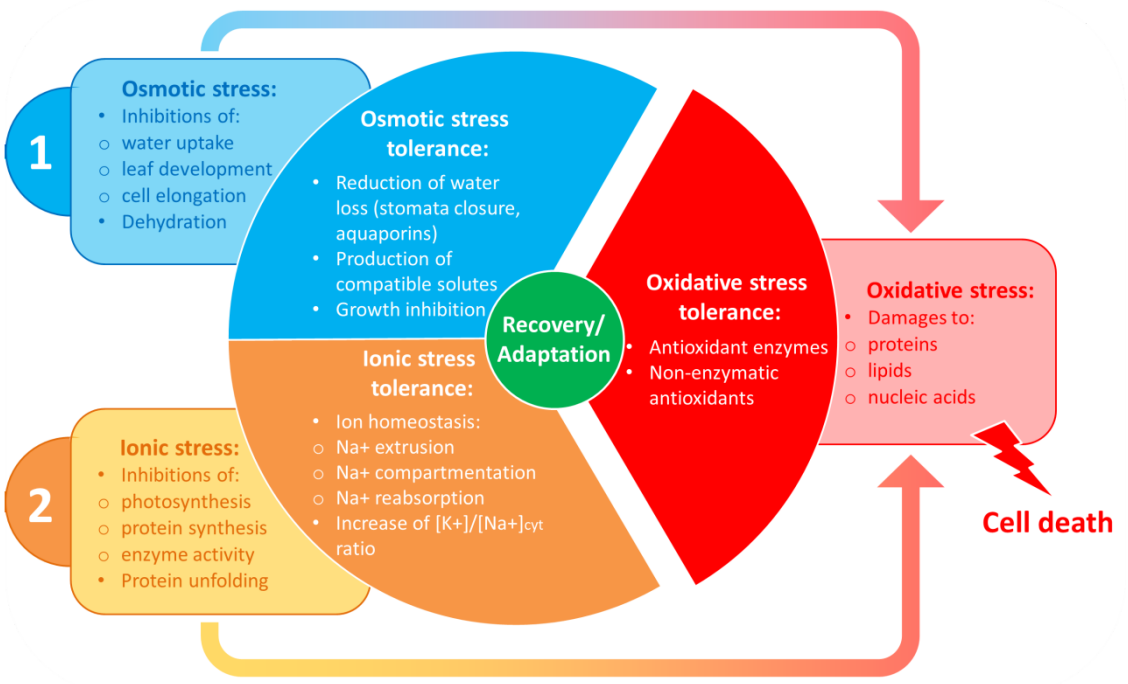

Figure 3. Effects of salt stress on plants and mechanisms of tolerance.

1.1.1 Osmotic stress

Osmotic stress is the first stress that plants undergo when roots are exposed to high salt concentrations. This stress reduces plant's ability to absorb water due to the high osmotic pressure exerted by the dissolved salt in the soil (Munns and Tester, 2008).
At the level of the whole plant, osmotic stress stimulates a response that is very similar to that of water deprivation: in fact, the reduced absorption of water from the soil induces the immediate closure of the stomata allowing the plant to considerably reduce water loss by evaporation. This process, however, is not sufficient to compensate the lack of water, and cells gradually lose turgor (Shabala and Cuin, 2007). This phenomenon, which on one hand allows the normal metabolic processes to continue, on the other hand inhibits the distension of the cells, with consequent reduction of leaves and roots growth. This process is carried out a few seconds after exposure of plants to a salty soil and continues for a few hours until the volume and cell turgor are restored. Despite this immediate response, cell division and distension are inhibited (Munns and Tester, 2008).

Mechanisms of osmotic stress tolerance

To cope with the osmotic stress plants try to limit water loss by regulating the permeability of the membranes and the production of compatible solutes that allow counteracting the osmotic pressure (Boursiac *et al*., 2005; Munns and Tester, 2008; Chen *et al*., 2007). A first response consists in reducing the plasma membrane permeability to water, so preventing its efflux when salt concentration outside the roots is high. This type of response is mediated by the modulation of the activity of aquaporins, that are proteins present in the plasma membrane, "Plasma Membrane Intrinsic Proteins" (PIPs) and in the tonoplast, "Tonoplast Intrinc Proteins" (TIPs), involved in the transport of water through the membranes (Boursiac *et al*., 2005; Maurel *et al*., 2008). Accordingly, the expression of aquaporins is reduced for example both in Arabidopsis roots (Boursiac *et al*., 2005) and in barley roots (Horie *et al*., 2011b) when affected by salt-stress. A second mechanism that plants use to counteract the effects of osmotic stress is to accumulate compatible solutes at high levels, either ions, such as K^+, or organic solutes, such as glycine betaine or proline, which can be produced in large quantity without toxic effects on the plant (Bohnert and Shen, 1999). Some tolerant species are able to accumulate directly Na + within the vacuole by using it as compatible solute. Compatible solutes also act as chaperones in the cytosol protecting membrane structures and enzyme functionality from salt damage. They can also in some cases act as scavengers of reactive oxygen species (Hare *et al*., 1988; Cuin and Shabala, 2008).

1.1.2 Ionic stress

Ionic stress arises later after exposure to saline soil when Na^+ and/or Cl^- concentration reaches toxic levels inside the cells. Since Cl^- entry seems to be a slow process, Cl^- toxicity is of main concern only for plants that are able to manage Na^+ transport better than Cl^- transport, such as grapevines. Therefore, the majority of research is focused on Na^+ effects.
Ionic stress can have serious effects on growth and development of plants, but these effects require long times due to the slow Na^+ accumulation, and in fact appear much later than those of

osmotic stress. Even sensitive plants in fact can show no symptoms before 2-3 days of exposure to salt (Munns and Tester, 2008).
Although the availability of Na^+ as a 'cheap' osmoticum is generally beneficial, a large excess of Na^+ ions over K^+ is not, for several reasons. Firstly, the similar physicochemical structures of Na^+ and K^+ mean that Na^+ competition at transport sites for K^+ entry through both high and low affinity K^+ transporters may result in K^+ deficiency. In addition, an excessive influx of Na^+ depolarizes the plasma membrane farther inhibiting K^+ entry through passive transport channels and rather causing K^+ output through "outward-rectifyng" channels activated by membrane depolarization. Secondly, cytoplasmic Na^+ competes for K^+ binding sites and hence inhibits metabolic processes that crucially depend on K^+, such as the synthesis of new proteins, the activity of many enzymes and photosynthesis (Shabala and Cuin, 2007).
Salt accumulation has adverse effects on older leaves initially. In fact, since they can no longer expand, they cannot dilute the content of salt. If stress is prolonged, the damage may also extend to other younger plant organs such as buds or young leaves, inducing chlorosis and necrosis. If the death rate of the leaves is higher with respect to the growth of new ones, a reduction of plant productivity occurs and early senescence is induced (Munns and Tester, 2008).

Mechanisms of ionic stress tolerance

One of the main mechanisms by which plants cope with ionic stress consists in maintaining a high K^+/Na^+ ratio in the cytosol. Plants try therefore to reduce Na^+ concentration in the cytosol and instead to increase K^+ concentration (Maathuis and Amtmann, 1999; Munns and Tester, 2008).
There are three main mechanisms that allow the plant to reduce the Na^+ concentration in the cytosol and in the shoots: the extrusion from the cytoplasm, the compartmentalization inside the vacuole and the reabsorption in the xylem.
The extrusion of Na^+ from the cytosol is mediated by the plasma membrane Na^+/H^+ antiporter (SOS1), which acts in concert with the H^+ -ATPase pumps and the K^+ high-affinity transport systems in the "Salt Overly Sensitive" (SOS) pathway (Ji *et al*., 2013).
Compartmentation in vacuoles is achieved by tonoplast Na^+/H^+ antiporters such as those belonging to the Na^+/H^+ exchanger (NHX) family in Arabidopsis, which allows the entry of Na^+ in exchange with protons. The activity of these antiporters is supported by the proton gradient generated from two independent proton pumps: the vacuolar H^+-ATPase and the V-PPase (vacuolar H^+-translocating pyrophosphatase) (Bassil *et al*., 2012). It has been reported that overexpression of one of the vacuolar Na^+/H^+ antiporters, AtNHX1, increases salt tolerance of the transgenic Arabidopsis plants (Apse *et al*., 1999).
One-third reduction of Na + toxicity involves the HKT transporters (High Affinity Potassium Transporter). In rice two classes of HKT transporters were identified so far, both involved in tolerance to salt stress. The first class consists of transporters selective for Na^+ expressed on the plasma membrane of cells surrounding the xylem vessels. Their function is to remove the excess Na^+ present inside the vessels and therefore limit its accumulation in photosynthetic tissues. This process has been demonstrated both in Arabidopsis thaliana plants that in some monocotyledons (Hauser and Horie, 2010), emphasizing the importance of these transporters in salt stress tolerance. The HKT transporters belonging to the second class, which is not present in Arabidopsis, seem to be expressed at the level of the tonoplast and act together to transporters involved in the compartmentalization of Na + into the vacuole (Schroeder *et al*., 2013).
K^+ enters the cells through the activity of specific potassium channels and transporters (Zhu, 2003). Among these, Shaker channels (Bertl *et al*., 1997), Tandem Pore K^+ (TPK) channels

(Sharma et al., 2013) and High-affinity HAK transporters (Santa-María *et al*., 1997) show a high K^+/Na^+ discrimination and thus are very important during salt stress, when Na^+ ions outside the roots are in excess.
The "Shaker-type K^+ channels" are triggered by changes in membrane potential (voltage-dependent) and localize on the plasma membrane. "Shaker-type K^+ channels" in plants are divided into three functionally distinct categories: "inward-rectifying K^+ channels", activated by hyperpolarization of the membrane, which mediate the entry of K^+ into the cells; "outward-rectifyng K^+ channels", activated by membrane depolarization that mediate of K^+ out of the cell; "weakly-rectifyng K^+ channels", which can mediate both the entry or the exit of K^+ depending on its concentration gradient. This family is composed of 9 members in Arabidopsis (Véry and Sentenac, 2002; Aramemnon database http://aramemnon.uni-koeln.de/). Studies of the "Shaker-type K^+ channels" showed that *Arabidopsis* KAT1 suppressed the salt-sensitive phenotype of yeast mutants, while AKT1 channels are negatively regulated in the presence of salt probably because they also allow Na + entry, being less specific for K + (Obata *et al*., 2007; Golldack *et al*., 2003).
In the model plant Arabidopsis thaliana the family of the "Tandem Pore-K + (TPK) channels" is composed of six members, TPK1-TPK5 and KCO3 (TPK6). TPK1, TPK3, TPK4 and KCO3 have been studied in Arabidopsis. TPK1 is localized to tonoplast, TPK4 is localized to plasma membrane, TPK3 to thylakoids (Carraretto *et al*., 2013), and KCO3 is located to the tonoplast (Rocchetti *et al*., 2013).
K^+ transporters of group I of the HAK/KT/KUP family were suggested as major contributors to high-affinity K^+ uptake in several plant species (Rodríguez-Navarro and Rubio, 2006). AtHAK5, in particular, is required for root elongation in presence of external K^+ concentrations below 10 µM (Qi *et al*., 2008). Under saline conditions, *athak5* plants showed reduced growth with respect to the WT. Therefore, AtHAK5 plays a crucial role in K^+ acquisition and thus probably also in salt stress (Nieves-Cordones *et al*., 2010).

1.1.3 Oxidative stress

Reactive oxygen species (ROS), including hydrogen peroxide (H_2O_2), superoxide radical ($O_2^{\bullet -}$), hydroxyl radical ($OH^{\bullet}$) and singlet oxygen ($^1O_2$) etc., resulting from excitation or incomplete reduction of molecular oxygen, are harmful by-products of basic cellular metabolism in aerobic organisms (Miller *et al*., 2010). Under optimal growth conditions, intracellular ROS are maintained at a low level. However, ROS production dramatically increases during stress. Salt stress, in fact, is expected to encourage the generation of ROS in plants for many reasons. First: plants respond to salt stress by decreasing stomatal conductance to avoid excessive water loss. This in turn decreases the internal CO_2 concentrations and slows down the reduction of CO_2 by Calvin cycle. This response leads to depletion of the oxidized NADP+, which acts as a final acceptor of electrons in PSI, and alternatively increases the leakage of electrons to O_2 forming O_{-2}. Furthermore, Na^+/Cl^- toxicity resulting from salt stress could disrupt the photosynthetic electron transport and provoke electron leakage to O_2. Second: the decrease in internal CO_2 slows down the reactions of Calvin cycle and induces photorespiration, resulting in generation of more H_2O_2 inside the peroxisome. Third: salt stress increases the rates of respiration with the consequence of respiratory electron leakage to O_2 (Abogadallah, 2010). In addition to organelles, plasma membrane is the main site for ROS generation in response to endogenous and exogenous stimuli. Several types of enzymes, such as NADPH oxidases, amineoxidases and a large family of class III

peroxidases localized at the cell surface contribute to produce apoplastic ROS (Apel and Hirt, 2004; Gill and Tuteja, 2010; Noctor *et al.*, 2014).

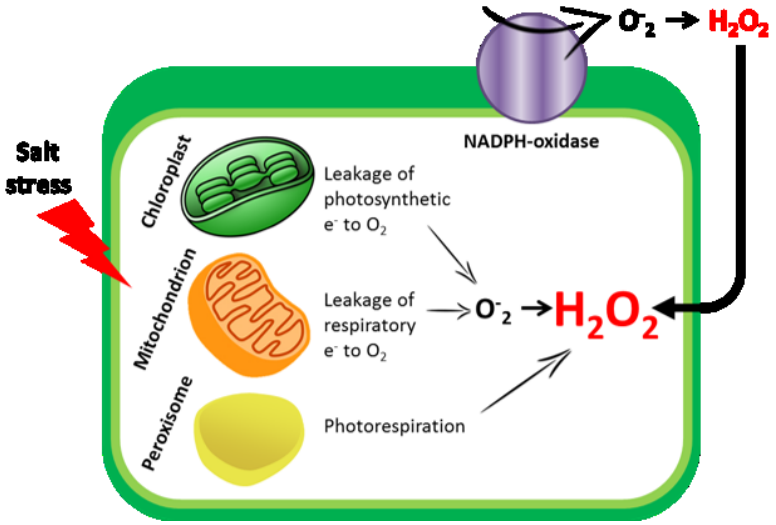

Figure 4. Main sites of ROS generation under salt stress.

Mechanisms of oxidative stress tolerance

Plants have evolved both enzymatic and non-enzymatic antioxidative systems to protect themselves against oxidative damage. ROS-scavenging enzymes of plants include superoxide dismutase (SOD), ascorbate peroxidase (APX), catalase (CAT), glutathione peroxidase (GPX), monodehydroascorbate reductase (MDHAR), dehydroascorbate reductase (DHAR), glutathione reductase (GR), glutathione S-transferase (GST), and peroxiredoxin (PRX). SOD acts as the first line of defense converting O_2•⁻ into H_2O_2. CAT, APX, and GPX then detoxify H_2O_2. APX is involved in an ascorbic acid (AsA) and/or a glutathione (GSH) regenerating cycle, known as the Foyer-Halliwell-Asada cycle, comprising also MDHAR, DHAR, and GR (Foyer and Halliwell, 1977; Asada, 1999; Noctor *et al.*, 2014). Non-enzymatic antioxidants include AsA, GSH, carotenoids, tocopherols, and flavonoids that are also crucial for ROS homeostasis in plant (Gill and Tuteja, 2010).

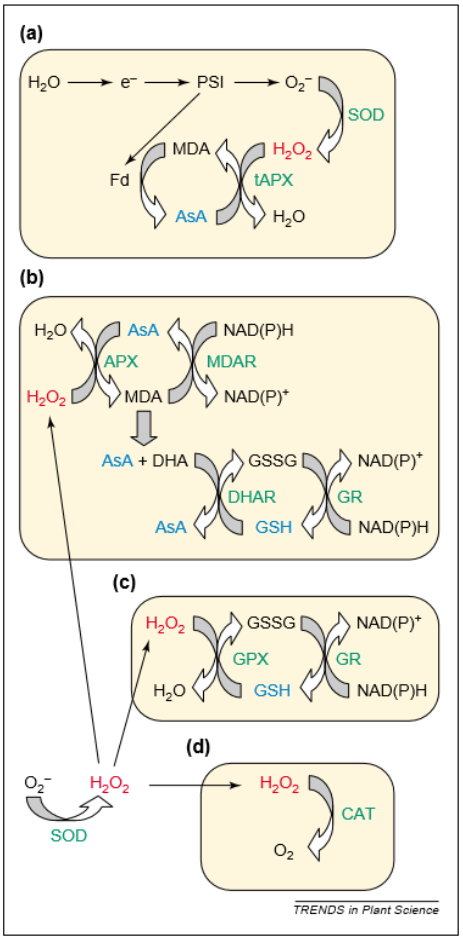

Figure 5. Pathways for reactive oxygen species (ROS) scavenging in plants. (a) The water–water cycle. (b) The ascorbate–glutathione cycle. (c) The glutathione peroxidase (GPX) cycle. (d) Catalase (CAT). ROS are indicated in red, antioxidants in blue and ROS-scavenging enzymes in green. Abbreviations: AsA, ascorbate; APX, AsA peroxidases; DHA, dehydroascorbate; DHAR, DHA reductase; Fd, ferredoxin; GSH, glutathione; GR, GSH reductase; GSSG, oxidized glutathione; MDA, monodehydroascorbate; MDAR, MDA reductase; PSI, photosystem I; SOD, superoxide dismutase; tAPX, thylakoid-bound APX (Mittler, 2002).

1.1.4 Cell death

Salinity can challenge plants to a degree that may even lead to cell death. Elevated concentrations of ROS, often combined with other molecules such as NO (usually highly induced by salt stress, Valderrama et al., 2007) pose a significant threat that may eventually trigger programmed cell death (PCD; Gechev and Hille, 2005). Programmed cell death is an active, genetically controlled process in which cells are selectively eliminated through involvement of specific proteases and nucleases. Being essential for cell and tissue homeostasis and differentiation, PCD also plays an important role in mediating plant adaptive responses to various abiotic stresses and also to salinity (Katsuhara and Kawasaki, 1996). Nevertheless, stress-induced PCD significantly affects plant yield and productivity and is therefore of fundamental impact on agriculture (Mittler and Blumwald, 2010). PCD is often associated with the occurrence of specific biochemical and morphological features such as condensation of the nucleus and cytoplasm, fragmentation of genomic DNA ('DNA laddering') and fragmentation of the cell into membrane-contained vesicles (apoptotic

bodies; Hoeberichts and Woltering, 2003) that are used in the identification and characterization of the event.

1.2 Sensing and signalling

The perception of salt stress and its signal transduction are critical steps to switch on adaptive responses in plants exposed to high salinity. Our current knowledge of how salt stress is sensed by plant tissues is severely limited. As already discussed above, plants experience multiple constraints under saline conditions. These include reduced water availability, elevated Na^+ levels, a massive disturbance to the cytosolic K^+ homeostasis and a dramatic increase in ROS accumulation in plant tissues (Munns and Tester, 2008). Each of these constraints may theoretically be sensed by either membrane-bound or cytosolic sensors, and then translated into a broad array of physiological and genetic alterations that optimize plant performance under saline conditions. A recently discovered osmo-sensing mechanism involves the "reduced hyperosmolality-induced $[Ca^{2+}]$ increase 1" (OSCA1), a plasma membrane-localized protein that is responsible for increased Ca^{2+} influx in response to osmotic stress (Yuan *et al*., 2014). Whether it is also involved in salt stress sensing has yet to be evaluated.
Sensors specific to Na^+ must exist, but their nature has not yet be discovered. In Arabidopsis, it is speculated that SOS1, a plasma membrane Na^+/H^+ antiporter part of the SOS pathway mentioned above, senses Na^+ by its C-terminal tail, predicted to reside in the cytoplasm (Shabala *et al*., 2005).
Key signalling molecules known for being involved in salt stress response are Ca^{2+} and ROS.

1.2.1 Calcium (Ca^{2+})

In plant cells the resting cytosolic concentration of calcium, $[Ca^{2+}]$cyt, under normal condition is maintained at nanomolar level, whereas the concentration of Ca^{2+} in cell wall, vacuole, endoplasmic reticulum and mitochondria is at 1–10 mM. However, specific signals, such as those triggered by several kind of stresses can induce a sudden increase in the $[Ca^{2+}]$cyt level up to micromolar level, transducing the signal to subsequent responses.
Under salinity, the earliest cellular response seems to be a rapid increase in free cytosolic Ca^{2+} within 1–5 s via influx through either NSCCs or a mechanosensitive calcium channel in the plasma membrane (i.e. OSCA1), which can then be amplified through the release from internal stores, especially the vacuole (Knight *et al*., 1997; Donaldson *et al*., 2004).
Within seconds after sensing of salinity stress, a transient, stable or oscillating change in $[Ca^{2+}]$cyt concentration is elicited. This change is required for activating the downstream response mechanisms either through induction or downregulation of the responsive genes. The nature of the $[Ca^{2+}]$cyt signal in terms of amplitude, frequency and duration of the peak or signal likely has specific role in encoding the particular information for plants under salinity stress.
Tracy *et al*. (2008) found that the osmotic and ionic components of salinity stress induced differential increases in $[Ca^{2+}]$cyt in Arabidopsis root cells. They reported that the heterogeneous $[Ca^{2+}]$cyt changes under NaCl stress were restricted to the root. Also in experiments on rice protoplasts, as well as on quince protoplasts, different $[Ca^{2+}]$cyt changes were obtained under sodium and osmotic stress (Kader and Lindberg, 2010). The rise in cytosolic Ca^{2+} may be relayed

by Ca^{2+} sensors such as SOS3, a calcineurin B-like protein. Increases in cytosolic Ca^{2+} likely facilitate the dimerization of SOS3 and its subsequent interaction with SOS2, a calcineurin B-like interacting protein kinase (CIPK24). The SOS3/SOS2 complex is targeted to the plasma membrane through myristoylation and subsequently phosphorylates the Na^+/H^+ antiporter, SOS1 (Zhu, 2002).

1.2.2 Reactive Oxygen Species (ROS)

While ROS have the potential to cause oxidative damage to cells during environmental stresses, as already discussed above, recent studies have shown that ROS play a key role in plants as signal molecules that regulates plant development, stress adaptation, and programmed cell death (PCD) (Apel and Hirt, 2004; Mittler *et al*. 2004; Torres and Dangl 2005; Gechev and Hill, 2005). ROS-mediated signalling is controlled through a delicate balance between its production and scavenging. To influence such diverse processes in different tissues and at different developmental stages, the biological response to altered ROS levels requires remarkable specificity. The biological outcome of ROS signalling is heavily related to the chemical identity of ROS, intensity and subcellular localization of the signal, and is dose dependent (Gechev *et al*., 2002; de Pinto *et al*., 2006). Low doses of H_2O_2 have been shown to induce protective mechanisms and acclimation responses against oxidative and various abiotic stress, while high doses trigger cell death (Gechev *et al*., 2002; Gechev and Hill, 2005). Interestingly, cell death initiated by high doses of H_2O_2 and $^1O_2$ can be distinguished from necrosis, which is caused by even higher doses of these ROS (Van Breusegem and Dat, 2006). Interactions with other signalling molecules, such as nitric oxide, are also key determinants of the final outcome of ROS signalling (Gechev and Hill, 2005).

The rapid increase in ROS production, referred to as 'the oxidative burst', was shown to be essential for many processes, and genetic studies have shown that respiratory burst oxidase homolog (Rboh) genes, encoding plasma membrane-associated NADPH-oxidases, are the main producers of signal transduction-associated ROS in cells during these processes (Mittler *et al*., 2004; Torres and Dangl, 2005). In particular, NADPH oxidase AtrbohD and AtrbohF seem to have an important function in ROS-dependent regulation of Na^+/K^+ homeostasis in *Arabidopsis* under salt stress (Ma *et al*., 2012).

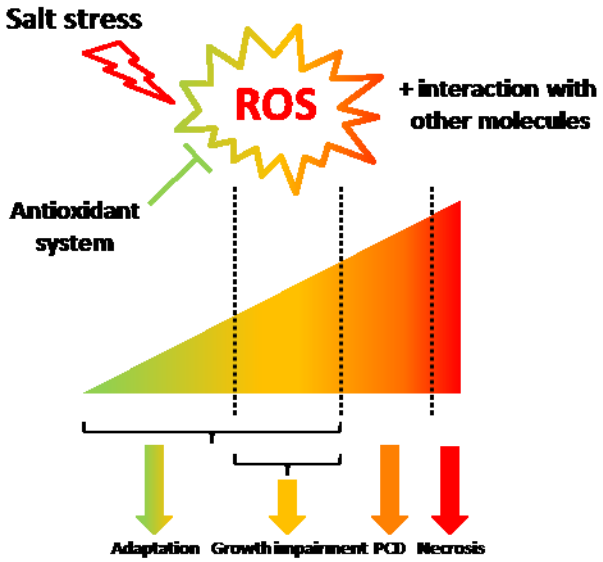

Figure 6. An overview of the role of ROS in response towards salt stress. Salinity stress is known to lead to the production of ROS. The antioxidant system prevent dangerous elevations of ROS levels. The outcome of ROS signalling depends mainly on the ROS concentration, but other factors as interaction with other signals like NO and Ca^{2+} are also integrated into the response. In general a stress-induced slight rise in ROS quantities activates tolerance mechanisms leading to adaptation. However, severe stress usually causes massive accumulation of ROS and the initiation of PCD, or in extreme cases even necrosis.

1.3 Rice

Different plant species have a wide-ranging capacity for salt tolerance, from the very sensitive species (glycophytes), such as the model plant *Arabidopsis*, to the very tolerant species (halophytes), such as *Atriplex spp*. (saltbush). Cereal crops are classified as glycophytes; however, different crop species can also have different capacities and mechanisms to tolerate salt stress (Munns and Tester, 2008). Within a species there can also be present naturally occurring genetic variation in salt tolerance that can be usefully exploited for breeding programs of salt-tolerant crops (Roy *et al*., 2011).

Rice (*Oryza sativa*) is the most salt sensitive among cereals and is in risk of greater exposure to brackish water due to the elevation of sea level, especially in the delta regions where it is mainly produced (Wassmann et al. 2009). Rice is one of the most important cereal crops in tropical and temperate regions, feeding the majority of the world's population. More than 90% of world's rice is grown and consumed in Asia where 60% of the earth's people and about two-thirds of the world's poor live (Khush and Virk, 2000). However, it also has economical relevance for developed countries, like the USA. In Europe, though neither a staple food nor a major crop, rice has a sociocultural significance and ecological importance in several Mediterranean countries. Therefore, the study of salt tolerance mechanisms in this cereal is of paramount importance, whether its cultivation is for subsistence or economic gain. Italy is the leading European rice producer with a total of 220,000 ha exploited for rice cultivation with an annual production of about 11 million tons, equal to 0.25% of world production. Italians do not eat much rice, but in the north part of Italy where the "risotto" dish is very popular and a number of rice varieties of the subspecies japonica temperate have been developed for this purpose. Instead, the 2/3 of rice produced in Italy is exported to both European and non-EU countries (Enterisi). This crop is grown

mainly in the Po' basin (Piemonte, Lombardia, Veneto and Emilia Romagna). In particular, the Delta of the Po' river, where high quality rice varieties are cultivated, has been experiencing an increase in soil salt concentration causing negative effects on rice productivity in that area (Fig.7).

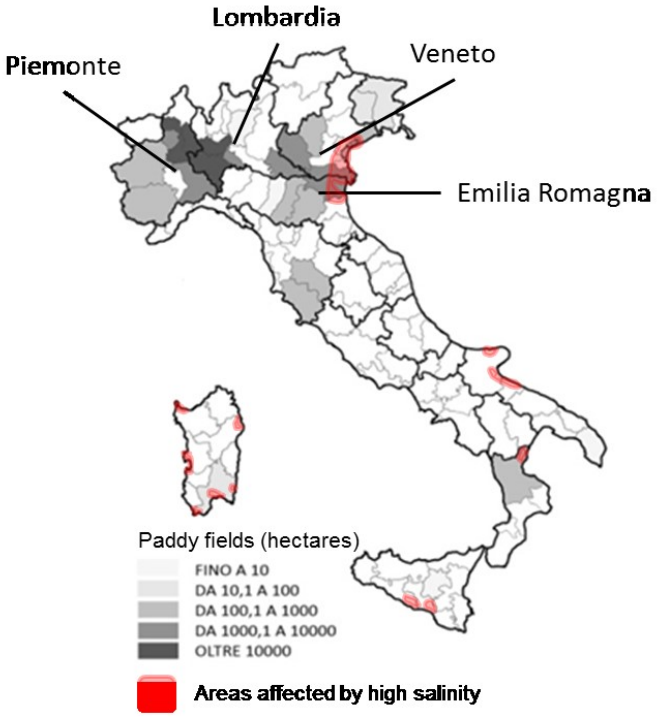

Figure 7. Distribution of paddy fields and salt affected areas in Italy (modified from EnteRisi).

1.3.1 Rice and salt stress

Plants root is the only organ in contact with the ground and therefore directly involved in the absorption of solutes and ions dissolved in it. These solutes can enter the root at the epidermal level, but the apoplastic flow is interrupted by the Caspary band, a suberin barrier covering endodermic cells. This barrier avoids the non-selective entry of solutes and water towards the stele. In fact, in order to continue their flow towards the stele, after reaching the Caspary band, solutes must necessarily cross the plasma membrane of cells where an active selection of the input substances occurs (Horie *et al.*, 2012). Rice is one of the most sensitive among crops. This sensitivity may be determined by the presence of an apoplastic flow (bypass flow) of Na^+ inside the roots of rice plants, which leads to the uncontrolled entry of Na^+ and its accumulation to toxic levels.

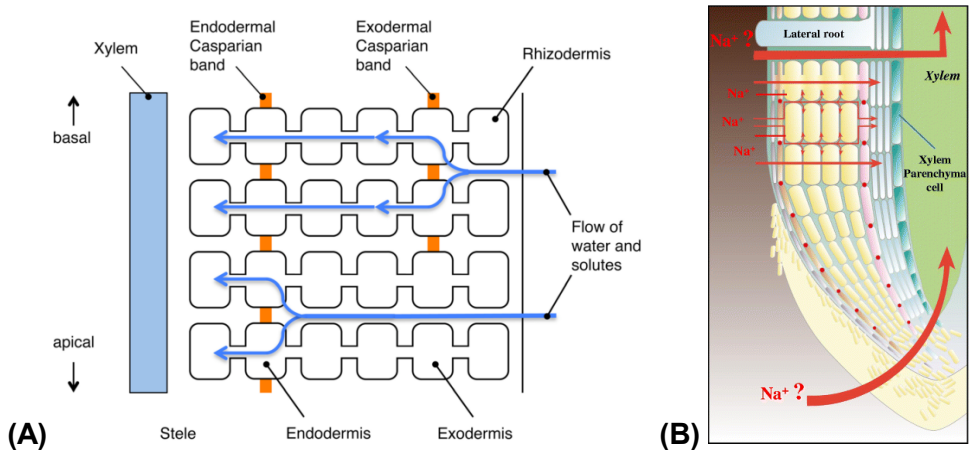

Figure 8. (A) Schematic diagram of a longitudinal section of a root illustrating general concept of radial movement of water and solutes. (B) Schematic representations of several entries for Na^+ influx into roots including cell-to-cell and apoplastic pathways. Thick red arrows represent hypothetical Na^+ entry sites for the apoplastic bypass flow (Horie *et al*., 2012).

In rice, in fact, numerous studies have shown the existence of a passive stream of Na^+ at the apoplastic level, known as the bypass flow, which runs through the Caspary band and enters in the xylem, drastically increasing Na^+ levels inside the plant (Yeo *et al*., 1987). Bypass flow is a small percentage of the transpirational volume flow, but it becomes important in ion transport at high transpiration rates and at high external ions concentration (Yeo *et al*., 1987; Flowers and Flowers, 2005). Many studies have been trying to find the physical location of this pathway. Faiyue *et al*., (2010), using a water-soluble, non-toxic, fluorescent substance that does not cross cell membranes, indicates a possible role for the lateral roots of rice in this uncontrolled entry of Na^+. A reduction in bypass flow have been shown to increase the resistance of rice to salt. For instance, adding silicon to the rooting medium reduced bypass flow and Na^+ uptake and extended the survival of seedlings growing under salt stress (Gong *et al*., 2006).

Osmotic tolerance in rice

As discussed earlier, reduction of membrane permeability is the first step that plants put in place to try to withstand osmotic stress. As previously shown in *Arabidopsis* (Maurel *et al*., 2008), salt stress reduced the activity and the expression of aquaporins in rice, suggesting the importance of these water channels in salt tolerance also in a cereal (Guo *et al*., 2006, Li *et al*., 2008). Rice also produces compatible solutes. However, lacking the choline monooxidase (CMO) that converts choline to betaine aldehyde, it cannot synthesize glycine betaine. Introduction of spinach CMO genes into rice plants promotes the synthesis of glycinebetaine and enhances salt stress tolerance in the transgenic rice plants (Sakamoto *et al*. 1998). Nevertheless, proline content has been shown to increase under salt stress and the transcript of gene encoding for P5CS (delta1-Pyrrolline-5-carboxylate synthetase) is up regulated under salinity stress (Bagdi *et al*., 2015). When *P5CS* gene was overexpressed, the transgenic rice plants showed both an increased production of proline and increased salt tolerance (Zhu *et al*., 2001). Conversely, rice seedling with a knockout mutation in *OsP5CS2* were more sensitive to salt stress than wild-type seedlings (Hur *et al*., 2004). Moreover, exogenous applied proline has been shown to promote recovery of rice seedlings from salt-stress (Nounjan *et al*., 2012).

Ionic tolerance in rice

As already described in Arabidopsis, the maintenance of a high ratio K^+/Na^+ in the cytosol turned out to be one of the major mechanisms of salt tolerance also in rice (Horie *et al*., 2012). For this reason, most of the studies on the responses to salt stress in rice focus on the analysis of the activity of Na^+ and K^+ channels and transporters.
As discussed above, one of the mechanisms to cope with ionic stress requires the removal of Na^+ from the cytosol through the SOS pathway or its compartmentalization into the vacuole.
In rice, cDNA coding for the proteins OsSOS1, OsSOS2 and OsSOS3 have been isolated. OsSOS1 transporters demonstrated a capacity for Na^+/H^+ exchange in plasma membrane vesicles of yeast cells, reduced their cellular Na^+ content and could coordinately function with AtSOS proteins. Moreover, OsSOS1 suppressed the salt sensitivity of sos1 mutants of *Arabidopsis*. The protein kinase OsSOS2 and its Ca^{2+}-dependent activator OsSOS3 could act coordinately to activate OsSOS1 in yeast cells and they could be exchanged with their *Arabidopsis* counterpart and suppressed the salt sensitivity of sos2 and sos3 mutants of *Arabidopsis* (Martinez-Atienza *et al*., 2007). Moreover, salt stress increases the expression levels of *OsNHX1* and its overexpression improved the salt tolerance of transgenic rice cells and plants (Fukuda *et al*., 2004). These results suggest that these mechanisms have been conserved also in rice where they are important factors determining salt tolerance.
HKT transporters have also been identified in rice. The most studied HKT transporters involved in the response to salt stress are OsHKT1;5 and OsHKT1;4, both involved in the processes of exclusion of Na^+ from the xylem and therefore from the photosynthetic tissues. Moreover, OsHKT1;5 also facilitate the entrance of K^+. These two transporters appear to act in salt stress tolerant cultivars by allowing accumulation of Na^+ in the older leaf to avoid the damaging of the new ones (Cotsaftis *et al*., 2012).
Another mechanism adopted to cope with ionic stress is the increasing of K^+ concentration in the cytosol.
Also in rice the activity of K^+ channels OsKAT1 seems to play a role for stress tolerance. In particular, OsKAT1 was found to suppress the salt-sensitive phenotype of a mutant yeast, and the K^+ transport-defective phenotype of another one indicating the function of OsKAT1 in K^+ uptake. Moreover, cellular Na^+ was decreased in OsKAT1-expressing yeast following the increase of K^+. This was true also for rice cells overexpressing OsKAT1(Obata *et al*., 2007). It should be noted that while AtKAT1 is well known to function in the guard cells of stomata (Nakamura *et al*., 1995), OsKAT1 expression was restricted to internodes and rachides of wild-type rice (Obata *et al*., 2007). Rice genome encodes three different isoforms of TPK channels. The rice TPK channels (OsTPKa and OsTPKb) exhibit different vacuolar localization. OsTPKa is targeted to the tonoplast of central lytic vacuole while OsTPKb is localized to the tonoplast of protein storage vacuoles (Isayenkov *et al*., 2011). It has been proved that in conditions of K^+ deficiency or salt stress, plants with elevated OsTPKa expression level exhibit better growth rates and decreased Na^+ accumulation in plant tissues, thus an overall increase in salt tolerance (Isayenkov *et al*., 2015). Overexpression of OsTPKb, instead, was found to increase rice osmotic and drought tolerance (Ahmad *et al*., 2015).
At least seventeen genes encoding KT/HAK/KUP transporters are present in the rice genome (Banuelos *et al*., 2002). Notably, it has been reported that constitutive expression of OsHAK5 in cultured-tobacco BY2 (*Nicotiana tabacum* cv. Bright Yellow 2) cells enhanced the accumulation of K^+ but not Na^+ during salt stress, conferring increased salt tolerance (Horie *et al*., 2011). Moreover, in rice overexpression of OsHAK5 increased the K^+/Na^+ ratio in the shoots and thus salt stress

tolerance, while knockout of OsHAK5 decreased this ratio, resulting in higher sensitivity to salt stress (Yang *et al*., 2014).

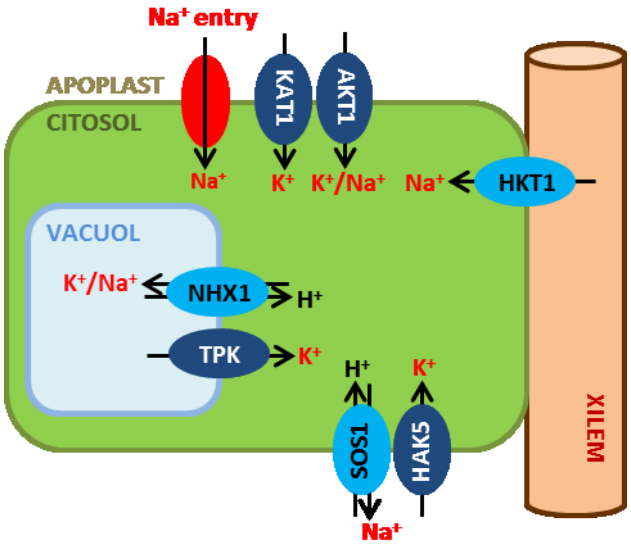

Figure 9. Schematic representation of important K^+ and Na^+ channels and transporters.

Chapter 2:

A prompt and specific response to salt stress at the origin of the tolerance of an Italian rice variety

2.1 Introduction

Soil salinity is a major constraint on crop production worldwide, particularly in agricultural lands close to the sea (Zhu *et al.*, 2001; Tester and Davenport, 2003). Salinization affects at least 33% of arable lands, and more areas are expected to deteriorate in coming years because of changes in global climate (FAO, http://www.fao.org/3/a-i4373e.pdf).

Plants respond differently to saline soil, with some very sensitive (glycophytes) and others more tolerant (halophytes). Unfortunately, most crop species are in the glycophyte group, and rice, one of the most important staple food crops in the world, is the most salt-sensitive of the cereals (Flowers and Yeo, 1995).

Soil salinity imposes two primary stresses on plants, osmotic and ionic. Osmotic stress establishes early after the onset of the stress, whereas ionic stress depends on ion accumulation in aerial parts of the plant (Munns and Tester, 2008). The osmotic pressure at the level of roots causes water loss and reduced turgor that in turn leads to a decrease in cell expansion and plant growth. Ion toxicity, in particular, that due to Na^+ accumulation, affects cellular metabolism, photosynthesis and induces oxidative stress.

Plants try to cope with salt stress by adopting, more or less effectively, multiple strategies that employ mechanisms to reduce water loss while improving water uptake. Sodium is excluded from sensitive leaf tissues either by reducing the flux of the toxic ion towards aerial parts or by decreasing the concentration in the cytosol, primarily by compartmentalization into vacuoles.

To respond effectively to salt stress, plants evolved the capability to perceive the hyperosmotic and ionic components of the stress, although the molecular identity of such receptors continues to be debated.

Regarding the osmotic component of stress, arrested growth and stomata closure are common features observed in responses to salinity that occur early from the onset of the stress. Specific calcium signatures are detected in early responses to salt stress, which suggest that mechano-sensitive ion channels may be involved in the perception of osmotic stress, causing calcium influx that leads to a specific response (Kurusu *et al.*, 2015). The recent discovery of the calcium channel OSCA1 from *Arabidopsis thaliana* that mediates hyperosmolarity-induced cytosolic calcium increase (OICI, Yuan *et al.*, 2014) may indicate that a central component in the perception of the osmotic component of salinity has been identified. In rice, 10 genes (Li *et al.*, 2015) were isolated with similarity to the OSCA family from *Arabidopsis*, and among them, *OsOSCA1.1*, *OsOSCA1.3*, *OsOSCA3.1/ERD4* and *OsOSCA2*.5 were specifically up-regulated in roots after salt treatment.

Perception of the stress at the membrane level is followed by a Ca^{2+}-mediated oxidative burst (Dubiella *et al.* 2013), which is likely involved both in local and in long-distance signalling (Miller *et al.*, 2010). Plasma membrane NADPH oxidases (NOXs) of the RBOH family are responsible for salt-induced apoplastic H_2O_2 production. In *Arabidopsis*, 10 genes have been found (*rbohA-J*), but only isoforms D and F are apparently involved in the salt stress response (Ma *et al.*, 2012). In particular, RBOH F likely regulates root-to-shoot Na^+ transport (Jiang *et al.*, 2012). These enzymes are modulated directly via Ca^{2+} binding to the EF-hands domains in the C-terminus of the protein and by gene up-regulation (Bánfi *et al.*, 2004). In rice roots, H_2O_2 is produced 5 minutes after exposure to salt stress (Hong *et al.*, 2009), possibly by activation of OsRBOHA, whose gene is regulated by salt (Wang *et al.*, 2016).

Although how plants sense Na^+ remains obscure, more information is available on the mechanisms adopted to avoid ion toxicity. Na^+ accumulation in the cytosol causes membrane depolarization, protein misfolding, and K^+ and water loss. Successful strategies for salt tolerance

likely rely primarily on the maintenance of a high $[K^+]/[Na^+]$ ratio in the cytosol (Hasegawa *et al.*, 2000). A cost-effective way to regain cellular turgor, and avoid impaired metabolism, is to use Na^+ as an inorganic osmolyte, e.g., by accumulation into vacuoles, and simultaneously increase cytosolic K^+, e.g., by release from vacuoles or uptake from the apoplast (Shabala and Pottosin, 2014). Several membrane transporters are involved in sodium exclusion or compartmentalization into vacuoles (Blumwald, 2000). Na^+/H^+ antiporters on the plasma membrane (SOS1) and the tonoplast (NHXs) are conserved systems that are observed in many vascular plants with involvement in tissue tolerance to ionic stress (Munns and Tester, 2008; Barragán *et al*., 2012; Amin *et al.,* 2016; Fukuda *et al*., 2004 and 2011). Potassium levels in the cytosol can be increased by release from intracellular storage, in particular from vacuoles in which a role for TPK outward K^+ channels in *Arabidopsis* and rice was demonstrated (Maathuis 2011; Ahmad *et al.* 2016; Isayenkov *et al.* 2011), and by uptake from the apoplast, most likely through an HAK5 K^+ transporter that confers salt tolerance when overexpressed in rice (Horie *et al.*, 2011).

Production of osmolytes is also a common mechanism that contributes to regaining cellular turgor (Hasegawa *et al.* 2000) and counteracts the oxidative stress induced by salt. Proline is the primary compatible solute synthesized after osmotic stress in rice, and a stress-inducible gene encoding for D-pyrroline-5-carboxylate synthetase 2 (*P5CS2*) was isolated, with this gene conferring salt and cold tolerance when overexpressed (Hur *et al*., 2004).

At the whole-plant level, sodium exclusion from the shoot is essential to avoid photosynthetic damage and crop yield loss. HKT-type $K^+(Na^+)$ transporters located on the plasma membrane of xylem parenchyma cells are involved in Na^+ unloading from the xylem sap. In rice, two members of the HKT family have been studied intensively, and the results indeed demonstrate their involvement in sodium exclusion from the shoot (HKT1;5; Hauser and Horie 2010) and from young leaves (HKT1;4; Cotsaftis *et al*., 2012; Suzuki *et al.*, 2016).

Therefore, salinity tolerance is a complex trait in which different components are involved in counteracting all the changes induced by salt stress.

Despite our understanding of the roles of many genes involved in salt tolerance, attempts to obtain fully salt resistant plants have often resulted in unwanted phenotypes, e.g., susceptibility to other environmental conditions in the field (Roy *et al.*, 2014). These unwanted phenotypes suggest that strategies other than single gene transfer are required to obtain crop plants with better productivity in challenging environmental conditions. To improve the salinity tolerance of crops, various traits should be incorporated, including ion exclusion, osmotic tolerance and tissue tolerance (Roy *et al.*, 2014).

Although *Oryza sativa* is a salt sensitive species, exploration of genetic variability and identification salt tolerant varieties is possible. Studies have been conducted with more than a few varieties, in particular, those from the indica group, identified with improved salt tolerance (Gregorio *et al.*, 2002; Ismail, 2007; Mohammadi-Nejad *et al.*, 2010; Yeo *et al.*, 1990). Based on physiological studies to evaluate salinity tolerance mechanisms, these varieties did not show simultaneous accumulation of different traits for tolerance (Akbar *et al.*, 1972; Yeo *et al.*, 1990). Thus, to ultimately combine different mechanisms in a new variety with a high level of salt tolerance, an increase in the understanding of new salinity tolerance mechanisms is required.

Developing a variety with an improved level of tolerance could contribute significantly to maintaining high levels of rice productivity. Approximately 75% of the world's rice is produced in irrigated paddy fields (www.irri.org), most of which are located next to rivers (e.g., the Mississippi in the US, the Nile in Egypt, the Mekong in Vietnam, the Yangtze in China, and the Po in Italy). The delta of the Po River basin in Italy, an area naturally dedicated to the production of high-quality Italian rice, is currently challenged by the serious threat of increased soil salinization, with soils now compromised (www.enterisi.it).

Therefore, in this work, two Italian rice varieties in the japonica group that showed the greatest contrast in salinity tolerance were selected from several varieties and were comprehensively characterized to unveil the mechanisms that provide salt tolerance.
To accomplish this goal, morpho-physiological and transcriptomic studies were conducted to develop an initial, general picture of the different behaviours of the two varieties. To complete the picture, these results were then integrated with molecular analyses of the early events in the perception of salt stress.

2.2 Results

Salt stress response in a salt sensitive and a tolerant Italian rice variety

In a pilot study, approximately 20 Italian rice varieties (ssp. japonica “temperate”) were tested for their salt sensitivity and then classified into 3 groups: tolerant, intermediate and sensitive. None of the varieties was fully resistant to salt stress (Bertazzini and Forlani, 2011).
Among the initially tested varieties, the two selected showed the greatest contrast in behaviour in response to salt exposure, the tolerant Baldo (B) and the sensitive Vialone Nano (VN). These varieties were compared to determine the molecular mechanisms that conferred tolerance rather than sensitivity.
The most effective concentration of salt ultimately chosen to highlight differences in salt response was 100 mM NaCl. Treated seedlings (vegetative growth stage 2, according to Counce *et al.*, 2000) showed reduced shoot growth and senescent leaves, with slight but significant differences between the two varieties. Six days after treatment, multiple senescent leaves were detected only on the sensitive VN variety (Fig.1 a, lower right panel); whereas on the tolerant B variety, the phenomenon was restricted to the first leaf (Fig.1 a, lower lane, second picture).

Growth parameters and water content

Based on detailed analysis of the growth parameters, we observed that the tolerant variety B showed a rapid reduction in growth rate (13.8% of the control; Fig.1 b, day 1) at the level of the first inter-collar (inter-collar 1; Fig. S1). Additionally, a limited loss (7%) in leaf relative water content was detected 3 days after treatment (Fig.1 c), which was likely due to the rapid reduction in stomatal aperture upon the perception of stress (Fig.1 d). Growth recovered (Fig.1, day 2), and new leaves eventually emerged (Fig.1 e).
By contrast, in the sensitive variety VN, the reduction in the first inter-collar growth rate was slower (35.5% of the control, Fig.1 b, day 1), more leaf water content was lost (44.7%) after 3 days of treatment (Fig.1 c), and the stomata aperture was not reduced after 24 h of stress (Fig.1 d). As a result, leaf yellowing ensued (Fig.1 a), and no new leaves appeared (Fig.1 e).

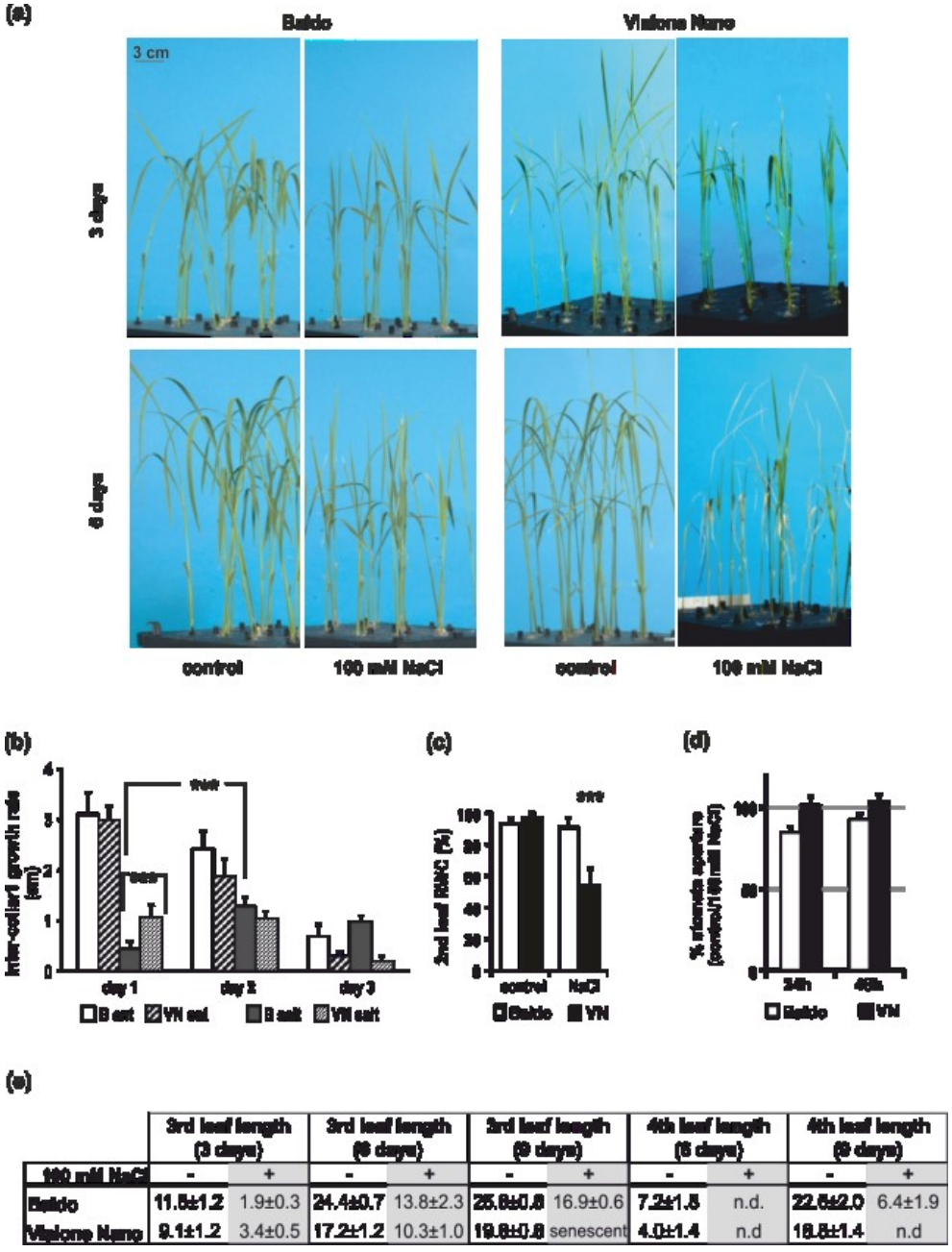

(e)

	3rd leaf length (3 days)		3rd leaf length (6 days)		3rd leaf length (9 days)		4th leaf length (6 days)		4th leaf length (9 days)	
100 mM NaCl	-	+	-	+	-	+	-	+	-	+
Baldo	11.5±1.2	1.9±0.3	24.4±0.7	13.8±2.3	25.6±0.8	16.9±0.6	7.2±1.5	n.d.	22.6±2.0	6.4±1.9
Vialone Nano	9.1±1.2	3.4±0.5	17.2±1.2	10.3±1.0	19.6±0.8	senescent	4.0±1.4	n.d	18.5±1.4	n.d

Figure 10. Morphological analyses of Baldo (left panels) and Vialone Nano (right panels) rice plants in control and stress conditions. (a) Seedlings have been cultured in hydroponics until the 2nd leaf stage and then challenged with salt solution for 3 (upper panels) or 6 days (lower panels). (b) Inter-collar 1 growth rate measured each 24 h (data are expressed as mean ± confidence interval, n > 100, p< 0.05). (c) Relative water content of 2nd fully expanded leaf (n = 6). (d) Stomatal aperture (relative to control plants) in the 2nd leaf after 24 h and 48 h from the treatment (data are expressed as mean ± confidence interval, n > 45, p< 0.05). (e) Length of 3rd and 4th leaves in treated and untreated plants: senescent and new emerged leaves are indicated (n > 100, data are expressed as mean ± SD) (* p < 0.05; ** p < 0.01; ***p < 0.001). B: Baldo; VN: Vialone Nano.

Evaluation of photosynthetic response in salt-treated plants

The effect of salt treatment (treated plants, T) on photosynthesis was evaluated by monitoring PSII maximum quantum yield (Φ_{PSII}) in seedlings (Fig.2, see the methods for details) for 13 days, with plants not exposed to salt stress used as controls (control plants, C).
For both varieties, this parameter was stable over time in control leaves (Figs.2 a and 2 c). When plants were treated with salt (Figs.2 b and 2 d), the responses diverged depending on the leaf age. The first (oldest) leaf of treated B plants showed a decrease in Φ_{PSII} after the 6th day (Fig.2 b). The second (fully expanded) leaf also showed the same strong decrease but only after the 10th day. By comparison, no major reduction was observed in the third leaf, and the fourth leaf, which emerged in the presence of salt, showed the same photosynthetic efficiency as that of the control samples (Fig.2 b). The behaviour of VN plants was in contrast to that of B plants, and after only 3 days of salt stress, both the first and the second leaves showed a large decrease in Φ_{PSII}, which indicated that photosynthesis was drastically impaired. The third leaf remained photosynthetically active until the 6th day, when again the Φ_{PSII} drastically decreased (Fig.2 d). Moreover, with salt treatment, further photoautotrophic growth was not supported in VN plants, and therefore, a fourth leaf was not produced (Fig.2 d). Fluorescence measurements used for the photosynthesis evaluation were performed using an imaging apparatus (see M&M) that could monitor the behaviour of different parts of a leaf. In Fig.2, the images of the PSII maximum quantum yield for the second leaves of B (Fig.2 e) and VN (Fig.2 f) plants under salt stress clearly show that the decrease in Φ_{PSII} for B plants was not homogeneous. For example, the decrease in PSII maximum quantum yield observed after 10 days of salt treatment (~0.5; Fig.2 b) was due to a strong reduction of Φ_{PSII} in the apical part of the leaf, whereas the basal part of the leaf remained fully photosynthetically active (~0.8; Fig.2 e). In the sensitive variety, this differentiation was not observed, and the entire leaf showed a strong, homogeneous decrease in Φ_{PSII} (Fig.2 f).

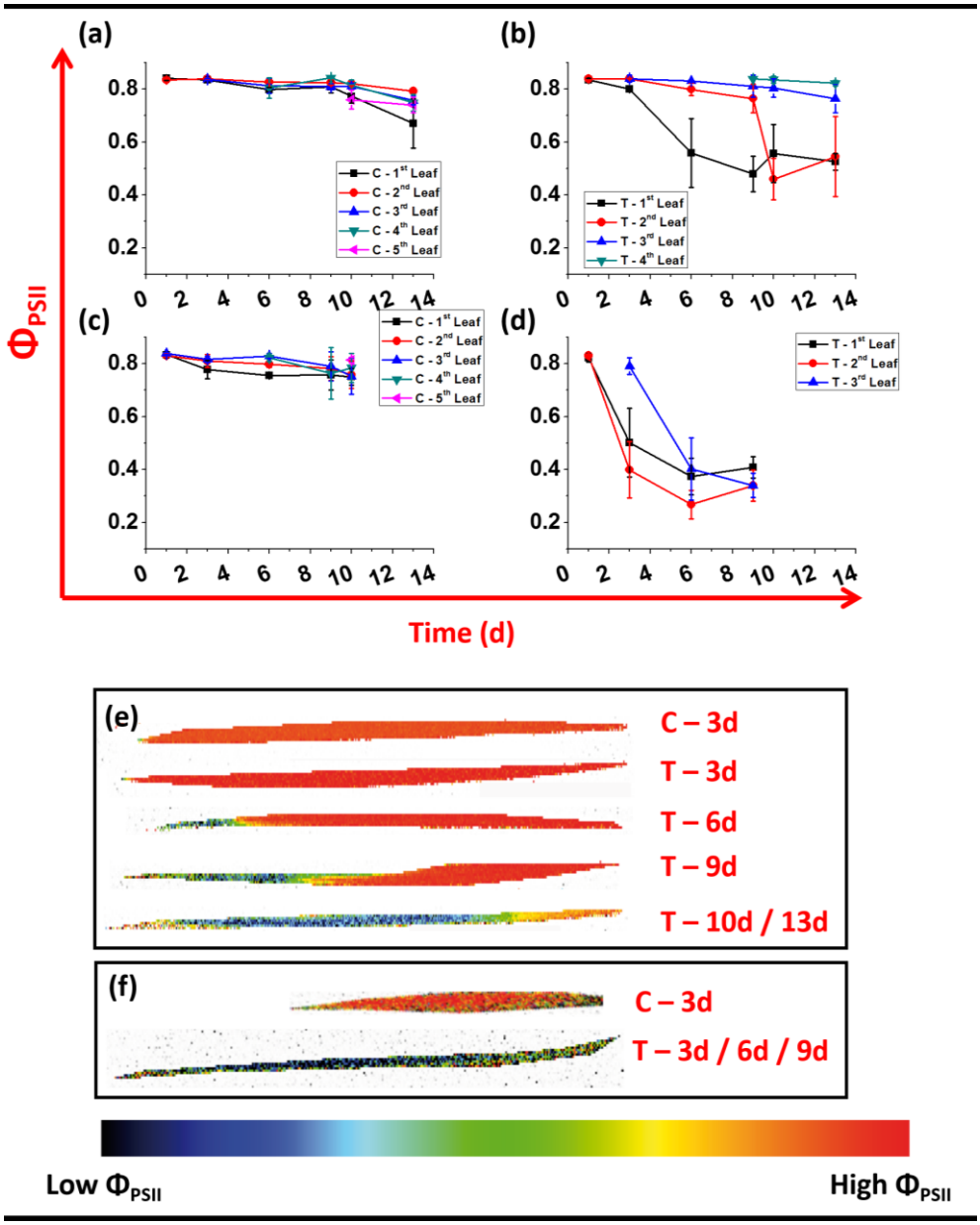

Figure 11. PSII maximum quantum yield (ΦPSII) evaluation during 13 days of salt treatment for rice plants (v. Baldo and v. Vialone Nano). (a) and (b) PSII maximum quantum yield for rice plants v. Baldo in control (a) and in salt treatment (b). (c) and (d) PSII maximum quantum yield for rice plants v. Vialone Nano in control (c) and in salt treatment (d); black – first leaf, red – second leaf, blue – third leaf, green – fourth leaf, violet – fifth leaf. Data are expressed as average of 6 biological replicates ± SD. Fluorescence images depicting PSII maximum quantum yield values for the whole second leaf area of Baldo (e) and Vialone Nano (f) plants. The region on the left represents the apical part of the leaf. Plants not exposed to salt treatment - C; Plants exposed to salt treatment – T.

Chlorophyll fluorescence measurements can also provide information on the ability to respond to intense light, with the excess energy dissipated through heat. This mechanism of non-photochemical quenching (NPQ) evolved in photosynthetic organisms to avoid the photo-oxidative damage (production of reactive oxygen species) caused by the over-excitation of PSII (Erikson *et al.*, 2015). The activation of NPQ is enhanced by exposure to abiotic stress (Zhu *et al.,* 2011). Figure 3 shows this parameter for the second leaf of B plants after 3 (Fig.3 a) and 6 days (Fig.3 b) of salt treatment. The NPQ was higher in treated plants than that in controls (red curves in Figs. 3

a and 3 b). Using the imaging system, we observed that the high NPQ was particularly evident in areas of the leaf that maintained their PSII functionality (Fig.3 c).
By contrast, in VN plants, we did not observe any strong NPQ activation compared with control plants (data not shown), and not even in those specific leaf regions in which the PSII functionality was unaffected (Fig.3 d).

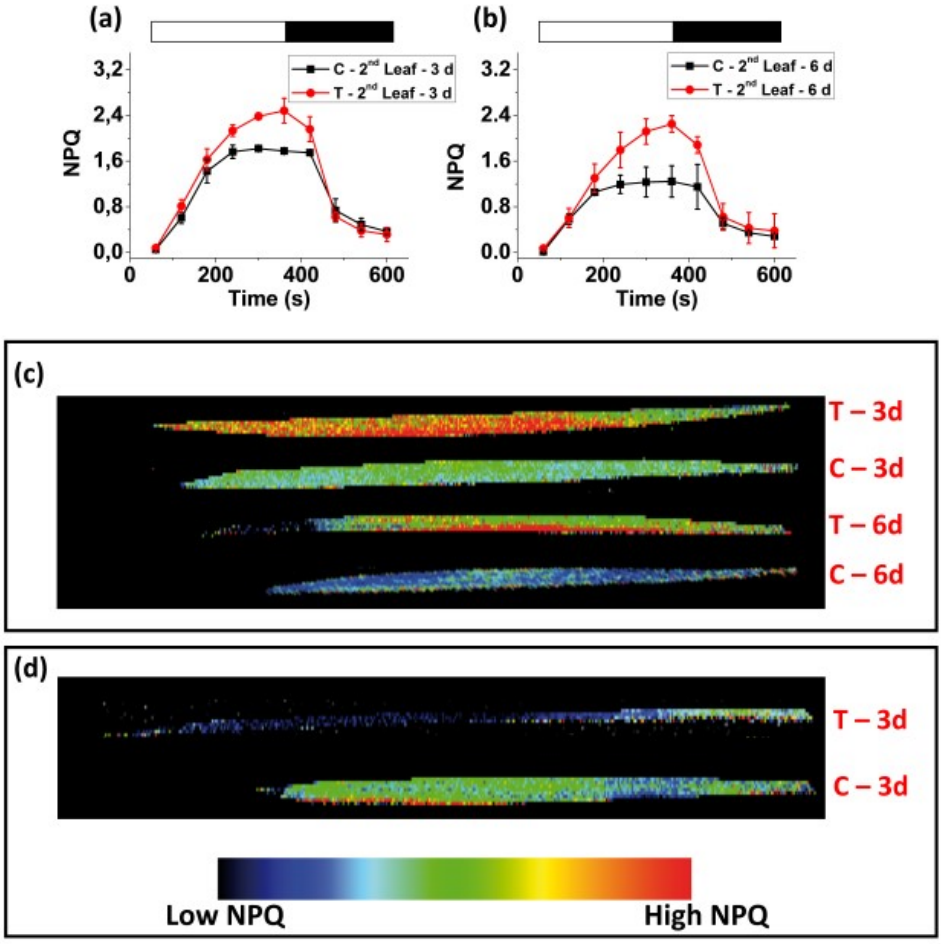

Figure 12. NPQ activation kinetics for salt-treated plants. NPQ kinetics for the second leaf of rice plants v. Baldo, after 3 (a) and 6 days (b) of salt treatment. White bars - light induction, black bars – dark relaxation (see methods for the detailed protocol). In red, salt treated plants – T; in black, control plants – C. Data are expressed as average of 6 biological replicates ± SD. Fluorescence images depicting NPQ values for the whole second leaf area for v. Baldo (d) and v. VN (d) plants. Images were taken after 3 or 6 days of salt treatment (T), using plants not exposed to salt stress as reference (Control – C). The region on the left represents the apical part of the leaf.

Recovery from saline stress

An experiment on the recovery of growth was conducted to evaluate the tolerance of B plants further. Plantlets grown in hydroponics enriched with 100 mM NaCl for 6 days were transferred into new, fresh medium without salt. After 7 days of culture in salt-free medium, the recovery capacity of the two varieties was assessed. The length of the 3rd and 4th leaves and the Φ_{PSII} were monitored for both varieties to evaluate not only the eventual capacity for growth to recover but also the recovery of photosynthetic performance (Table I and Fig.4).

Our results showed that the tolerant variety recovered completely after 6 days of treatment, whereas in the sensitive variety, the percentage of dead plants reached 76% (Table I), and photosynthesis in the remaining plants was greatly compromised (not shown).
Despite the recovery period, the salt also affected B plants, since the first leaf was photosynthetically compromised much more than that of the control plants (Fig.4). However, B plants withstood the stress and began a recovery process, and the newly emerged leaves (3rd and 4th) were not affected by the stress (Fig.4).

Table I. Length of 3rd and 4th leaves after 6 days of salt stress followed by 7 days in salt-free medium. The column + indicates seedlings under salt stress and the column – indicates the corresponding controls.

	3rd leaf length (6 + 7 days)		**4th leaf length (6 + 7 days)**	
100 mM NaCl	-	+	-	+
Baldo	24.2±0.4	16.7±0.3	28.3±0.8	24.6±2.1
Vialone Nano	17.9±.0.9	3.7±2.1*	20.5±1.4	5.0±2.8*

* 76% of dead plants (n=42)

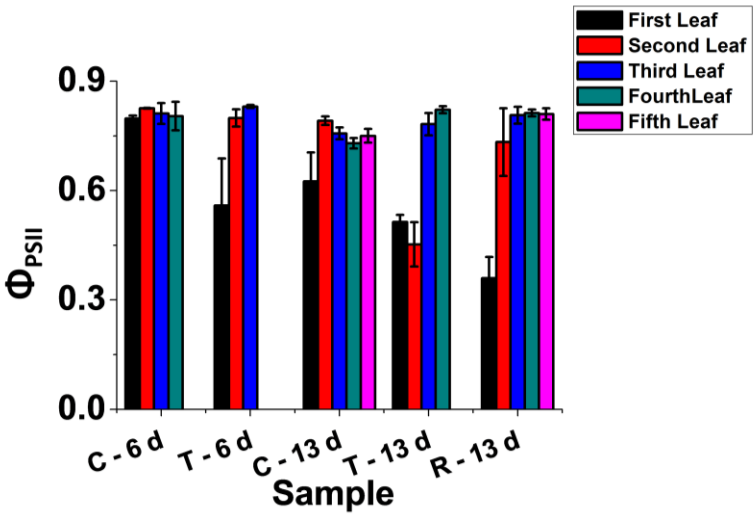

Figure 13. PSII maximum quantum yield (ΦPSII) evaluation after recovery from salt stress for rice plants v. Baldo. PSII maximum quantum yield (ΦPSII) during salt treatment prolonged for 6 days and after putting the plants in a recovery medium (R) without salt, for 7 days. Data for the recovery of VN plants PSII functionality are missing since plants, at this time point, were dead. C- plants not exposed to salt treatment; T - plants exposed to salt treatment; R – plants in the recovery medium. black – first leaf, red – second leaf, blue – third leaf, green – fourth leaf, violet – fifth leaf. Data are expressed as average of 6 biological replicates ± SD.

Differential salt effects on root apparatus

Much evidence suggests that salinity and osmotic stress induce morphological changes in Root System Architecture (RSA). Some modifications may also be involved in stress tolerance, although the mechanism remains unclear (Galvan-Ampudia and Testerink, 2011).
To test the hypothesis that a different adaptation of RSA might be involved in the tolerance or sensitivity of plants, we analysed the root morphology of the two varieties. Total root length and topological index were determined using WinRhizo software.
Morphological analyses showed that tolerant and sensitive varieties displayed contrasting root patterns in response to salt treatment (Fig.5 a). In the susceptible variety, a significant decrease in total root length (expressed in cm) was observed 2 days after the salt treatment compared with that in the control group, which led to arrested growth in the following days. By contrast, in the tolerant variety, no differences in total root length were observed after salt treatment.
Root architecture was also analysed to identify specific root characteristics of the tolerant variety. The topological index did not differ significantly between B and VN control roots (Fig.5 b), with both showing a dichotomous pattern. However, significant changes ($p < 0.05$) in the root topology of the tolerant variety were observed 4 days after salt treatment. As VN roots stopped growing and maintained their initial structure (topological index: 0.67 ± 0.006), the roots of B plants expressed a more herringbone topological pattern (topological index: 0.70 ± 0.004; Fig.5 b).

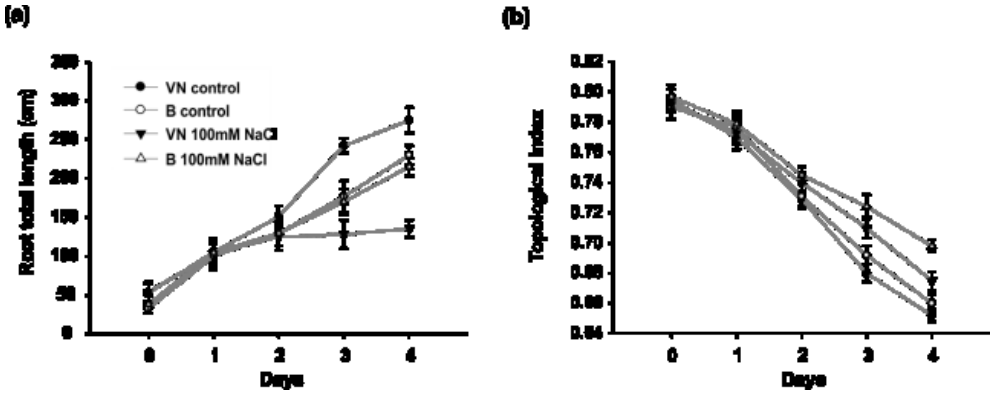

Figure 14. Root total length (a) and topological index (b) of the sensitive and tolerant cultivar are shown in presence (black symbols) and absence (empty symbols) of salt. The tolerant cultivar shows a change in RSA in response to stress (b), while the sensitive plants display an irreversible growth arrest (a). Data are expressed as mean ± SEM, n = 9, $p < 0.01$.

Tolerant plants allocate sodium differently in roots and shoot

In response to salt stress, VN plants showed symptoms that photosynthesis was impaired (Fig.2) and that senescence was anticipated (Fig.1 a). By contrast, in B plants, only older leaves were sacrificed, and the young ones survived (Figs.3 and 4).
To evaluate the response to ion toxicity, sodium content was measured in roots and leaves.
In the tolerant variety, Na^+ was restricted to the roots and the first and second leaves, with salt-excluded from the third leaf (Fig.6 a). However, in the sensitive variety, Na^+ was more uniformly partitioned in roots and shoot, and salt accumulation was observed in all the leaves (Fig.6 a). The

[K^+]/[Na^+] ratio was lower in the shoots of the sensitive variety than in those of the tolerant variety (Fig.6 b), which indicated greater ionic stress in the sensitive plants.

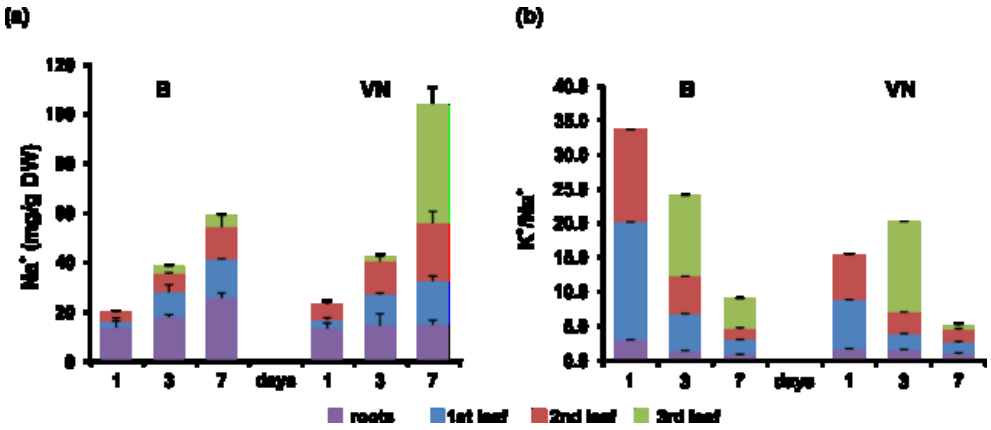

Figure 15. Sodium pattern distribution (a) and [K^+]/[Na^+] ratios (b) in roots and leaves (first, second and third) at 1, 3 and 7 days of treatment.

Salt susceptibility unveils a wide, not specific modulation of genes

To understand the molecular basis of salt tolerance, we compared transcriptional profiles of the two varieties obtained by mRNA sequencing. The analyses were conducted in roots and leaves three days after the salt stress, when both varieties were beginning their specific programme in response to salt stress: adaptation (growth recovery) in B plants, and senescence in VN plants.
A total of 542,309,740 single-end, 50 nt long reads were obtained from the sequencing experiments (mean per sample of 22,596,239 with a standard deviation of 3,817,253), which were reduced to 536,477,150 after preprocessing (mean per sample of 22,353,215 with a standard deviation of 3,792,380). Most of the reads (93.1%) were successfully mapped to the rice genome and met the requirements described in the methods section; of these, 3.48% mapped in multiple positions and were discarded.
Sequencing data were analysed as described in the methods section and also by exploiting metabolic pathways from the KEGG database. The results are summarized below and available online at http://admiral.fmach.it/projectview/stqWgH/.
Separately for each variety, pairwise comparisons were considered between treated and untreated samples, amongst leaves or roots.
As shown in Table II, in the sensitive variety VN, many more genes (DEGs) were regulated, almost fourfold the number regulated in B, both in leaves (5992 and 1572, respectively) and roots (7221 and 2263, respectively).

Table II. Number of DEGs and DE pathways for each comparison. The acronym are built with the following elements: V: Vialone Nano; B: Baldo; R: root; L: leaves; T: treated (3 days salt-stressed seedlings); C: control (without salt stress). The first column summarizes the results of the edgeR pipeline, whereas the last two summarizes the enrichment analysis (performed with DEAP).

Comparison	Diff. Expr. Genes	Diff. Expr. Pathways	Genes in Pathways
VRT vs VRC	7221	57	1219
BRT vs BRC	2263	23	384
VLT vs VLC	5992	67	996
BLT vs BLC	1572	29	435

In the first raw analysis, we gathered all DEGs represented by the following GO terms: response to salt stress, to osmotic stress, to water stimulus, to desiccation, to water deprivation, and to oxidative stress. In the sensitive variety, approximately 3- to 4-fold of the number of genes found in tolerant plants was modulated both in leaves and in roots (343 and 440 in VN and 130 and 167 in B, respectively). Only 94 and 138 of these genes were in common between the two varieties in leaves and roots, respectively.

Among the common genes, we detected those that coded for salt/drought-induced proteins, including aquaporins, dehydrins, late embryogenesis abundant proteins, and annexins, which indicated that both varieties responded to salt. Notably, the genes involved in ROS detoxification (i.e., peroxidases and catalases) were shared only in roots, with sodium mostly confined to roots in B plants (Fig.6 a). Genes unique to the VN variety suggested that these plants were experiencing strong oxidative stress (genes for NADPH oxidoreductase, catalases, superoxide dismutases, and ascorbate peroxidases) and cellular damage (genes for DNA helicases and heat shock proteins) in both roots and leaves. These results confirmed that the plants of the VN variety were previously exposed to ionic stress (Fig.6 a).

To better interpret the many DEGs, a pathway enrichment was performed: genes were assigned to clusters of orthologous groups from the KEGG database (4th column in Table II), gene networks (topology) were created, and finally, the expression data were combined with the pathway topology to compute an enrichment score (see the methods section for further details). Thus, we obtained a list of enriched pathways and their modulated components for each pairwise comparison. The number of enriched pathways was proportional to the number of DEGs and therefore was higher in the sensitive variety (Table I), suggesting a wider response to salt stress in the VN variety.

Tables III and IV show all enriched pathways in leaves and roots, respectively. The number of genes in the most differentially expressed path within the pathway is reported for each comparison. Some pathways (22 in leaves and 20 in roots) were common between the two varieties. Among these pathways, a few included different DEGs (i.e., “Selenocompound metabolism”, “Fructose and mannose metabolism”, “Pantothenate and CoA biosynthesis”, and “Purine metabolism” in leaves; “Arginine and proline metabolism” and “Arginine biosynthesis” in roots). The redundancy of genes could account for this discrepancy because no difference in the regulation of those pathways was observed. Only two exceptions were noted: “Selenocompound metabolism” in leaves, which in VN, shifted clearly towards Se-Met synthesis (Fig. S3), and “Arginine and proline metabolism” in roots in which the up-regulation of proline biosynthesis in B and the up-regulation of polyamines in VN were observed (Fig. S4).

Regarding the pathways identified only for the B variety (2 in roots and 6 in leaves), for “Phenylalanine, tyrosine and tryptophan biosynthesis,” the up-regulation of indole (IAA precursor)

synthesis was noticeable (Fig. S5), and for "Pyrimidine metabolism," the salvage pathway was apparently activated (Fig. S6), which is a process previously observed in salt-stressed mangrove trees (Suzuki-Yamamoto *et al.* 2006). Concerning the pathways characterizing only the VN variety (31 in roots and 45 in leaves), compared with the B variety, those involved in chlorophyll metabolism, carbon fixation, oxidative stress response, autophagy, and basic metabolism (glycolysis, riboflavin and protein synthesis) were affected by salt stress. In particular, in leaves, the genes involved in photosystems assembly were down-regulated, whereas those implicated in nitrogen reallocation (i.e., glutamine synthetase) and autophagy were up-regulated; thus, an active chloroplast dismantling followed by reassimilation of nitrogen, typical of a process of leaf senescence, was demonstrated (Fig.1 a, Tables III and IV). Of note, the "Plant-pathogen interaction" pathway was enriched in VN roots, which consists of a group of 159 genes that were mostly up-regulated, representing an example of a mistargeted stress response in the sensitive variety.

Notably, in both B and VN varieties, many hormone biosynthetic and signalling pathways were modulated (carotenoid biosynthesis for ABA, diterpenoid biosynthesis for GAs, cytokinins and brassinosteroid biosynthesis) both in roots and leaves (Tables III and IV).

Table III. Enriched pathways in leaves. The number of up- or down-regulated genes is reported for each pathway. VN, Vialone Nano; B, Baldo.

Differentially expr. Pathway in leaves	**v.**	**up**	**down**	**notes**
Amino acid metabolism				
Alanine, aspartate and glutamate metabolism	VN	6	8	Glutamine synthesis, leaf senescence (Cai *et al* 2009, Kamachi *et al* 1992)
Arginine biosynthesis	VN	4	3	
Cysteine and methionine metabolism	VN	22	19	
Histidine metabolism	VN	0	4	
Lysine biosynthesis	B, VN	3, 1	6, 8	2 genes with opposite expression
Lysine degradation	VN	2	0	
Phenylalanine metabolism	VN	11	14	
Phenylalanine, tyrosine and tryptophan biosynthesis	B	13	3	
Tyrosine metabolism	B, VN	15, 15	10, 10	7 genes with opposite expression
Valine, leucine and isoleucine biosynthesis	VN	5	1	
Metabolism of other amino acids				
Cyanoamino acid metabolism	VN	19	14	
Glutathione metabolism	VN	42	24	
Selenocompound metabolism	B, VN	1, 3	3, 1	no genes in common, Se-Met synthesis in VN
Carbohydrate metabolism				
Amino sugar and nucleotide sugar metabolism	B, VN	17, 16	6, 6	1 extra gene up in B, 2 genes with opposite expression
Ascorbate and aldarate metabolism	VN	6	13	
Butanoate metabolism	VN	4	5	
C5-Branched dibasic acid metabolism	VN	1	2	

Fructose and mannose metabolism	B, VN	4, 18	11, 11	only 10 genes in common
Galactose metabolism	B, VN	16, 15	7, 5	3 extra genes up in B
Glycolysis / Gluconeogenesis	VN	13	5	
Glyoxylate and dicarboxylate metabolism	VN	8	9	
Inositol phosphate metabolism	VN	9	5	
Pentose phosphate pathway	B, VN	16, 15	16, 20	46 genes in common, 2 genes with opposite expression
Propanoate metabolism	VN	8	1	
Pyruvate metabolism	VN	36	28	
Starch and sucrose metabolism	VN	16	26	
TCA cycle	VN	10	6	
Energy metabolism				
Carbon fixation in photosynthetic organisms	VN	7	19	
Nitrogen metabolism	VN	5	5	
Oxidative phosphorylation	B	13	7	
Sulfur metabolism	B, VN	3, 2	7, 8	1 gene with opposite expression
Environmental adaptation				
Circadian rhythm - plant	VN	3	5	
Folding, sorting and degradation				
Protein processing in endoplasmic reticulum	B	10	1	
SNARE interactions in vesicular transport	VN	6	2	
Sulfur relay system	B, VN	0, 0	4, 4	
Glycan biosynthesis and metabolism				
Glycosaminoglycan degradation	VN	1	5	
Glycosphingolipid biosynthesis - globo series	B, VN	3, 3	1, 1	
N-Glycan biosynthesis	VN	6	0	
Lipid metabolism				
Cutin, suberine and wax biosynthesis	B	1	4	
Fatty acid biosynthesis	B, VN	3, 6	12, 17	3 extra genes up in VN, 1 extra gene down in B, 6 extra genes down in VN
Fatty acid degradation	VN	13	1	
Glycerolipid metabolism	VN	27	19	
Steroid biosynthesis	VN	4	7	Biosynthesis of plant hormones
Synthesis and degradation of ketone bodies	VN	7	1	
Metabolism of cofactors and vitamins				
Biotin metabolism	VN	0	9	
Folate biosynthesis	VN	2	7	
Nicotinate and nicotinamide metabolism	VN	7	2	
One carbon pool by folate	B, VN	8, 4	10, 14	6 genes with opposite expression
Pantothenate and CoA biosynthesis	B, VN	1, 3	3, 4	no genes in common

Porphyrin and chlorophyll metabolism	VN	2	9	
Riboflavin metabolism	VN	0	7	
Thiamine metabolism	B, VN	0, 0	2, 2	
Ubiquinone and other terpenoid-quinone biosynthesis	B, VN	1, 0	4, 6	1 extra gene in VN
Vitamin B6 metabolism	VN	5	1	
Metabolism of terpenoids and polyketides				
Brassinosteroid biosynthesis	B, VN	2, 1	5, 6	Biosynthesis of plant hormones, 2 gene with opposite expression
Carotenoid biosynthesis	VN	2	14	Biosynthesis of plant hormones, zeaxanthin and violaxanthin are affected
Diterpenoid biosynthesis	B, VN	10, 8	4, 5	Biosynthesis of plant hormones, 1 extra gene up in B, 1 gene with opposite expression
Limonene and pinene degradation	B	1	0	
Terpenoid backbone biosynthesis	VN	7	17	Plant hormone metabolism
Zeatin biosynthesis	B, VN	0	3	Biosynthesis of plant hormones
Biosynthesis of other secondary metabolites				
Flavone and flavonol biosynthesis	VN	1		
Isoquinoline alkaloid biosynthesis	B, VN	7, 6	7, 3	9 genes are in common, 2 with opposite expression, 3 extra genes up in B, 2 extra genes down in B
Monobactam biosynthesis	B, VN	3, 1	6, 8	2 genes with opposite expression
Phenylpropanoid biosynthesis	VN	26	10	
Stilbenoid, diarylheptanoid and gingerol biosynthesis	VN	8	3	
Nucleotide metabolism				
Purine metabolism	B, VN	55, 38	40, 72	42 genes are in common, 25 of them have opposite expression
Pyrimidine metabolism	B	68	28	
Signal transduction				
Phosphatidylinositol signalling system	VN	20	19	
Plant hormone signal transduction	B, VN	9, 8	5, 6	ABA, 1 gene with opposite expression
Translation				
Aminoacyl-tRNA biosynthesis	VN	1	4	
Transport and catabolism				
Endocytosis	VN	3	0	
Regulation of autophagy	VN	8	1	

Table IV. Enriched pathways in roots. The number of up- or down-regulated genes is reported for each pathway. VN, Vialone Nano; B, Baldo.

Differentially expr. Pathways in roots	**v.**	**up**	**down**	**notes**
Amino acid metabolism				
Alanine, aspartate and glutamate	VN	11	9	

metabolism				
Arginine and proline metabolism	B, VN	9, 15	2, 6	4 genes in common, proline synthesis in B, polyamine synthesis in VN
Arginine biosynthesis	B, VN	1, 6	5, 6	only 3 genes in common, 1 with opposite expression
Cysteine and methionine metabolism	B, VN	15, 20	30, 24	31 genes in common, the rest are redundant
Glycine, serine and threonine metabolism	VN	12	27	
Histidine metabolism	B, VN	1, 2	2, 1	1 gene with opposite expression
Lysine biosynthesis	VN	8	1	
Lysine degradation	VN	8	6	
Tryptophan metabolism	VN	7	4	
Valine, leucine and isoleucine biosynthesis	VN	7	1	
Valine, leucine and isoleucine degradation	VN	6	2	
Metabolism of other amino acids				
beta-Alanine metabolism	VN	13	7	
Glutathione metabolism	B, VN	42, 42	22, 22	5 genes with opposite expressin
Selenocompound metabolism	B, VN	1, 0	6, 8	1 gene with opposite expression, 1 extra gene down in VN
Carbohydrate metabolism				
Butanoate metabolism	VN	8	1	
Fructose and mannose metabolism	B, VN	11, 12	26, 25	7 genes with opposite expression
Galactose metabolism	VN	8	11	
Inositol phosphate metabolism	VN	11	21	
Pentose and glucuronate interconversions	VN	6	14	
Pentose phosphate pathway	VN	15	21	
Propanoate metabolism	VN	5	2	
Pyruvate metabolism	B, VN	20, 24	36, 32	5 genes with opposite expressin, 2 extra genes up in B, 2 extragenes up in VN, 2 extra genes down in B
Starch and sucrose metabolism	VN	27	37	
Energy metabolism				
Nitrogen metabolism	B, VN	1, 1	6, 8	
Oxidative phosphorylation	VN	10	38	
Sulfur metabolism	B, VN	5, 7	12, 7	1 extra gene up in B, 3 extra genes down in B, 1 extra gene down in VN
Environmental adaptation				
Circadian rhythm - plant	B, VN	1, 4	6, 3	3 genes with opposite expression
Plant-pathogen interaction	VN	113	46	
Folding, sorting and degradation				
Sulfur relay system	VN	3	0	
Glycan biosynthesis and metabolism				
Glycosaminoglycan degradation	B, VN	4, 4	2, 3	1 extra gene down in VN, 2 genes with opposite expression
Glycosphingolipid biosynthesis - ganglio series	B	5	1	

Glycosphingolipid biosynthesis - globo series	B	6	2	
Glycosylphosphatidylinositol(GPI)-anchor biosynthesis	VN	6	2	
Lipid metabolism				
Ether lipid metabolism	VN	6	12	
Fatty acid biosynthesis	VN	11	19	
Fatty acid elongation	VN	1	10	
Glycerophospholipid metabolism	VN	25	30	
Steroid biosynthesis	B, VN	7, 9	5, 5	Biosynthesis of plant hormones, 2 extra genes up in VN
Synthesis and degradation of ketone bodies	VN	1	4	
Metabolism of cofactors and vitamins				
Folate biosynthesis	VN	8	0	
Nicotinate and nicotinamide metabolism	B, VN	2, 1	7, 6	1 extra gene up and 1 down in B
One carbon pool by folate	B, VN	5, 10	13, 8	6 genes with opposite expression
Pantothenate and CoA biosynthesis	B, VN	2, 6	4, 1	3 genes with opposite expression, 1 exta gene up in VN
Vitamin B6 metabolism	VN	5	0	
Metabolism of terpenoids and polyketides				
Brassinosteroid biosynthesis	VN	1	9	Biosynthesis of plant hormones
Carotenoid biosynthesis	B, VN	9, 9	4, 4	Biosynthesis of plant hormones, 2 gene with opposite expression
Diterpenoid biosynthesis	B, VN	10, 8	2, 1	Biosynthesis of plant hormones, 2 extra genes up in B, 1 extra gene down in B, 2 genes with opposite expression
Sesquiterpenoid and triterpenoid biosynthesis	VN	1	3	
Terpenoid backbone biosynthesis	B, VN	20, 20	7, 8	Biosynthesis of plant hormones, 6 genes with opposite expression, 1 extra gene up in VN, 1 extra gene up in B
Zeatin biosynthesis	VN	1	3	Biosynthesis of plant hormones
Biosynthesis of other secondary metabolites				
Flavone and flavonol biosynthesis	VN	0	3	
Monobactam biosynthesis	VN	8	1	
Phenylpropanoid biosynthesis	VN	54	109	
Nucleotide metabolism				
Purine metabolism	VN	20	30	
Signal transduction				
Phosphatidylinositol signalling system	VN	13	26	
Plant hormone signal transduction	VN	12	12	ABA
Transport and catabolism				
Phagosome	B, VN	0	12	

Tissue tolerance in Baldo is due to Na^+ compartmentalization

The response to salt stress involves modulation of ion transport systems, particularly the channels and transporters of potassium and sodium, some of which play key roles in salt tolerance mechanisms (Munns and Tester, 2008, Horie *et al.*, 2012). To determine the mechanisms involved in the different patterns of Na^+ distribution adopted by the two varieties, changes in the expression profile of genes encoding for channels, transporters and carriers obtained with the transcriptomic data were identified and analysed in detail (Table S2).

As previously noted, the sensitive variety modulated many more genes than the tolerant variety. After 3 days of salt stress, sensitive plants regulated genes that encoded mostly for aquaporins, NSCCs (nonselective cation channels, GLR and CNGC), ATPases, K^+ transporters (HAK), and proline and monosaccharide transporters, primarily in roots. Furthermore, genes involved in Na^+ and Cl^- transport (i.e., NHX, ClC, CCC, and HKT) were modulated only in the VN plants, which suggested that susceptible plants after 3 days continued to suffer osmotic stress, water deficit and ion toxicity.

As the results show in Table S2, no significant indications of the role of these genes in tolerant plants were provided after 3 days of treatment; therefore, representative members for each category of transporter gene were selected and their expression analysed at earlier times (1, 6 and 24 h) after salt stress (Fig.7 a).

OsAKT1.1, SKOR and KAT1 are root specific shaker-like K^+ channels for which the expression has been investigated extensively (Fuchs *et al.*, 2005; Schmidt *et al.*, 2013; Obata *et al.*, 2007). In our studies, *OsAKT1.1* and *SKOR* were down-regulated, whereas *OsKAT1* was induced by salt, as expected (Fig.7 a), in both B and VN varieties, which confirmed that both varieties responded to the stress.

Tonoplast transporters, putatively involved in Na^+ compartmentalization or $[K^+]_{cyt}$ homeostasis, were analysed. TPKa and TPKb as members of the two-pore outward potassium channel family were up-regulated in the first hour in roots of B plants but only after 6 hours in VN roots. In leaves, no significant difference was observed between the two varieties. The gene encoding for the vacuolar cation/proton antiporter NHX1 was up-regulated early only in B roots (1 h) and leaves (6 h). The vacuolar H^+-translocating pyrophosphatase OVP1 encoding gene was up-regulated in the tolerant variety in roots and leaves after 1 h and 6 h, respectively, whereas in VN leaves, the gene was up-regulated later only at 24 h after treatment.

We also investigated the expression profiles of Na^+ transporters responsible for Na^+ unloading from the xylem sap. HKT1;4 and HKT1;5 were only slightly modulated, perhaps because of their very restricted cellular localization. HKT1;5 was down-regulated in VN roots after 1 h and was up-regulated in the tolerant variety 24 h after treatment. HKT1;4 was up-regulated in leaves of both varieties, but the up-regulation was earlier (1 h) in VN plants.

The gene encoding for the Na^+/H^+ antiporter OsSOS1, which contributes to sodium exclusion from the cytosol, was only slightly up-regulated in leaves of both B and VN (Fig. 7a) varieties after 6 h and 24 h, respectively.

Of the K^+ transporters, we selected HAK5, which is involved in the response to K^+ starvation and salt stress. The gene was modulated only in roots of VN plants in which it was down-regulated in the early phases of stress and then up-regulated after 24 h. In leaves, the gene was up-regulated early in both varieties, at 1 h and 6 h in VN and B plants, respectively.

Early response of tolerant variety to salt stress

Based on the results obtained with morpho-physiological and molecular approaches, the tolerant variety responded to salt stress more rapidly and in a more specific way than the sensitive variety. In the sensitive variety, the response was wide, unselective and relatively slow, which led to a chaotic, not manageable physiological condition that induced senescence.

To provide support for this hypothesis, we analysed the expression profiles of some genes induced by salt/drought at very early stages of the stress, such as the genes involved in osmosensing (*OsOSCA1.1* and *3.1*), signal transduction pathway (*OsDREB2A* and *RbohA*; Mallikarjuna *et al*. 2011; Wang *et al.* 2016), early ROS events (superoxide dismutase: *SODCC2*; catalase isozyme A: *CatA*; cytosolic ascorbate peroxidase 1: *APX1*; glutathione S-transferase: *GSTU6*) and proline synthesis (*P5CS2*).

The expression profiles of these genes clearly showed that roots of the tolerant variety B responded to stress in the first hour of treatment (Fig.7 b, BR 1h), whereas in leaves, the same genes were up-regulated after 6 h (Fig.7 b, BL 6h). The response was similar in VN plants, with some of the genes up-regulated but with a slight delay (i.e., after 6 h and 24 h in roots and leaves, respectively).

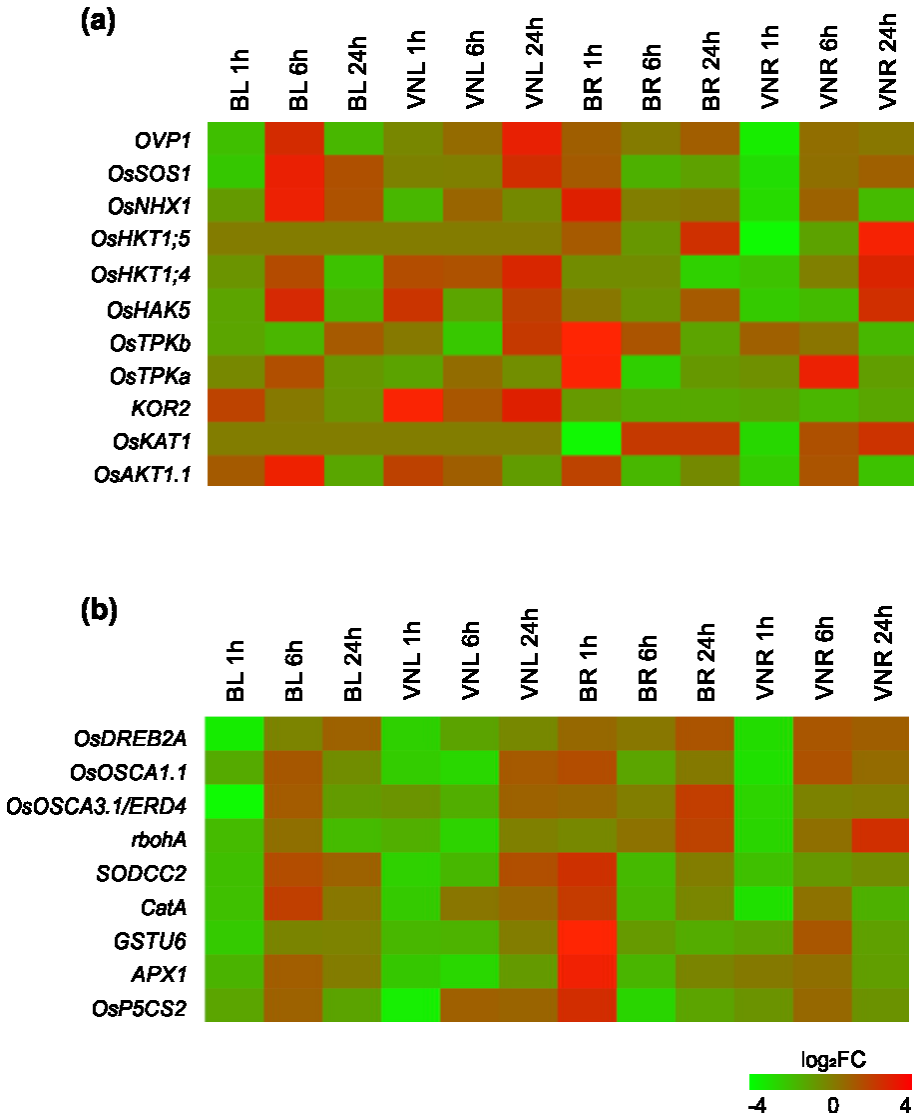

Figure 16. Gene expression profile after 1, 6 and 24 h of stress. (a) Genes involved in K^+ release to the cytosol (HAK5, TPKa and b) and in Na^+ exclusion (HKT1;5 or HKT1;4, SOS1) or compartmentalization (NHX1, OVP1). The genes coding for K^+ channels OsAKT1.1, SKOR and KAT1 have been used as a control in roots where they are known for being modulated by salt. (b) Genes involved in salt stress perception (OsOSCA1.1 and 3.1), signal transduction (OsDREB2A), early ROS events (OsRbohA) and scavenging (SODCC2, CatA, APX1, GST, P5CS2) Data are expressed as log2 of fold change (ΔΔCT method). B: Baldo; VN: Vialone Nano; L: leaves; R: roots.

2.3 Discussion

Tolerance to salt stress is a complex trait that is not dependent on a single mechanism. In this study, two Italian rice varieties (Vialone Nano and Baldo) that differed in salt sensitivity were investigated with the aim to determine some of the mechanisms that explained their different responses to stress. Based on an accurate morpho-physiological characterization in addition to a transcriptomic analysis of plants exposed to salt stress for 3 days, we described in detail how stress affected the behaviour of the two rice varieties. The results from these experiments were then integrated with an expression analysis of selected genes modulated early by salt stress.
Salinity challenges plants with both osmotic and ionic stress. Osmotic stress is established in minutes to hours, whereas ionic stress requires hours to days or weeks, depending on the amount and speed of ion accumulation in the aerial parts of a plant (Munns and Tester, 2008). Based on our results, the B variety had distinctive features that made those plants more tolerant than VN plants to both osmotic and ionic stress under conditions of high salinity.

Morpho-physiological traits: tolerant Baldo responds quickly and shows adaptive features

Biometric measures (Fig.1 b) showed a greater osmotic tolerance in B plants, which was demonstrated by the more effective reduction in stem growth rate than that in VN plants (86.2% and 64.5%, respectively) at 24 h after treatment and by the simultaneous, temporary closing of stomata (Fig.1 d) to limit water loss (Fig.1 c).
Sodium accumulation in older leaves represents a typical strategy adopted by plants to counteract ionic toxicity, and therefore, is responsible for the decline in photosynthetic efficiency and leaf senescence (Munns and Tester, 2008; Cotsaftis *et al.*, 2012; Suzuki *et al.*, 2016). Differences in sodium allocation might explain how and why the B variety was more tolerant to ionic stress than the sensitive variety. In B plants, sodium was restricted primarily to roots and later to the oldest leaves, whereas in the sensitive variety, sodium partitioning was clearly uniform between roots and leaves (Fig.6). As a result, in B plants, PSII functionality was affected in the 1st and 2nd leaves and not in the 3rd and 4th (Figs.2 and 3). By contrast, VN plants were strongly affected by salt treatment and showed large impairments in photosynthetic efficiency. Furthermore, with the use of an imaging system, compared with the more common pulse-amplitude modulation (PAM) instruments (Du *et al.*, 2010; Zhu *et al.*, 2011; Zulfugarov *et al.*, 2014), we observed that photosynthetic efficiency did not decrease homogenously in B plants, and although some parts of the leaves were sacrificed, photosynthesis was unaffected in the other parts. The sensitive variety VN did not have this response, and VN leaves were completely affected by salt. These patterns were likely matched by the activation of specific mechanisms of sodium allocation among and within leaves, which highlighted that B plants likely evolved mechanisms to compartmentalize Na^+ in contrast to VN plants. This strategy could also be advantageous for photosynthesis; rather than loose efficiency in all the cells, it is better to sacrifice a part of a leaf completely while keeping the rest intact to function.
Additionally, the recovery experiments demonstrated the capacity for B plants to limit the stress response to the first leaf, which was sacrificed to support the photosynthetic activity of the other leaves and continue the photosynthetic growth of the entire plant with the emergence of new leaves (Fig.4). For the evaluation of the activation of the NPQ mechanism, the results found in this

study were consistent with literature data that report the induction of a stronger NPQ activation in plants exposed to abiotic stresses (e.g., salt and drought) in several species. For example, salt tolerant plants (e.g., *Brassica campestris*) show a faster NPQ activation kinetic, which also leads to higher NPQ amplitude after light exposure (Zhu *et al.*, 2011). This event was also described in *Physcomitrella. patens*, which is a representative of the early land colonization stage of plants (Azzabi *et al*., 2012) and highlights how NPQ activation evolved in plants immediately after colonization of terrestrial habitats. These results suggest that an increase in NPQ activation could be used in combination with Φ_{PSII} as a biomarker of the response to salt stress, providing evidence of an appropriate response in a plant. Therefore, application of PAM instruments could provide a first evaluation of salt exposure directly in the field, highlighting the severity of the stress.
The effect of salt on the root apparatus was evaluated by analysing root topology, which is an indicator of ecophysiological differences in adaptations to environmental stresses (Fitter and Stickland, 1991; Fitter, 1996). In this study, the root topology of B plants was strongly modified by salt treatment, and upon exposure to salt stress, these plants tended to develop a root system topology approximating a herringbone pattern, which could be interpreted as an explorative strategy of a root system to rapidly reach lower soil layers. By contrast, VN plants retained a dichotomous topology because of an irreversible block in changing the growth response to stress.
This first set of results indicated that the two varieties reacted differently to the imposed stress. VN plants responded by slowly stopping the growth of roots and the shoot. By contrast, the B plants began as an initial prompt decrease in the growth of the shoot, which was followed by the induction of tolerance mechanisms, such as sodium exclusion from young leaves, an increase in NPQ (photoprotection) and a change in RSA to improve nutrient uptake.

Transcriptomic analysis unveils a more specific response to salt stress in the tolerant variety

The response at the molecular level was evaluated with a transcriptomic analysis performed 3 days after the stress when both varieties were initiating their specific programmes in response to salt stress: adaptation (recovery in growth) in B plants versus senescence in VN plants. Based on the quality and quantity of regulated genes, the response of the sensitive variety was broad and not too specific compared with that of the tolerant variety. The number of regulated genes was 4-fold higher in VN plants, but the genes modulated were also apparently involved in responses to other types of stress, such as that to pathogens in roots (see above and Table IV). However, in VN leaves, many DEGs were involved in carbon metabolism and nitrogen remobilization (Table III), which indicated the onset of a genetically controlled cellular dismantling process. The pattern of up- and down-regulated genes was also more clearly defined in B plants than that in VN plants for which a clear pattern was not observed. As a consequence of these differences, a chaotic physiological condition was established, and senescence events were initiated in the sensitive variety, whereas in the tolerant variety, as a general feature, the response to salt stress was more limited and specific.

Tolerance is achieved in Baldo plants by sodium sequestration and $[K^+]/[Na^+]$ homeostasis

As reported by Munns and Tester (2008), roots are more salt tolerant than leaves; therefore, by maintaining salt in the roots for as long as possible, the B variety adopted a successful strategy. Simultaneously, a high Na^+ tolerance was implied for B roots, which was likely related to efficient ion sequestration in root cell vacuoles.

The early activation of genes encoding for tonoplast transporters involved in Na^+ sequestration into the vacuoles (NHX1 and OVP1; Barragán *et al.*, 2012; Gaxiola *et al.*, 2001; Zhang *et al.*, 2011) and K^+ release to the cytosol (TPKs, Fig. 7a) provided strong indication that a tissue tolerance mechanism was activated in B plants.

Notably, in the leaves of tolerant plants, *OsNHX1* and *OVP1* were highly expressed 6 h after stress. Because sodium was not in the leaves yet (Fig.6), we hypothesized a different role for NHX1 than that of Na^+ antiporter. In *Arabidopsis*, a role in K^+ transport and turgor maintenance was recently demonstrated for NHX1 (Andrés *et al.*, 2014; Barragán *et al.*, 2012), and therefore, in this context, *NHX1* might be a reliable molecular marker of salt tolerance.

The molecular analysis provided support for our hypothesis that the resilience of B plants in salty conditions might be due to the capability of the root system to retain more sodium, possibly by storage in vacuoles, and to avoid nutrient starvation through morphological changes (Fig.5). Leaves are also involved in this resistance by the regulation of the genes involved in osmotic homeostasis (*TPKs*, *NHX1*, *OVP1*, Fig.7 a) and by the rapid stomatal closure (Fig.1 c), which might explain the ability to preserve water content (Fig.1 c).

Timing of early response is apparently important in obtaining salt tolerance

Based on recent evidence, the difference between tolerance and susceptibility to a stress might be the result of different mechanisms used to perceive stress or the timing of signal transduction during the response to stress (Ismail *et al.*, 2014).

In roots, calcium and H_2O_2 waves through OSCA hypersensitive-gated Ca^{2+} channels and plasma membrane NADPH oxidase are likely responsible for salt perception and root-to-shoot signalling (Evans *et al.*, 2016; Mittler *et al.*, 2011) that lead to sodium exclusion in the shoot (Jiang *et al.*, 2012). By analysing the expression of genes involved early in the salt response, a more rapid osmotic response was confirmed in the tolerant variety, and the genes involved in osmosensing, osmoregulation and ion homeostasis (*OSCA1.1*, *P5CS2*, *NHX1*, *OVP1*) and those involved in signal transduction (*OsDREB2A*; Agarwal *et al.,* 2006; Mallikarjuna *et al.*, 2011) and H_2O_2 signalling (*RbohA*; Wang *et al.*, 2016) were up-regulated in roots in the first hour after treatment (Fig.7). The same genes were also activated early in leaves (6 h), likely through fast signalling from roots to shoots, causing a rapid stress response in the photosynthetic organ, long before the sodium accumulation began.

2.4 Conclusions

Timing is important to obtain a specific salt tolerant response

In combination, the results of this report indicated that tolerant plants rapidly perceived salt stress and responded by activating a typical osmotic response in the first 24 h, which led to the development of an adaptive programme that allowed growth to resume with the appearance of new unaffected leaves (Fig.1 e). At the root level, the topology moved towards a herringbone pattern, which is an explorative strategy of the root system aimed to reach lower soil layers rapidly. Additionally, plants of the B variety responded to ion toxicity by rapidly inducing the up-regulation (1 h) of two-pore outward potassium channels, namely, TPKa and b, and the Na^+/H^+ antiporter NHX1 (Fig.7 a) in roots, which allowed the cytosolic $[K^+]/[Na^+]$ concentration to remain high, preventing deleterious ion effects at the cellular level.
By contrast, the sensitive variety reduced stem growth more slowly and did not close its stomata. These plants were less tolerant to osmotic stress and based on the uniform allocation of sodium in the shoot and roots, were also less tolerant to ionic stress. Based on molecular analyses, VN plants responded more slowly to salt stress, and this delay apparently resulted in a huge molecular response regarding the quantity and quality of genes that were up- and down-regulated. The result was not cooperation to build a specific response but a chaotic physiological condition, which led to plant senescence. Thus, the absence of a prompt initial response (Fig.7) to the imposed stress seems to imply less specificity in activating cellular mechanisms necessary to establish an adaptive programme.
The results produced in this work are fully consistent with the proposal by Ismail *et al.* (2014). In that paper, the authors suggest that the timing of a response to salt stress is a very important factor in inducing an adaptive outcome versus cell death. In particular, because the stress-induced signals (Ca^{2+}, H^+, ROS) did not confer specificity *per se*, they propose that the timing is important for when these signals appear and disappear to induce specificity.
In conclusion, the timing followed by a specific response explained salt tolerance in the B variety of rice; thus, timing was apparently connected to specificity.

Acknowledgements

This work was supported by Progetto AGER grant n° 2010-2369 to FLS.
This work was done in collaboration with the laboratory of Prof. Morosinotto (Department of Biology, University of Padova, Padova, Italy) for the photosynthetic parameters evaluation, the laboratory of Prof. Sacchi (Department of Agricultural and Environmental Sciences - Production, Landscape, Agroenergy, University of Milan, Milan, Italy) for the determination of the ionomic content, the laboratory of Dott. Stefano Toppo (Department of Molecular Medicine, University of Padova, Padova, Italy) for the bioinformatic analysis and the laboratory of Dott. Piergiorgio Stevanato (Department of Agronomy, Food, Natural Resources, Animal and Environment, DAFNAE, University of Padova, Legnaro, Italy) for the root morphology analysis.

2.5 Materials and Methods

Plant material and morphological analyses

Dehulled seeds of Italian rice varieties (*O. sativa* L. spp. japonica "temperate") were sterilized for 1 min in 70% ethanol and rinsed 5 times with deionized water. Seeds were sown on water-wetted filter paper in Petri dishes and left to germinate for 48 h at 24 °C in the dark. Uniformly germinated seedlings were transferred to agar-filled (0.55% w/v) seed-holders in an Araponics system (www.araponics.com) with a modified Hoagland solution (Hoagland and Arnon, 1938; Table S1). Plants were grown until the vegetative stage V2 (collar formation on the second leaf; Counce *et al*., 2000) at approximately 6 days in a growth chamber at 26/21 °C, with a 16/8 h photoperiod, an approximate RH of 70%, and light of 120-150 µmol photons m-2 s-1.
Six-day-old seedlings were grown with or without 100 mM NaCl, 10 mM CaCl2, 20 mM MgSO4, and 10 mM Na2SO4, and the distance between leaf collars (inter-collar, Figure S1) was measured daily. Leaves (blade + sheath), stems and roots (washed carefully) were collected. For ionomic analysis, samples collected at different times (1, 3 and 7 days) from control and treated plants were dried at 40°C for 48 h and stored in plastic boxes. For RNA-seq analysis, 3-day treated samples (leaves and roots) were frozen in liquid nitrogen. To minimize the effect of individual polymorphisms, each biological replicate was a mix of 6 plants. Three biological replicates were used in each experiment.

Stomata aperture measurements

Stomata of the second leaf were observed under a light microscope (Leica 5000b, Leica Microsystems, Wetzlar, Germany) with a 100x objective. The length of the longitudinal axis was measured in control and treated plants at 24 and 48 h after the superimposition of salt (100 mM NaCl; $n > 50$, $p < 0.01$) with ImageJ software (Schneider *et al*., 2012).

Relative water content

Sections of 5 cm2 of the second leaf were cut with scissors and immediately weighed (W). Then, the sections were hydrated in water in 15 mL test tubes for 4 h in a growth chamber under light. After rapid drying, the samples were weighed to obtain the turgid weight (TW). Dry weight was measured after oven-drying at 40 °C for 48 h.
Relative water content was determined using the following formula (Barr and Weatherley, 1962):
RWC (%) = [(W-DW) / (TW-DW)] x 100 (n = 6)

Photosynthetic parameters evaluation

In vivo chlorophyll fluorescence measurements were performed with an imaging apparatus (FluorCam FC-800; Photon Systems Instruments, Brno, Czech Republic). Plants were dark adapted for 30 min and later sacrificed. The chlorophyll fluorescence value of dark-adapted samples (F0) was measured applying a non-actinic white light source (intensity < 0.05 µmol photons m-2 s-1).

By contrast, the maximum chlorophyll fluorescence value of dark-adapted samples (Fm) was measured applying a saturating light pulse (intensity = 3500 µmol photons m-2 s-1 and 800 ms duration).
PSII functionality was expressed as PSII maximum quantum yield (ΦPSII) and was calculated according to (Maxwell and Johnson, 2000). PSII quantum yield was monitored over time, using control plants not exposed to salt as the reference. Leaves were then exposed to 500 µmol photons m^{-2} s^{-1} for 5 min to evaluate non-photochemical quenching (NPQ) activation kinetics. Later, the light was switched off for 3 min to evaluate NPQ relaxation. NPQ was calculated according to Maxwell and Johnson (2000).

RNA sequencing and data analyses

RNA purification and sequencing

Total RNA was extracted both from leaves (blade + sheath) and roots of 3-day treated and untreated plants (not exposed to salt) using an RNeasy Plant Mini Kit followed by in-column DNase treatment (Qiagen, Hilden, Germany). The RNA quality was measured using a Bioanalyzer 2100 (Agilent Technologies, Santa Clara, USA). IGA Technology Services (Udine, Italy) performed RNA sequencing using Illumina techniques on polyA+ RNA.

RNA-seq preprocessing

The processing of sequencing reads was performed with a procedure analogous to that described in Finotello *et al*. (2014) for single-end sequences. Illumina raw reads were preprocessed with FASTX Toolkit 0.0.13.2 (http://hannonlab.cshl.edu/fastx_toolkit/index.html) to trim adapter sequences and low-quality read terminals and discard reads containing ambiguous 'N' characters. The overall quality of preprocessed results was then manually inspected using the quality reports produced with FastQC (http://www.bioinformatics.babraham.ac.uk/projects/fastqc/).
Preprocessed reads were mapped with TopHat (Kim *et al*., 2013) on the Oryza sativa v. Nipponbare genome, which was downloaded from the MSU Rice Genome Annotation Project (version 7.0) (Kawahara *et al*., 2013), with the file of gene coordinates also provided to help map the reads spanning splice junctions (TopHat option '-G'). Reads multimapped were removed from the final results, together with those reads owning less than 96% identity with the reference. Finally, read counts were computed using bedtools (Quinlan and Hall, 2010).

Annotation

To expand the functional annotation of rice genes, the entire set of transcripts was annotated with the Argot web server (*Falda et al*., 2012 and 2016, *Lavezzo et al*., 2016), which assigned Gene Ontology terms to each input sequence (Gene Ontology Annotation database downloaded on 2013-12-29, PFAM release 27.0). This procedure increased the functional annotation of previously characterized genes and provided novel annotations for many genes with unknown function.

Differential analysis

The raw counts were used as input into a state-of-the-art differential expression analysis workflow (Anders et al. 2013), based on the edgeR bioconductor package (Robinson et al. 2010). A proper

design matrix was defined that compared the treated versus the corresponding control for both leaves and roots separately for the two varieties. Only reads with at least 1 count per million (cpm) in 3 samples were included in the following analysis. The primary steps of the Generalized Linear Model (GLM) based-pipeline were performed. The data were normalized; and given the design matrix, both “trended” (or, whenever not possible, “common”) and “tagwise” dispersion were computed before estimating the GLM for each feature and performing a likelihood ratio test. Finally, the differentially expressed genes (DEGs) were chosen, and a threshold equal to 0.05 was adopted for the p-values and corrected using the Benjamini and Hochberg approach (Benjamini and Hochberg, 1995). The processed data matrix was also stored for the following pathway enrichment analysis.

Pathway Enrichment Analysis

To perform pathway enrichment analysis, rice genes were assigned to clusters of orthologous groups from the KEGG database using blastKOALA (Kanehisa *et al*. 2016). Pathway information was downloaded from the KEGG database (Release 78.1, May 1, 2016) and parsed reconstructing gene networks. Following Sales *et al*. (2012), genes were directly connected when there was an intermediate interacting element (e.g., a chemical compound not measured), and complexes were expanded in groups of interacting nodes (cliques). This information on pathway topology was used as input in the Differential Expression Analysis of Pathways (DEAP) (Haynes *et al*., 2013). The DEAP algorithm was initially developed for microarray experiments; thus, we fed it with normalized cpm after log2-transformation (performed using the voom bioconductor package because of its ease of use (Law *et al*., 2014)). In this approach, the expression data are combined with the topology: the differential expression is computed for all possible paths within the graph. The type of relationship (catalytic or inhibitory) determines the summand sign. Each pathway is then assigned with the maximum absolute value of the differential expression among all its paths, which is then used to test the entire pathway using a random rotation approach (Langsrud, 2005). Finally, the enriched pathways are identified, in addition to their most differentially expressed paths.

RNA sequencing data validation

We tested the expression pattern of 20 DEGs from the RNA profiling experiment using an OpenArray-based nanofluidic RealTime-PCR technique (see the qPCR paragraph in M&M). A comparison of the data from the two approaches is shown in Table S3. Whether up- or down-regulated, the results for all the genes tested were similar using the two techniques.

Root morphology analysis

Root morphological traits were evaluated with a scanner-based image analysis system (WINRHIZO Pro; Regent Instruments, QC, Canada) that scanned, digitized and analysed root samples. The topological index (TI) was calculated as the ratio of the natural logarithm of the altitude (the most links between an external link and the base link) and the natural logarithm of the magnitude (terminal root sections between the meristem and the nearest branching point). Values of TI close to 0 indicate a dichotomous branching pattern, whereas those close to 1 reveal a herringbone pattern (Fitter and Stickland, 1991; Fitter, 1996).

Determination of the ionomic content in leaves and roots

For determination of the elements of interest, leaves (blade + sheath), stems and roots (washed carefully) were collected after 1, 3 and 7 days of treatment, dried at 40 °C for 48 h and stored in plastic boxes. Then, dry leaf and root samples were weighed and digested by a microwave digester system (MULTIWAVE-ECO, Anton Paar GmbH, Graz, Austria) in Teflon tubes filled with 10 mL of 65% HNO3 by applying a one-step temperature ramp (to 210 °C in 10 min, and maintained for 10 min). After 20 min of cooling time, the mineralized samples were transferred into polypropylene test tubes.
Samples were diluted 1:40 with MILLI-Q water, and the concentration of elements was measured by ICS-MS (Aurora-M90 ICP-MS, BRUKER DALTONICS S.r.l., Macerata, Italy). A 2 mg L-1 aliquot of an internal standard solution (72Ge, 89Y, 159Tb) was added both to samples and for the calibration curve to give a final concentration of 20 µg L-1.
Typical polyatomic analysis interferences were removed using CRI (Collision-Reaction-Interface) with an H_2 flow of 93 mL min-1 through a skimmer cone.

qPCR

qPCR was performed using the QuantStudio 12K Flex real-time PCR system and OpenArray technology (Thermo Fisher Scientific, CA, USA), following the manufacturer's instructions. TaqMan® OpenArray® Real-Time PCR Plate with Custom Gene Expression Assays (56 probes; Table S4) was designed and purchased from Thermo Fisher Scientific. The results were analysed using the ΔΔCT method (Livak and Schmittgen, 2001).

Statistical Analyses

Student's t-tests were applied to experiments with a sample number greater than 30. Wilcoxon-Mann-Whitney tests were applied for n < 30. Data from the root apparatus were analysed by ANOVA. For the analysis of RNA sequencing data, refer to the text above.

2.6 Supplementary materials

Table S1. Modified Hoagland solution. The final pH was 5.8

KNO_3	1.5 mM
$Ca(NO_3)_2$	1 mM
$MgSO_4$	0.5 mM
$NH_4H_2PO_4$	250 µM
H_3BO_3	46 µM
$MnCl_2$	9 µM
$ZnSO_4$	0.8 µM
$CuSO_4$	0.3 µM
$(NH_4)_6Mo_7O_{24}$	0.1 µM
FeNaEDTA	25 µM
Na_2O_3Si	30 µM

Table S2. Number of genes encoding channels, H^+ pumps and carriers gathered from the RNA sequencing data (see M&M par. "Differential Analysis").

	B		VN			B		VN	
	leaf	**root**	**leaf**	**root**		**leaf**	**root**	**leaf**	**root**
channels	**21**	**29**	**35**	**56**	**carriers**	**61**	**87**	**151**	**193**
OSCA-type channels	1	2	4	3	ClC family anion:proton antiporter	1	0	3	3
ammonium transporters	2	3	1	6	SWEET-type sugar efflux transporter	4	5	8	8
SLAC-type guard cell anion channels	3	1	3	1	HKT-type potassium/sodium cation transporter	0	0	2	1
GLR-type ligand-gated cation channels	0	3	1	9	HAK/KUP/KT-type potassium cation transporter	4	6	11	14
CNGC-type cyclic nucleotide-gated cation channels	1	1	1	3	auxin transporter	1	3	7	8
potassium cation channels	2	3	2	4	ProT-type proline transporter	1	0	3	2
aquaporin/small solute channels	3	4	9	14	CCC-type cation:chloride co-transporter	0	0	1	1
					monosaccharide transporters	2	8	10	20
active transport	**5**	**9**	**22**	**22**	NHX-type proton:sodium cation antiporter	0	0	2	1
V-type ATPase	0	0	9	8	CHX-type proton:monovalent cation antiporter	1	4	2	5
P-type ATPase	1	7	8	12	CAX-type proton:calcium cation exchanger	1	0	4	1
putative proton-translocating pyrophosphatase	2	0	3	0	CCX-type cation:calcium cation exchanger	1	0	1	2

Table S3. Validation of RNA sequencing data by OpenArray technique. The correlation coefficient is indicated. Numbers are log_2FC. FC: fold change. B, Baldo; VN, Vialone Nano; L, leaves; R, roots.

Gene_ID MSU	Gene_ID RAP	Gene_description	BL 72h	BL RNAseq		VNL 72h	VNL RNAseq
LOC_Os02g41580	Os02g0625300	phosphoenolpyruvate carboxylase kinase 2	-1.50	-1.67		-1.22	-1.07
LOC_Os07g40290	Os07g0592600	probable indole-3-acetic acid-amido synthetase GH3.8	2.80	2.00		3.82	1.86
LOC_Os09g31478	Os09g0491740	auxin efflux carrier	1.41	0.93		2.68	1.66
LOC_Os01g23580	Os01g0337500	OVP1	2.46	1.68		2.26	2.47
LOC_Os03g12820	Os03g0230300	OsSRO1c	1.93	1.49		2.65	2.43
LOC_Os03g26210	Os03g0379300	transcription factor bHLH47	-1.58	-2.61		-0.37	-1.45
LOC_Os04g09900	Os04g0178300	Syn-copalyl diphosphate synthase CPS4	2.59	2.17		3.24	2.02
LOC_Os02g09390	Os02g0186800	cytochrome P450	3.03	2.46		2.52	1.90
LOC_Os07g46990	Os07g0665200	superoxide dismutase [Cu-Zn] 2 (SODCC2)	1.61	1.05		1.01	1.00
LOC_Os06g21820	Os06g0323100	indole-3-acetate O-methyltransferase 1-like	1.86	1.62		3.03	2.83
LOC_Os01g62900	Os01g0848200	delta-1-pyrroline-5-carboxylate synthase-like (OsP5CS2)	1.26	1.26		2.38	0.90
LOC_Os09g26620	Os09g0437500	auxin-repressed protein	1.71	1.30		2.92	1.36
LOC_Os05g10670	Os05g0195200	zinc finger CCCH domain-containing protein 35	2.97	2.80		2.47	2.06
LOC_Os11g31540	Os11g0514500	BRASSINOSTEROID INSENSITIVE 1-associated receptor kinase 1	3.46	2.28		2.03	3.28
LOC_Os01g72360	Os01g0952900	expressed protein	-1.86	-2.67		-1.18	-1.65
LOC_Os01g50910	Os01g0705200	late embryogenesis abundant protein, group 3 (LEA3)	7.49	6.10		6.52	4.93
LOC_Os01g64310	Os01g0862800	NAC domain-containing protein 90	-2.18	-1.91		-2.39	-1.97
LOC_Os10g38470	Os10g0528100	glutathione S-transferase (GSTU6)	2.15	1.64		2.50	2.06
LOC_Os03g12510	Os03g0226200	non-symbiotic hemoglobin 2	-3.00	-2.31		-4.00	-4.54
LOC_Os11g26760	Os11g0454000	dehydrin Rab16C	2.73	3.21		3.24	4.42
		Correlation	**0.97909**			**0.93193**	
Gene_ID MSU	**Gene_ID RAP**	**Gene_description**	**BR 72h**	**BR RNAseq**		**VNR 72h**	**VNR RNAseq**
LOC_Os02g41580	Os02g0625300	phosphoenolpyruvate carboxylase kinase 2	-1.18	-0.95		-1.04	-1.78
LOC_Os09g31478	Os09g0491740	auxin efflux carrier	3.14	1.43		3.13	2.21
LOC_Os03g26210	Os03g0379300	transcription factor bHLH47	-2.48	-2.37		-2.30	-3.40
LOC_Os04g09900	Os04g0178300	Syn-copalyl diphosphate synthase CPS4	4.77	2.51		4.03	2.34
LOC_Os02g09390	Os02g0186800	cytochrome P450	2.62	2.18		2.76	1.96
LOC_Os07g13810	Os07g0241800	DIMBOA UDP-glucosyltransferase BX8	1.69	1.22		2.45	0.79
LOC_Os03g50490	Os03g0712800	glutamine synthetase cytosolic isozyme 1-3	3.33	1.29		2.80	2.28
LOC_Os04g36740	Os04g0445000	Potassium channel KOR2	-1.25	-1.21		-1.06	-1.53
LOC_Os02g02400	Os02g0115700	catalase isozyme A	2.37	1.96		3.39	2.08
LOC_Os01g45990	Os01g0648000	OsAKT1.1	-1.31	-1.76		-1.68	-2.19
LOC_Os01g62900	Os01g0848200	delta-1-pyrroline-5-carboxylate synthase-like (OsP5CS2)	2.93	1.96		3.07	1.88
LOC_Os09g26620	Os09g0437500	auxin-repressed protein	0.98	1.15		1.68	0.78
LOC_Os01g55200	Os01g0756700	OsKAT1	2.00	1.13		2.92	1.42
LOC_Os12g26290	Os12g0448900	alpha-DOX2	3.40	0.94		3.75	2.38
LOC_Os05g10670	Os05g0195200	zinc finger CCCH domain-containing protein 35	0.58	0.83		1.69	0.67
LOC_Os11g31540	Os11g0514500	BRASSINOSTEROID INSENSITIVE 1-associated receptor kinase 1	2.82	2.22		4.96	4.60
LOC_Os01g72360	Os01g0952900	expressed protein	-3.83	-3.61		-4.19	-4.81
LOC_Os01g64310	Os01g0862800	NAC domain-containing protein 90	-3.87	-2.60		-2.32	-1.86
LOC_Os10g38470	Os10g0528100	glutathione S-transferase (GSTU6)	2.14	1.40		4.48	1.64
LOC_Os03g12510	Os03g0226200	non-symbiotic hemoglobin 2	-1.55	-2.17		-4.45	-4.10
		Correlation	**0.953**			**0.97505**	
BL 72h	Baldo leaves qPCR 72 h						
VNL 72h	Vialone Nano leaves qPCR 72 h						
BL RNAseq	Baldo leaves RNAseq 72 h						
VNL RNAseq	Vialone Nano leaves RNAseq 72 h						
BR 72h	Baldo roots qPCR 72 h						
VNR 72h	Vialone Nano roots qPCR 72 h						
BR RNAseq	Baldo roots RNAseq 72 h						
VNR RNAseq	Vialone Nano roots RNAseq 72 h						

Table S4. List of Gene Expression Assays used in this work. Two housekeeping genes were used, elongation factor 1-alpha (REFA1) and ubiquitin-40S ribosomal protein S27a-1 (UBQ).

Assay_ID	Gene_ID MSU	Gene_ID RAP	Gene_description
AIPAEXL	LOC_Os02g41580	Os02g0625300	phosphoenolpyruvate carboxylase kinase 2
AIQJC3T	LOC_Os04g13140	Os04g0208200	senescence-specific cysteine protease SAG39
AIRSA91	LOC_Os07g40290	Os07g0592600	probable indole-3-acetic acid-amido synthetase GH3.8
AIT97MH	LOC_Os09g31478	Os09g0491740	auxin efflux carrier
AJ0IXD3	LOC_Os07g05570	Os07g0150100	OsOSCA3.1/ERD4
AJ0IXEA	LOC_Os03g49990	Os03g0707600	DELLA protein SLR1
AJ1RVKF	LOC_Os01g10110	Os01g0197700	Cytokinin dehydrogenase 2 (OsCKX2)
AJ1RVKK	LOC_Os05g27730	Os05g0343400	OsWRKY53
AJ39RWU	LOC_Os07g01810	Os07g0108800	OsTPKb
AJ39RWY	LOC_Os01g70490	Os01g0930400	OsHAK5
AJ6RN9A	LOC_Os01g10290	Os01g0200000	autophagy-related protein 3 (ATG3)
AJ70MFF	LOC_Os04g51830	Os04g0607600	OsHKT1.4
AJ70MFN	LOC_Os02g52230	Os02g0759700	transport inhibitor response 1-like protein
AJ89KLO	LOC_Os01g23580	Os01g0337500	OVP1
AJ89KLV	LOC_Os03g12820	Os03g0230300	OsSRO1c
AJAAZRG	LOC_Os02g15640	Os02g0255500	abscisic acid receptor PYL8
AJAAZRK	LOC_Os07g47100	Os07g0666900	OsNHX1
AJCSV3X	LOC_Os03g26210	Os03g0379300	transcription factor bHLH47
AJD1UAB	LOC_Os01g07120	Os01g0165000	OsDREB2A
AJFASGE	LOC_Os04g09900	Os04g0178300	Syn-copalyl diphosphate synthase CPS4
AJI1MY0	LOC_Os01g20160	Os01g0307500	OsHKT1.5
AJKAK47	LOC_Os05g32720	Os05g0393800	OsOSCA1.3
AJLJJBG	LOC_Os02g09390	Os02g0186800	cytochrome P450
AJN1FN3	LOC_Os07g13810	Os07g0241800	DIMBOA UDP-glucosyltransferase BX8
AJQJB0C	LOC_Os03g50490	Os03g0712800	glutamine synthetase cytosolic isozyme 1-3
AJQJB0J	LOC_Os03g54100	Os03g0752300	OsTPKa
AJS08CU	LOC_Os07g46990	Os07g0665200	superoxide dismutase [Cu-Zn] 2 (SODCC2)
AJS08CV	LOC_Os03g17690	Os03g0285700	L-ascorbate peroxidase 1, cytosolic (APX1)
AJX001S	LOC_Os04g36740	Os04g0445000	Potassium channel KOR2
AJY9Y72	LOC_Os02g02400	Os02g0115700	catalase isozyme A
Os03472546_m1	LOC_Os01g53294	Os01g0734200	respiratory burst oxidase homolog protein A (rbohA)
Os03495668_g1	LOC_Os06g21820	Os06g0323100	indole-3-acetate O-methyltransferase 1-like
Os03500929_mH	LOC_Os09g16510	Os09g0334500	probable WRKY transcription factor 30
Os03503633_m1	LOC_Os01g45990	Os01g0648000	OsAKT1.1
Os03504594_m1	LOC_Os01g62900	Os01g0848200	delta-1-pyrroline-5-carboxylate synthase-like (OsP5CS2)
Os03521969_m1	LOC_Os09g26620	Os09g0437500	auxin-repressed protein
Os03523224_m1	LOC_Os10g39130	Os10g0536100	OsMADS56
Os03524882_s1	LOC_Os12g24800	Os12g0435200	9-cis-epoxycarotenoid dioxygenase 2 (NCED2)
Os03529509_g1	LOC_Os01g55200	Os01g0756700	OsKAT1
Os03551356_m1	LOC_Os12g26290	Os12g0448900	alpha-DOX2
Os03566227_s1	LOC_Os05g10670	Os05g0195200	zinc finger CCCH domain-containing protein 35
Os03577339_g1	LOC_Os11g31540	Os11g0514500	BRASSINOSTEROID INSENSITIVE 1-associated receptor kinase 1
Os03581771_s1	LOC_Os01g72360	Os01g0952900	expressed protein
Os03584988_m1	LOC_Os01g35050	Os01g0534900	OsOSCA1.1
Os03586154_g1	LOC_Os02g04630	Os02g0138900	putative vacuolar cation/proton exchanger 4 (OsCAX4)
Os03597219_g1	LOC_Os01g50910	Os01g0705200	late embryogenesis abundant protein, group 3 (LEA3)
Os03615227_m1	LOC_Os01g64310	Os01g0862800	NAC domain-containing protein 90
Os03615512_g1	LOC_Os01g72210	Os01g0950900	OsOSCA2.5
Os03619633_g1	LOC_Os12g44360	Os12g0641100	OsSOS1
Os03639010_gH	LOC_Os01g55940	Os01g0764800	probable indole-3-acetic acid-amido synthetase OsGH3.2
Os03639305_gH	LOC_Os10g38470	Os10g0528100	glutathione S-transferase (GSTU6)
Os03640576_s1	LOC_Os03g12510	Os03g0226200	non-symbiotic hemoglobin 2
Os03643538_s1	LOC_Os11g26760	Os11g0454000	dehydrin Rab16C
Os03640561_s1	LOC_Os03g08010	Os03g0177400	elongation factor 1-alpha (REFA1)
AIS09F9	LOC_Os01g22490	Os01g0328400	ubiquitin-40S ribosomal protein S27a-1 (UBQ)

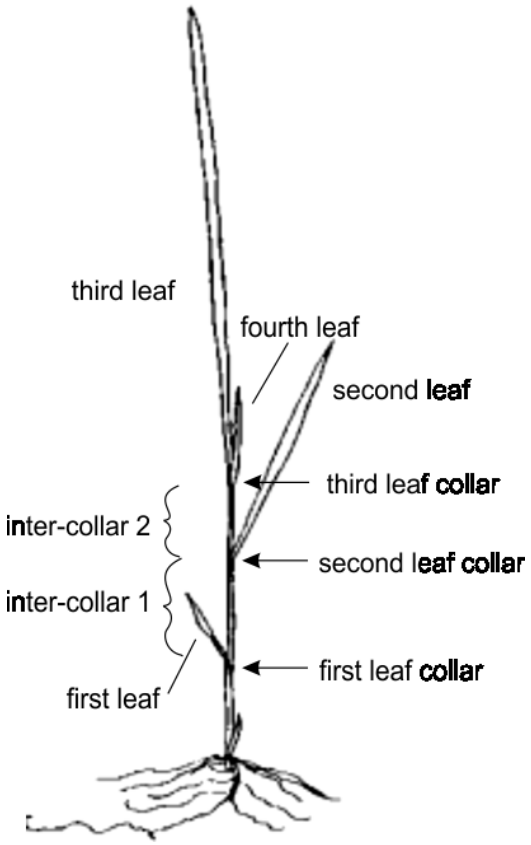

Figure S1. Representation of a rice seedling.

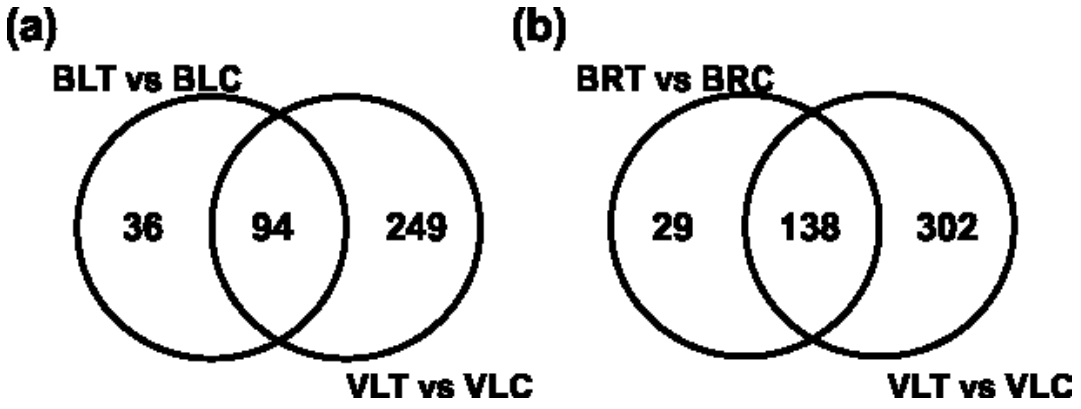

Figure S2. Venn diagram of DEGs annotated as responsive to salt, oxidative, water stresses (see text) in leaves (a) or roots (b). B, Baldo; V, Vialone Nano; L, leaves: R, roots; T, salt treated; C, control plants.

Baldo

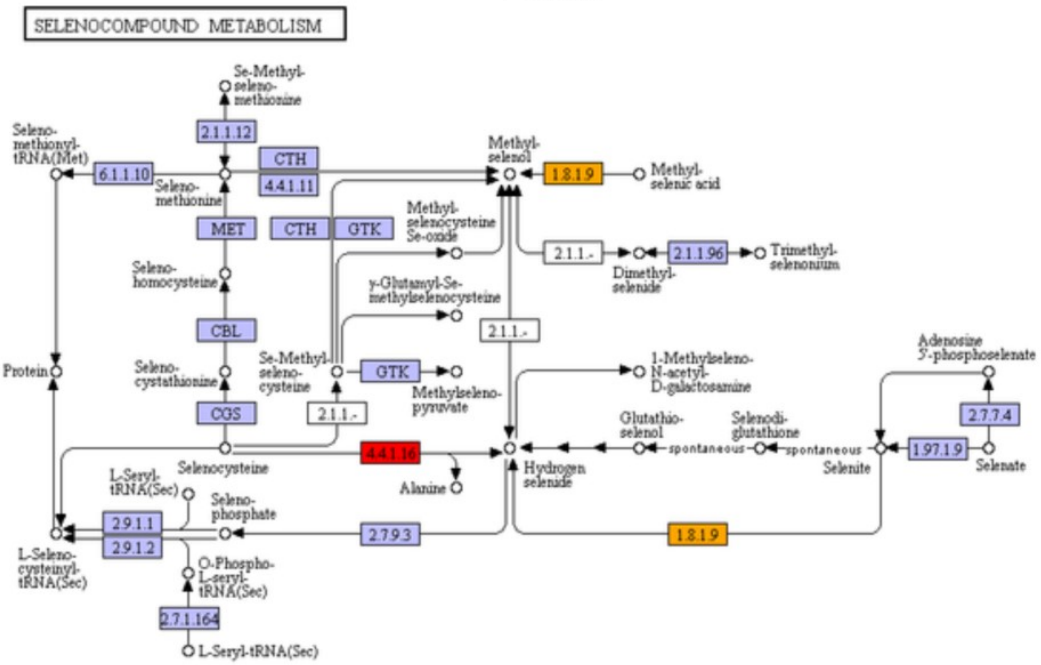

Vialone Nano

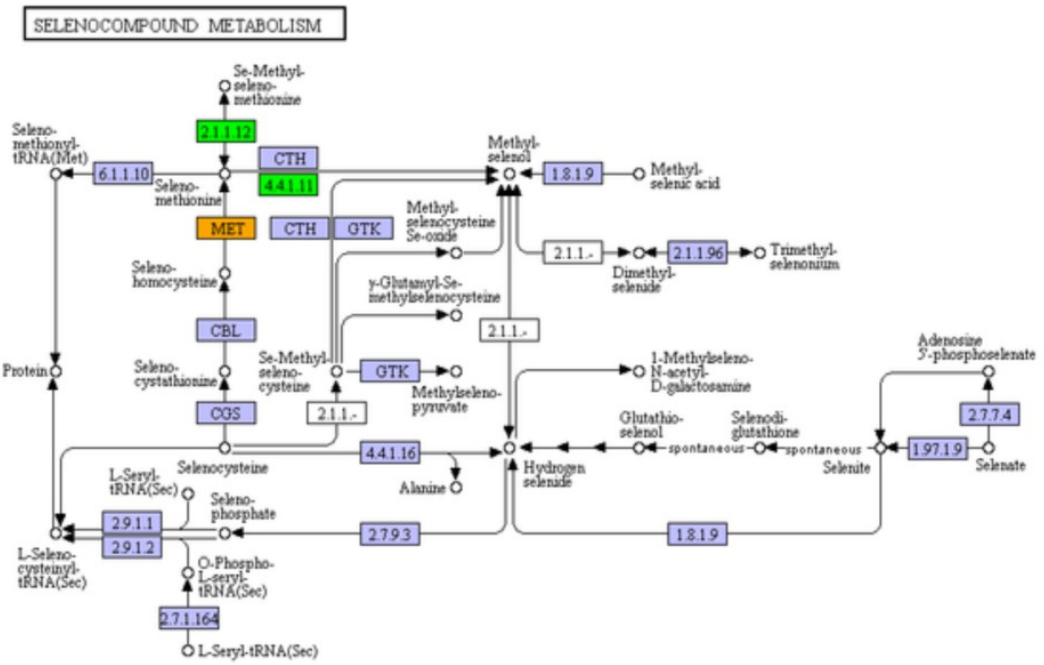

Figure S3. Selenocompound metabolism. (a) VN leaves. (b) B leaves. Colour code: green, all DEGs are up; red, all DEGs are down, Orange, DEGs are either up or down.

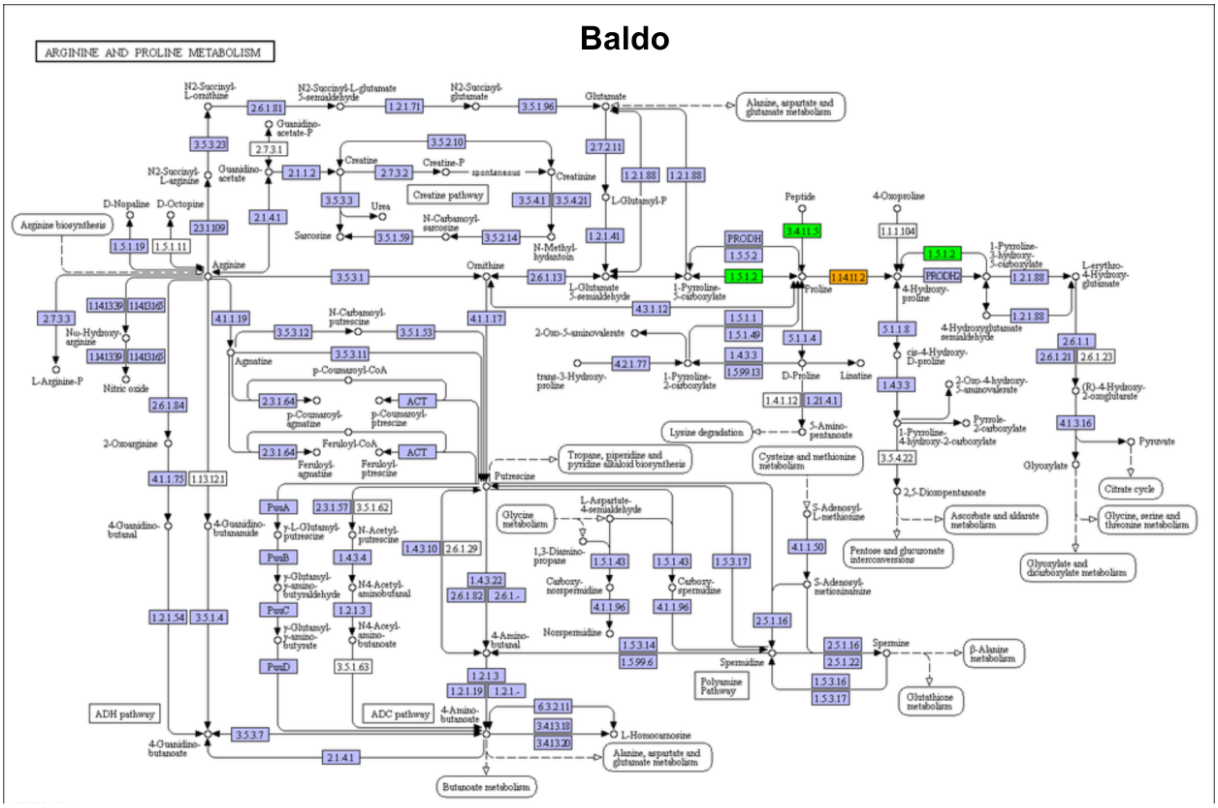

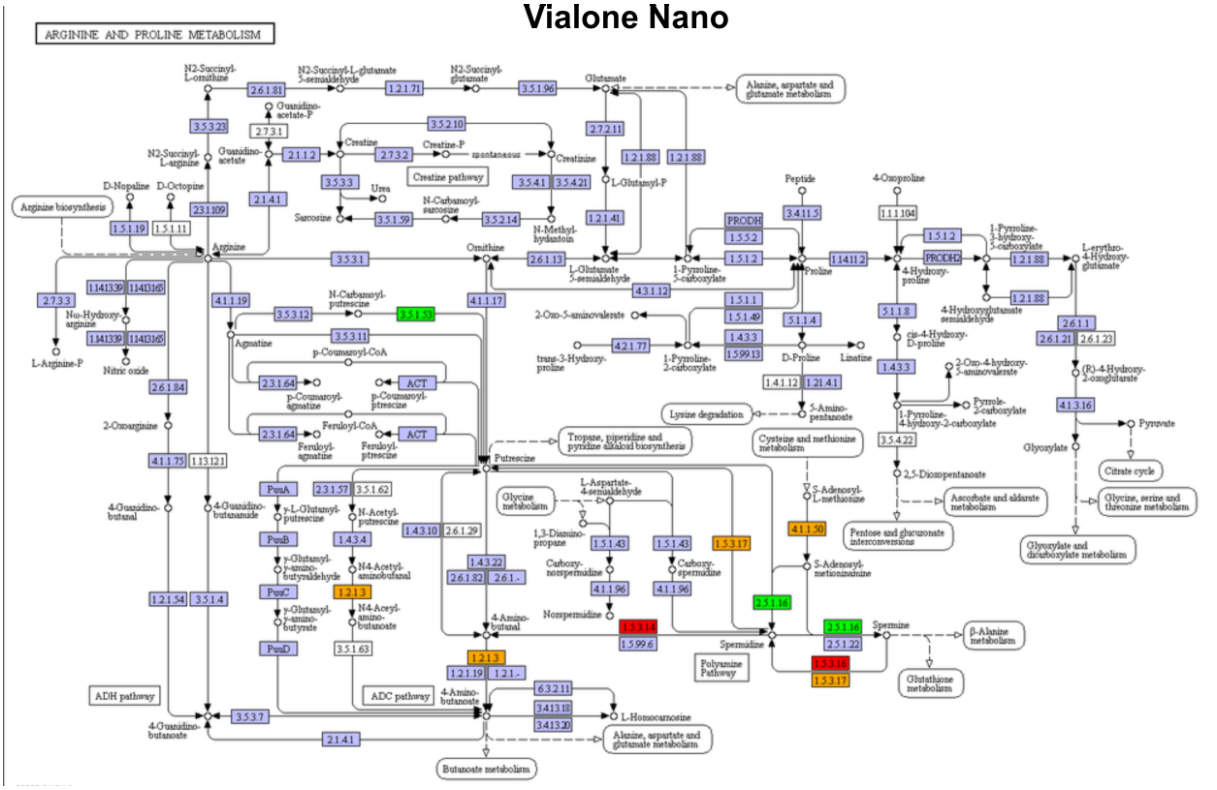

Figure S4. Arginine and proline metabolism. (a) VN leaves. (b) B leaves. Colour code: green, all DEGs are up; red, all DEGs are down, Orange, DEGs are either up or down.

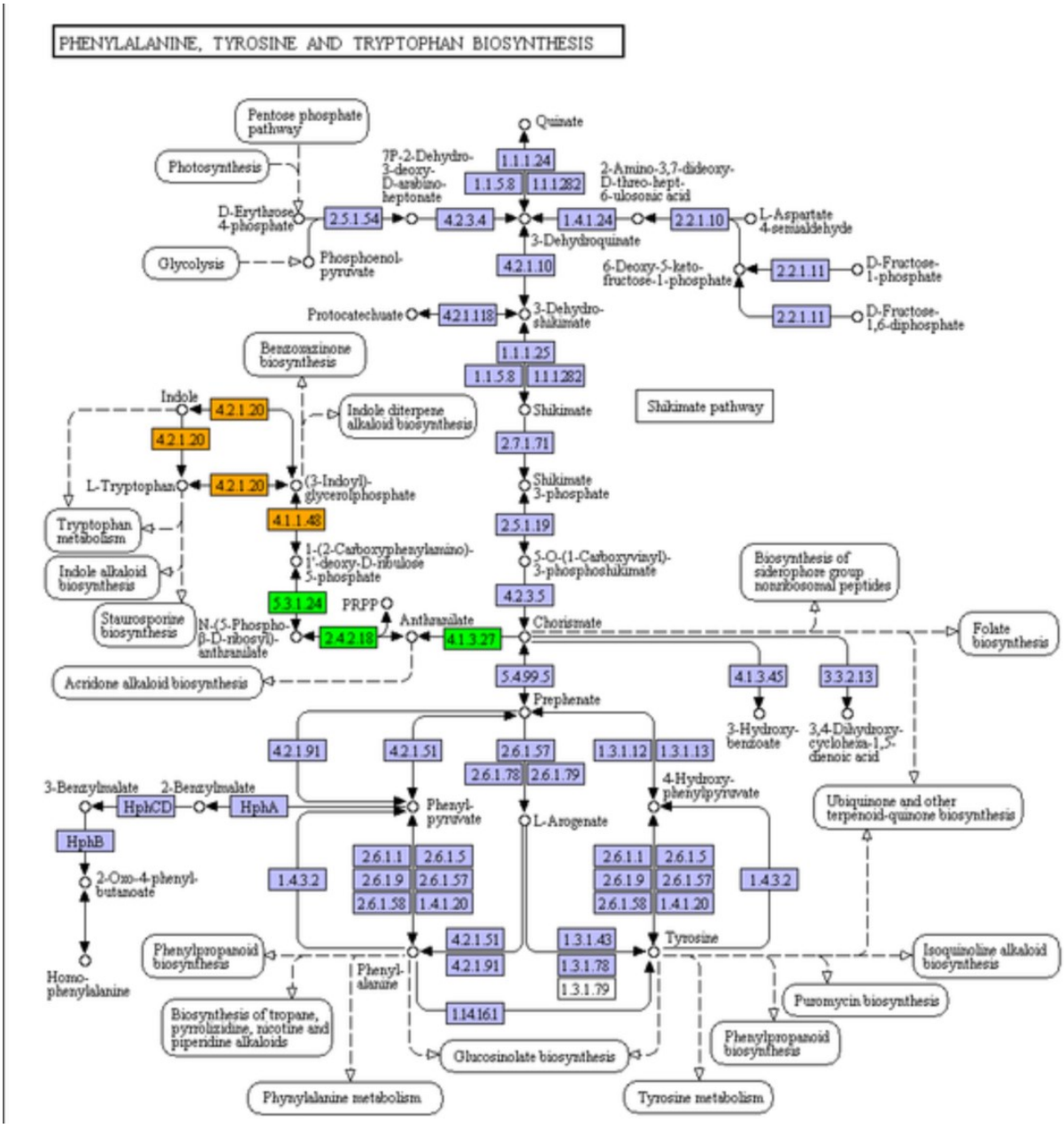

Figure S5. Phenylalanine, Tyrosine and Tryptophan biosynthesis in B leaves. Colour code: green, all DEGs are up; red, all DEGs are down, Orange, DEGs are either up or down.

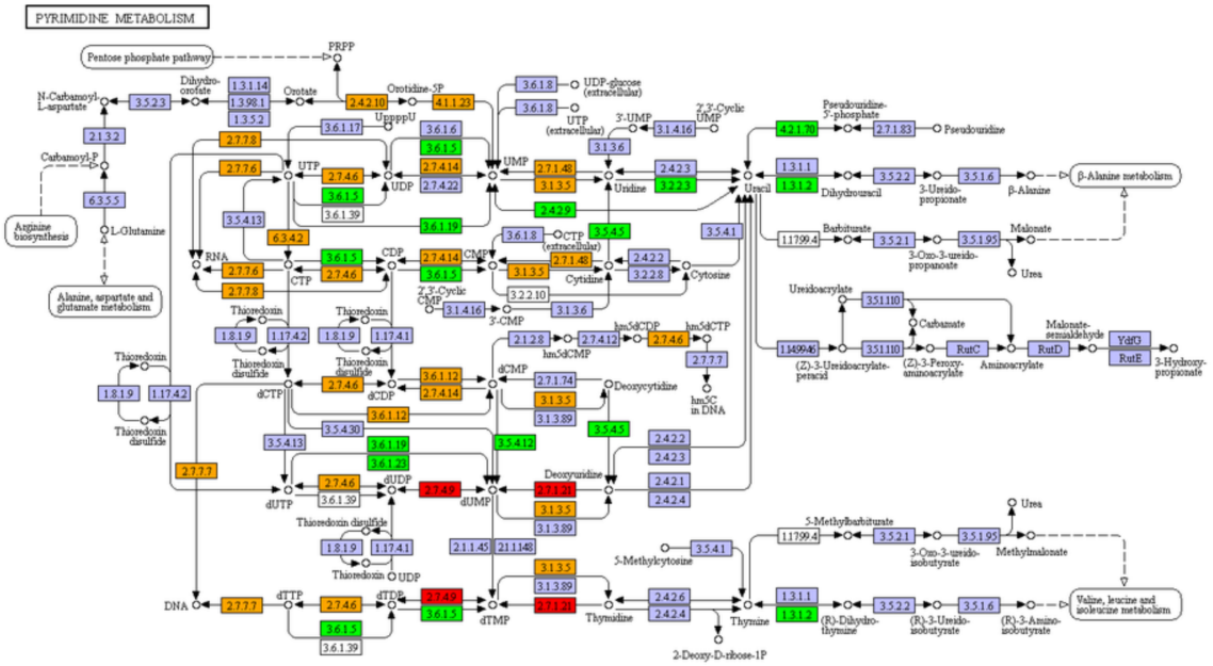

Figure S6. Pyrimidine metabolism in B leaves. Colour code: green, all DEGs are up; red, all DEGs are down, Orange, DEGs are either up or down.

Chapter 3:

Effective antioxidant defence systems and expression of K^+ transporter/channel genes explain differing salt sensitivity of two Italian rice varieties cultured cells

3.1 Introduction

Soil salinity is a major constraint on crop production worldwide, particularly in agricultural lands close to the sea (Zhu *et al.*, 2001; Tester and Davenport, 2003). Salinization affects at least 33% of arable lands, and more areas are expected to deteriorate in coming years because of changes in global climate (FAO, http://www.fao.org/3/a-i4373e.pdf).

Plants differ greatly in their tolerance to salinity, and they can be roughly divided into two main groups: salt-sensitive (glycophytes) and salt-tolerant (halophytes). Unfortunately, most crop species belong to the former group and rice is the most salt-sensitive among cereals (Flowers and Yeo, 1995).

Soil salinity imposes two primary stresses on plants, osmotic and ionic. Osmotic stress establishes early after the onset of the stress, causes water loss and reduced turgor that in turn leads to a decrease in cell expansion and plant growth. Ionic stress, instead, arises later after exposure to saline soil when Na^+ concentration, in particular, reaches toxic levels inside the cells affecting cellular metabolism and photosynthesis (Munns and Tester, 2008). Moreover, high salinity also induces the formation of ROS within plant cells, and their over accumulation results in oxidative damage of membrane lipids, proteins and nucleic acids (Dionisio-Sese and Tobita, 1998; Hernández *et al*., 2000; Sgherri *et al*., 2007, Gill and Tuteja, 2010; Gupta and Huang, 2014).

To cope with this adverse condition, plants have evolved a multi-faceted range of physiological and metabolic responses activating many stress-responsive genes and synthesizing diverse functional proteins and metabolites through a complex signal transduction network (Hirayama and Shinozaki, 2010).

Whereas all of these mechanisms are indeed important, their relative contribution may differ, depending on plant species, stress severity and duration, and experimental conditions.

To cope with the osmotic stress plants try to limit water loss by regulating the permeability of the membranes and the production of osmoprotectans (Boursiac *et al*., 2005; Munns and Tester, 2008; Chen *et al*., 2007).

Successful strategies for ionic stress tolerance likely consist in the maintenance of a high $[K^+]/[Na^+]$ ratio in the cytosol (Hasegawa *et al.*, 2000) often achieved by reducing Na^+ concentration and/or increasing K^+ concentration into the cytosol (Munns and Tester, 2008; Horie *et al*., 2012; Shabala and Pottosin, 2014).

There are three main mechanisms that allow plants to reduce Na^+ concentration in the cytosol and in the shoots: the extrusion from the cytoplasm, the compartmentalization inside the vacuole and the reabsorption in the xylem (Blumwald, 2000; Munns and Tester, 2008). Na^+/H^+ antiporters on the plasma membrane (SOS1, part of the SOS pathway) and the tonoplast (NHXs) are responsible for the first and the second mechanism respectively (Munns and Tester, 2008; Barragán *et al*. 2012; Amin *et al.,* 2016; Fukuda *et al*. 2004 and 2011). The third mechanism is accomplished by HKT-type $K^+(Na^+)$ transporters of xylem parenchyma cells that unload Na^+ from the xylem sap, preventing its accumulation in the shoot (HKT1.5) and in young leaves (HKT1.4) (Hauser and Horie, 2010; Cotsaftis et al., 2012; Suzuki et al., 2016).

Potassium levels in the cytosol can be increased by releasing it from intracellular storage or by the uptake from the apoplast. In stress conditions, the overexpression of tonoplast members of the OsTPK outward K^+ channel family (Maathuis, 2011; Ahmad *et al.*, 2016; Isayenkov *et al.*, 2011), of the plasma membrane high affinity K^+ transporter OsHAK5 (Qi et al., 2008; Horie *et al.,* 2011), and of the shaker-like inward-rectifier K^+ channel OsKAT1, all involved in the increase of $[K^+]$cyt, confer salt tolerance in rice (Obata *et al.*, 2007).

To prevent the oxidative damage, plants have evolved an efficient enzymatic and non-enzymatic antioxidative system. ROS-scavenging enzymes of plants include superoxide dismutase (SOD), ascorbate peroxidase (APX), catalase (CAT), monodehydroascorbate reductase (MDHAR), dehydroascorbate reductase (DHAR), glutathione reductase (GR), glutathione S-transferase (GST), and so on. Non-enzymatic antioxidants include AsA, GSH, carotenoids, tocopherols, and flavonoids that are crucial for ROS homeostasis in plant (Gill and Tuteja, 2010). Plants with high levels of constitutive antioxidants or that are able to induce such antioxidants have been reported to show greater resistance to oxidative damage (Parida and Das, 2005).

On the other hand, salinity can challenge sensitive plants to such an extent that cell death is induced. Cell death events are often caused by the inability of the plant to keep low ROS levels. In fact, elevated concentrations of ROS, in combination with other molecules induced by salt stress such as NO (Valderrama *et al*., 2007), pose a significant threat that eventually can trigger programmed cell death (PCD; Delledonne *et al*., 2001; Gechev and Hille, 2005; de Pinto *et al*. 2006). In contrast to necrosis, that is caused from even higher levels of ROS and NO (de Pinto *et al*. 2006) and that is not actively controlled, PCD is an active, genetically controlled process in which cells are selectively eliminated. This cell death pathway is associated with the occurrence of several markers among which genomic DNA fragmentation ('DNA laddering'; Hoeberichts and Woltering, 2003).

To activate a salt stress response, plants must have evolved the capability to perceive the osmotic and ionic components of this stress and to induce signalling transduction pathways to build an appropriate cellular programme. The molecular processes controlling early salt stress perception and signalling are not yet fully understood. Plant hyper-osmotic sensors are likely to be coupled with Ca^{2+} channels given that plants exhibit a rapid rise in cytosolic Ca^{2+} levels within seconds of exposure to NaCl or mannitol (Knight *et al*., 1997). Other second messengers can also be induced by salt stress, for example ROS (Jaspers and Kangasjarvi, 2010). In fact, recent studies have shown that ROS, well known as toxic cellular molecules, may play key roles in plants as signal transduction molecules that regulates plant development, stress adaptation, and programmed cell death (PCD) (Apel and Hirt, 2004; Mittler *et al*., 2004; Torres and Dangl, 2005; Gechev and Hill, 2005; de Pinto *et al*., 2012). Salt-induced ROS are predominantly represented by H_2O_2 (Yang *et al*., 2007; Pang and Wang, 2008). Extracellular ROS production depends on the activity of NADPH oxidases (NOXs) of the RBOH family (Ma *et al*., 2012). In rice (*Oryza sativa*), NADPH oxidase–dependent H_2O_2 production emerges within few minutes of salt stress (Hong et al., 2009). Thus, H_2O_2 production may initiate an early signal cascade that trigger salt response mechanisms. It is currently unknown how the H_2O_2 signal is perceived. However, a signal transduction cascade has been proposed in which a mitogen-activated protein kinase (MAPK) cascade and downstream transcription factors (TFs) represent key regulatory components of ROS signalling (Skopelitis *et al*., 2006; Pang and Wang, 2008). Recently, Schmidt *et al*. (2013) found out that the TF SERF1 regulates the expression of a salt-responsive MAPK cascade and of salt tolerance–mediating TF genes, thus behaving as a positive regulator of salt tolerance.

Rice feeds the majority of world's population and its cultivation deeply impacts the economy of many countries. Although *Oryza sativa* is a salt sensitive species, salt tolerant varieties may be found (Gregorio *et al*., 2002; Ismail, 2007; Mohammadi-Nejad *et al*., 2010). So far, few salt tolerant traits have been identified and not all of them are present in each variety simultaneously. Thus, an increase in the understanding of new salinity tolerance mechanisms is required to eventually combine all of them in a new variety with a high level of salt tolerance (Yeo *et al*., 1990).

The aim of this work has been the analysis of two Italian rice varieties, Baldo (B) and Vialone Nano (VN), showing contrasting salt-sensitivity, to unveil different response mechanisms to salt stress. This study has been performed on suspension cell cultures obtained from seeds of the two

varieties that allow performing detail experiments at cellular and molecular level on a homogeneous cellular population. In particular, early events leading to H_2O_2 production induced by salt stress have been analyzed in detail. This approach allowed the identification of different mechanisms explaining the contrasting salt sensitivity between the two rice varieties at cellular level. Notably, the role of H_2O_2 as signalling molecule involved in inducing either PCD or an adaptive response in a level-dependent manner has emerged in the two varieties.

3.2 Results

Cultured cells preserve differences in response to salt stress of their source plants

In a previous work, two Italian rice varieties, B and VN, differing in salt sensitivity, were compared to unveil mechanisms conferring salt tolerance. Based on physiological and molecular analyses, plants of the B variety proved to be the most tolerant by showing a preferential restriction of Na^+ in roots and older leaves, maintenance of a high $[K^+]/[Na^+]$ ratio and a faster growth arrest that allow the setting up of a tolerance response (MS in preparation).

To answer the question whether differences in salt sensitivity between the two varieties were manifested also at cellular level, suspension cell cultures from their respective seeds were established and characterized. The two cell lines were exposed to several salt concentrations (50, 100, 150 mM NaCl) and growth parameters along with measurements of cell death induced by treatment were determined.

By comparing the growth curves of the two cell lines, differences in salt sensitivity were observed (Fig.1 A and B). By measuring the percentage of cell death at different times during sub-culture cycles, cultured cells from v. VN reached 50% after 2 and 4 days of salt treatment at 150 and 100 mM NaCl, respectively (Fig.1 C). Cultured cells from v. B, instead, showed an initial slow increase of the percentage of cell death, reaching 20% and 25% at 2 days after exposure at 100 and 150 mM NaCl, respectively (Fig.1 D). These cell death levels remained almost stable up to 4 days after treatments, when they increased again by reaching 30% at 10 days in the presence of the 100 mM NaCl, and 50% in the presence of the highest concentration of salt (Fig.1 C and D). No significant differences were observed in presence of 50 mM NaCl.

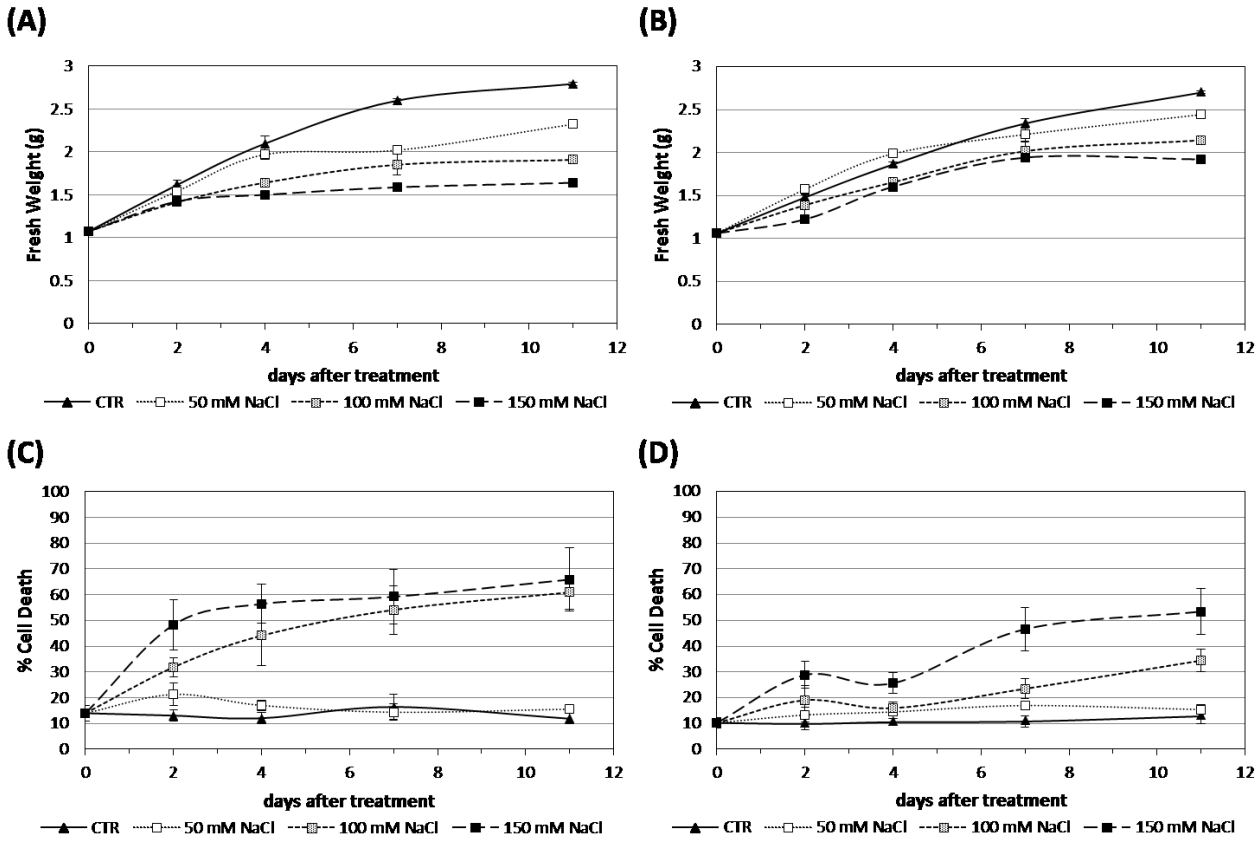

Figure 1. Cell growth and survival curves of B and VN suspension cultured cells in presence and absence of NaCl. Three-day-old VN (A and C) and B (B and D) cells were treated with different concentrations of NaCl. Closed triangles – straight line, Control; open squares – dotted line, 50 mM NaCl; grey squares – small-dashed line, 100 mM NaCl; closed squares – dashed line, 150 mM NaCl. (A) and (B), Fresh weight (g) of cells at different times after treatment. (C) and (D), Cell viability (Evans blue staining). Values represent the mean ± confidence interval ($p<0.05$) of three independent experiments performed in triplicate.

To define the nature of the process of cell death induced by salt stress, DNA laddering, a well-known hallmark of programmed cell death (PCD) in plants was analysed. DNA oligonucleosomal fragmentation was detected in VN cells after 7 days of treatment in presence of 100 mM NaCl, when the percentage of cell death reached almost 60%. By contrast, in B cells genomic DNA resulted unbroken, being the cell death level at that time point at the 20% (Fig. 2) .

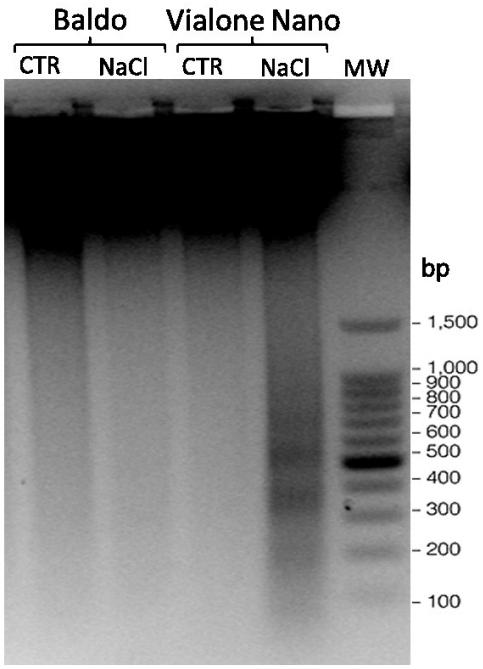

Figure 2. DNA laddering. Cells treated with 100 mM NaCl or with H_2O (CTR) for 7 days were harvested and their DNA extracted. 20 µg of DNA were subjected to electrophoresis to assess oligonucleosomal DNA fragmentation (laddering).

These results confirm a different salt sensitivity between the two varieties that was detectable also at cellular level. In fact, a process of PCD was induced in the sensitive variety after few days of treatment (100 mM NaCl), whereas the more tolerant cell line was able to cope with the same stress, keeping cell death to low levels, a condition probably necessary for activating salt tolerance mechanisms.

Signal Molecules in Salt Response: Hydrogen Peroxide and Nitric Oxide

Salt stress is known to induce ROS/RNS (reactive oxygen/nitrogen species) production (Gill and Tuteja, 2010; Gould *et al*., 2003). Depending on the levels, ROS can be involved in signalling pathways leading to different cell fate, i.e cell survival (low doses of hydrogen peroxide (H_2O_2); Baxter *et al*., 2013) or cell death (high levels of H_2O_2 probably combined with high levels of nitric oxide (NO); Delledonne *et al*., 2001; de Pinto *et al*., 2002; Gechev and Hille, 2005).
For these reasons, the production of H_2O_2 and NO, was investigated in the two suspension cell cultures in the presence of salt stress.
First, H_2O_2 release from the cells into culture medium was evaluated. A basic level of H_2O_2 around 20 nmoles g^{-1} DW was measured in the medium of untreated cells, whereas in salt treated cells, two distinct peaks of H_2O_2 production were induced, with a first burst at 5 min (for 100 mM and 150 mM NaCl; $p<0.05$, *t* test between control and treated cells) followed by a sustained second peak at 24 h (reaching around 35, 40 and 53 nmoles g^{-1} DW at 50, 100 and 150 mM NaCl, respectively; $p<0.01$, *t* test). Notably, H_2O_2 production occurred in a dose-dependent manner (Fig.3 A). By contrast, no H_2O_2 was detectable in the medium B cells, in spite of the concentration of salt applied to the cells (50, 100 or 150 mM NaCl; Fig.3 B).

Then, by using the fluorescent probe, dihydrorhodamine 123 (DHR123), the intracellular level of H_2O_2 was investigated under same experimental conditions. The VN cell line showed a broad peak of H_2O_2 production inside the cells after 1 h treatment ($p<0.01$, *t* test) followed by a slow but progressive increasing of H_2O_2 levels, as measured at 24, 48 and 72 h. In the more tolerant cell line, instead, salt treatment induced a very narrow early peak of H_2O_2 production inside the cells at 5 min ($p<0.01$, *t* test) in presence of the three NaCl concentrations and a later slow increase, that reaches its maximum at 48 h with 150 mM NaCl ($p<0.01$, *t* test) and at 72 h with 50 and 100 mM NaCl ($p<0.01$, *t* test). Also for the intracellular H_2O_2, the production occurred in a dose-dependent manner (Fig.3 C and D).

Successively, the intracellular NO production was recorded using the fluorescent probe 4-Amino-5-Methylamino-2',7'-Difluorofluorescein Diacetate (DAF-FM DA). In VN cells an initial increase in NO production (Fig.4 A) was detected both at 100 and 150 mM NaCl ($p<0.05$, *t* test) and this higher level was maintained almost steady until 72 h. In B cells, instead, only an early narrow peak (1 h; $p<0.01$, *t* test) of NO production was detected in presence of all three NaCl concentrations, and this was followed by a low increase of NO production only at the highest salt concentration (Fig.4 B).

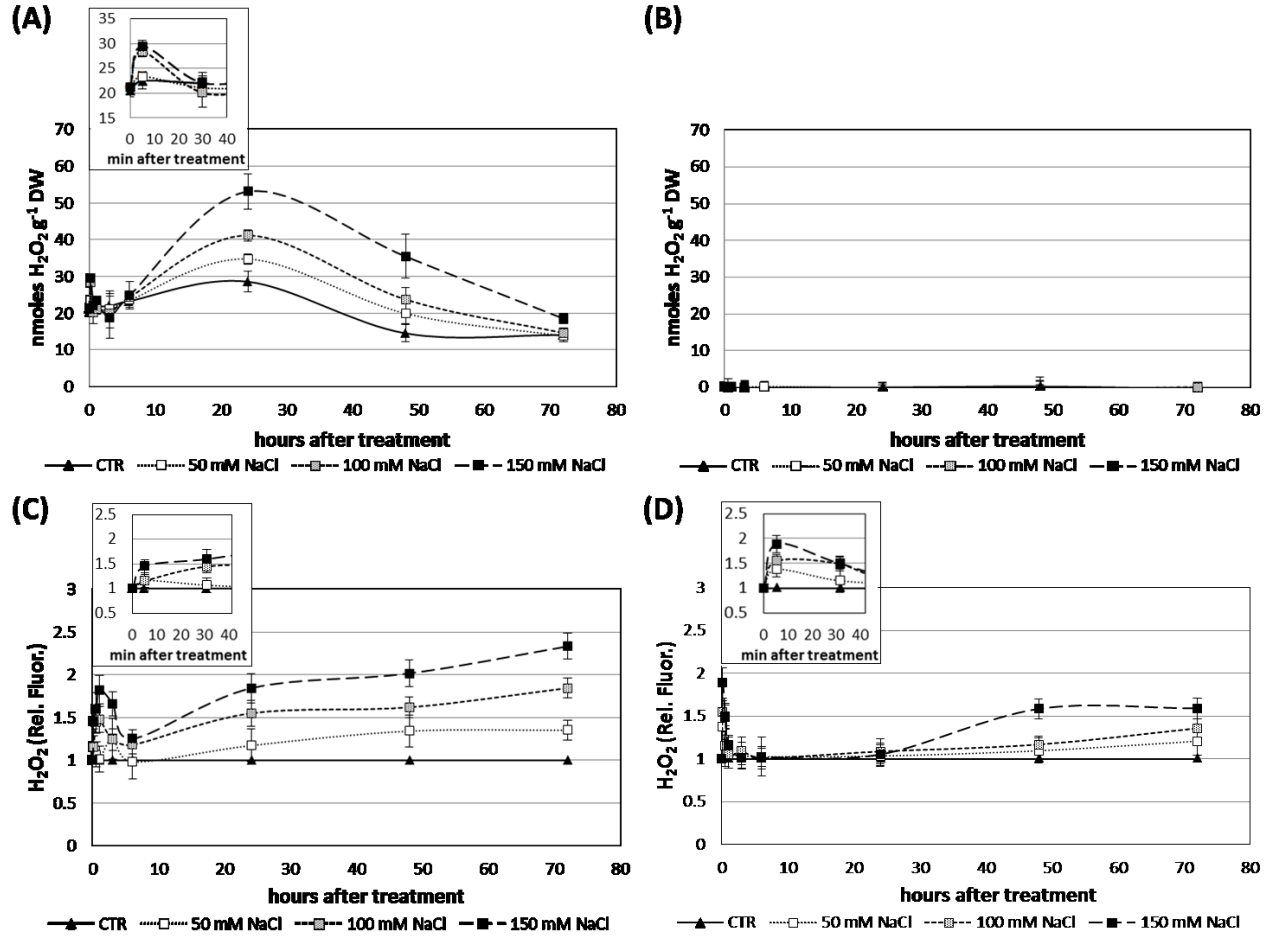

Figure 3. H_2O_2 produced by rice suspension cell cultures of VN (A and C) and B (B and D) and measured at different time points after salt treatment. Closed triangles – straight line, Control; open squares – dotted line, 50 mM NaCl; grey squares – small-dashed line, 100 mM NaCl; closed squares – dashed line, 150 mM NaCl. A and B, H_2O_2 released in the medium; DW, Dry weight. C and D, H_2O_2 measured by the DHR-123 method, values were normalized against the levels of control cells, which are given a value of 1 and therefore have no SD. Values represent the mean ± confidence interval ($p<0.05$) of at least two independent experiments. An enlargement of the first 40 min of treatment is in the insets.

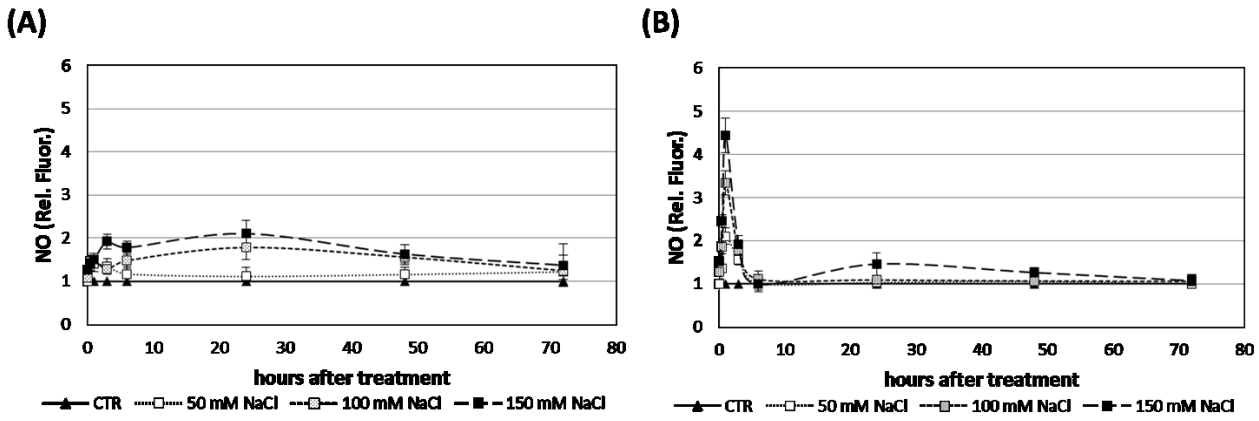

Figure 4. NO produced by rice suspension cell cultures of VN (A) and B (B) and measured at different time points after salt treatment. Closed triangles – straight line, Control; open squares – dotted line, 50 mM NaCl; grey squares – small-dashed line, 100 mM NaCl; closed squares – dashed line, 150 mM NaCl. Values were normalized against the levels of control cells, which are given a value of 1 and therefore have no SD. Values represent the mean ± confidence interval ($p<0.05$) of at least two independent experiments.

Given the larger amounts of H_2O_2 and continuous production of NO by the sensitive cell line exposed to salt stress, the expression profile of the *Fatty acid alpha-Oxidase* (or α-dioxigenase2; *α-DOX2*) and of the *Alternative Oxidase 1a* (*AOX1a*), both known to be regulated by NO and H_2O_2 and associated with PCD (Ponce De León *et al*., 2002; Koeduka *et al*., 2005; Mlejnek, 2013; Feng *et al*., 2013), was analysed. In VN cells, *α-DOX2* expression level highly increased at 48 h, reaching a peak at 72 h. The same trend was observed for the AOX1a gene. In B cell line, instead, a slight upregulation of the α-DOX2 gene was observed at 24h, followed by a downregulation at 72 h. Concerning the AOX1a gene, no expression changes were detected in the tolerant cell line (Fig.5 A and B).

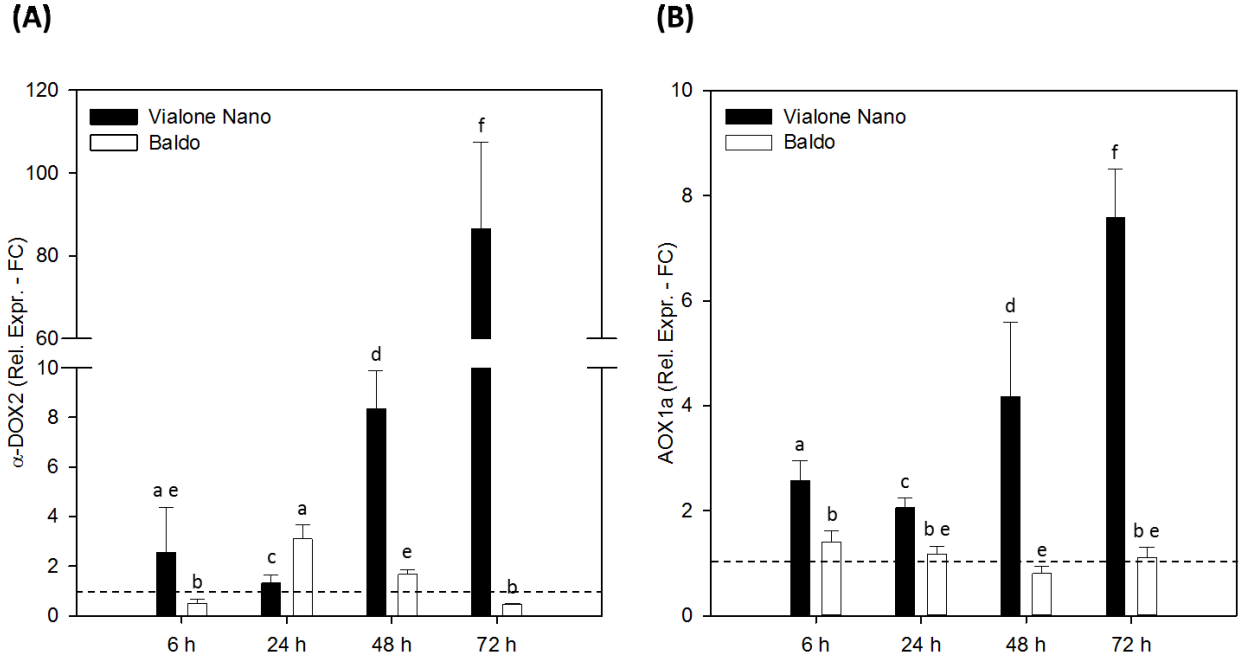

Figure 5. Relative expression (Fold Change) of (A) α-DOX2 gene and (B) AOX1a gene at different hours after treatment with 100 mM NaCl. Values represent the mean ± confidence interval ($p<0.05$) of three independent experiments in duplicate. Different letters indicate statistically different expression levels (Student's *t* test, $p<0.05$).

Genes involved in ROS signalling and modulation

In our experimental system a H_2O_2 burst was observed early in the tolerant line whereas a high level of H_2O_2 combined with sustained levels of NO was detected at a later time in the sensitive line. These two responses to salt stress are inducing signals leading to different fates, i.e. the induction of resistant mechanisms, in B cells, and of a cell death process, in VN cells.
To investigate this hypothesis in more details, the expression of genes linked to ROS and involved in early response to salt stress was investigated. First, the expression of *SALT-RESPONSIVE ERF1* (*SERF1*), a rice transcription factor (TF) gene that functions in H_2O_2-dependent salt stress signalling and required also for the induction of salt tolerance, was analysed (Schmidt *et al*., 2013). In B cells, *SERF1* expression was rapidly induced within 10 min of salt stress, while in VN cells, it showed slower induction, with a small peak at 30 min of exposure to salt stress (Fig.6 A).
Then, RBOHA gene expression was analysed. RBOHA belongs to the respiratory burst oxidase homologues (RBOHs) gene family, known to play a key role in the network of ROS production in plants (Suzuki *et al*., 2011). In fact, it is involved in the biosynthesis of H_2O_2, in particular by producing superoxide ions, then dismutated in H_2O_2 by the superoxide dismutase (SOD). Moreover, plasma membrane NADPH oxidases of the RBOH family are responsible for salt-induced apoplastic H_2O_2 production (Ma *et al*., 2012). *RBOHA*, in particular, resulted to be regulated by salt (Wang *et al*., 2016). In our system, B upregulated *RBOHA* 6 h after treatment, whereas VN upregulated this genes only after 24 h (Fig.6 B).

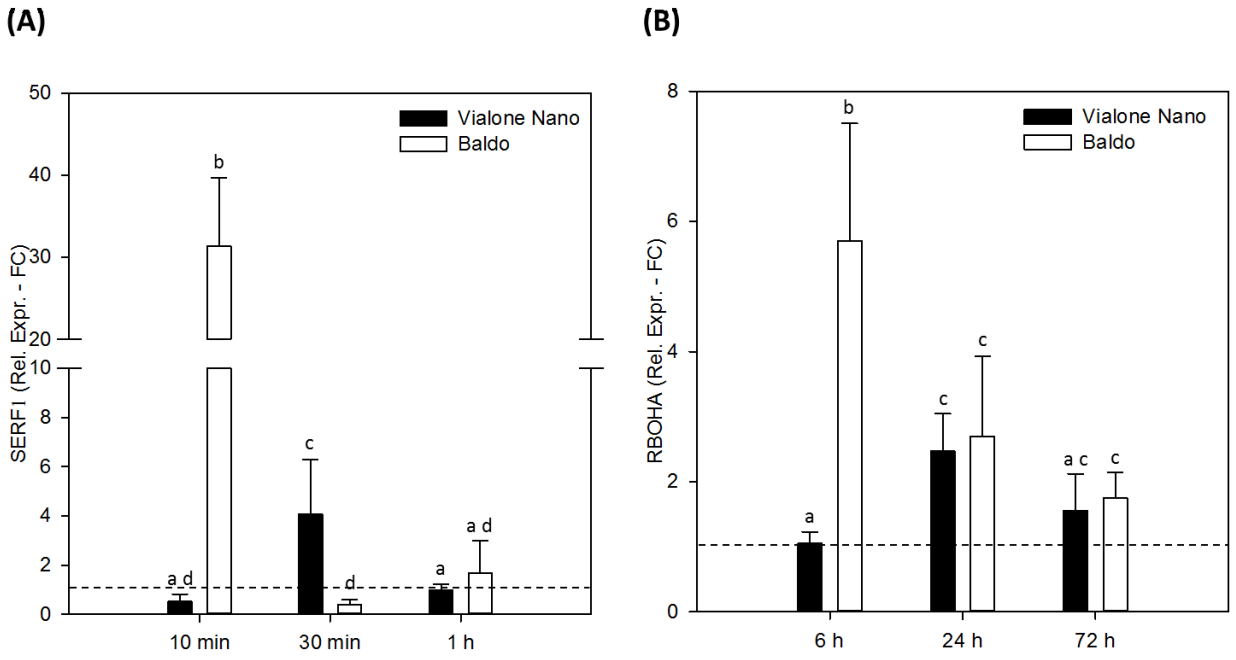

Figure 6. Relative expression (Fold Change) of (A) SERF1 gene and (B) RBOHA gene at different times after treatment with 100 mM NaCl. Values represent the mean ± confidence interval ($p<0.05$) of three independent experiments in duplicate. Different letters indicate statistically different expression levels (Student's *t* test, $p<0.05$).

We also analysed the expression of some of the genes coding for the most important antioxidant enzymes that regulate ROS levels inside the cells. The expression level of important genes, as the

ones coding for SOD (*SODCC2*), Glutathione S-transferase (*GSTU6*), cytosolic Ascobate Peroxidase 1 (*APX1*) and Catalase B (*CATB*), showed different patterns. In B cell line the expression level of *SODCC2* and *GSTU6* increased at highest level after 6 h treatment, while in VN cells the expression level of *SODCC2* increased at 24 h (Fig.7 A and B). Also the expression of *APX1* increased at 6 h and 24 h treatment in B cells while no differences can be observed in VN cells (Fig. 7 C). On the other hand, the expression of *CATB* showed a slightly and transient increase statistically significant at 6 h after treatment only in VN cells, while it remained constant in B cells (Fig. 7 D).

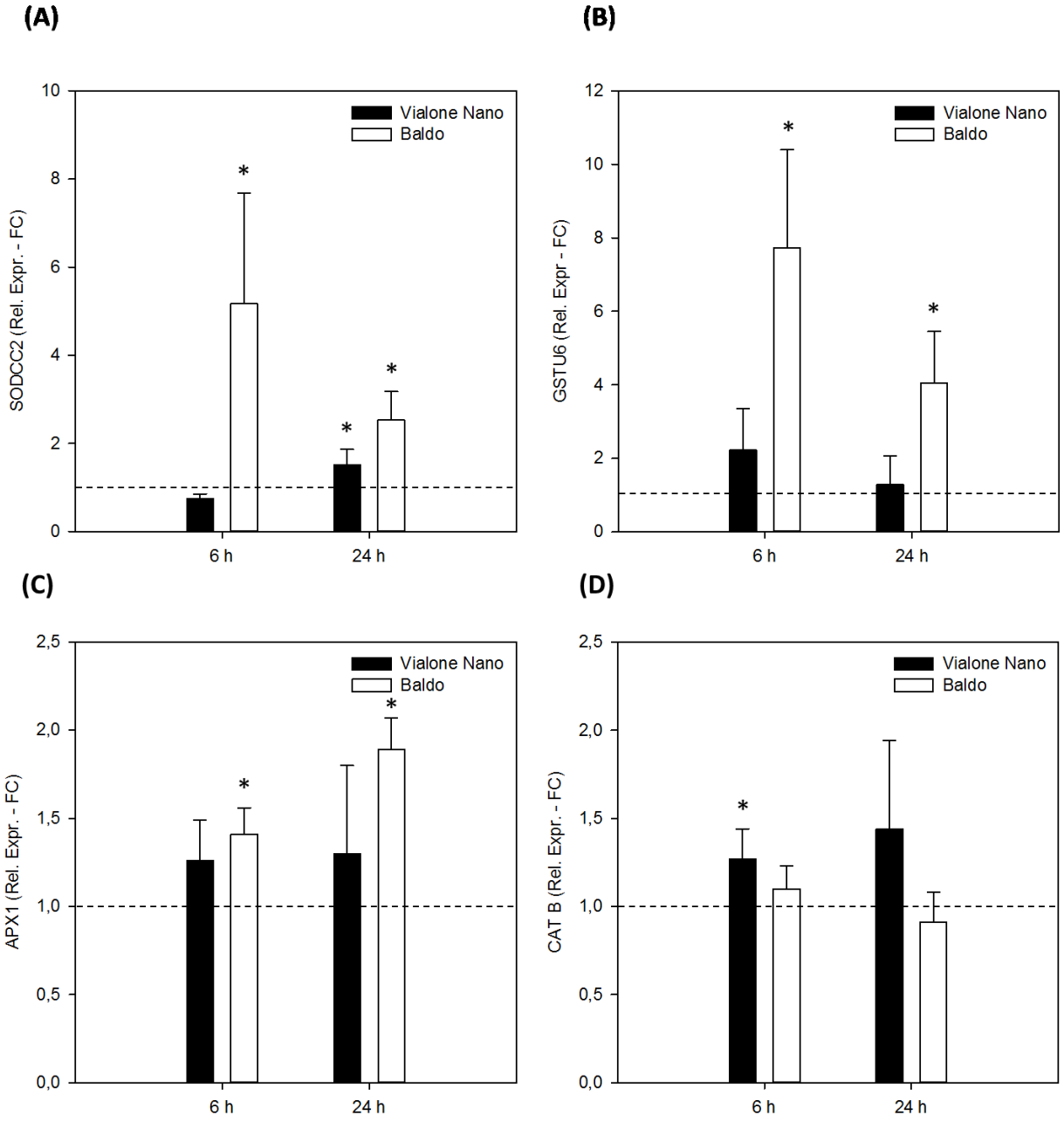

Figure 7. Relative expression (Fold Change) of (A) SODCC2 gene, (B) GSTU6 gene, (C) APX1 gene and (D) CATB gene at different times after treatment with 100 mM NaCl. Values represent the mean ± confidence interval ($p<0.05$) of three independent experiments at least in duplicate. The asterisk indicates values that are significantly different from those of untreated cells by Student's *t* test (* $p<0.05$).

No significant differences, instead, were detected between the two cell lines by analysing the expression of Catalase A (*CATA*) coding gene.

ROS regulation by enzymatic and non-enzymatic antioxidant systems

To utilize ROS as signalling molecules, non-toxic levels must be maintained in a delicate balance between ROS production, involving ROS-producing enzymes, and the metabolic counter-process involving ROS-scavenging pathways (De Gara *et al*., 2010; Foyer and Noctor, 2011; Suzuki *et al*., 2012). Thus, ROS levels depend on gene expression regulation but also on modulation of the involved enzyme activities. Therefore, the activity of the most important antioxidant enzymes was evaluated.

First, the activity of superoxide dismutases (SODs) that converts the dangerous superoxide produced by NADPH-oxidases in H_2O_2 was measured. In control cells, VN cell line showed a SODlevel activity higher than B cells; this is consistent with the higher amount of H_2O_2 released into cell culture medium by VN in control conditions (Fig.3 A). In presence of NaCl (100 mM) SOD activity showed a clear increase in both cell lines 24 h after treatment, in particular, a 43% increase in B tolerant cells and a 27% increase in VN sensitive cell line (Fig. 8).

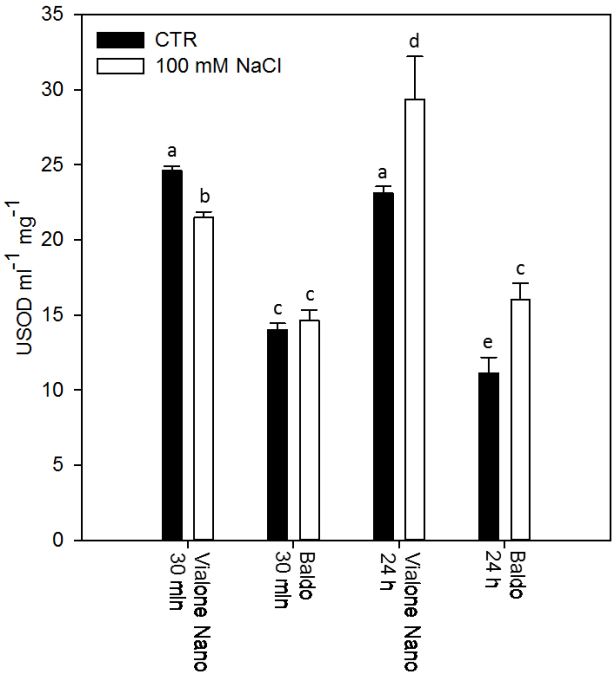

Figure 8. Effect of 100 mM NaCl on SOD activity determined at 30 min and 24 h after treatment. Values represent the mean ± SD of two independent experiments at least in duplicate. Different letters indicate statistically different activity levels by one-way ANOVA ($p<0.05$).

Considering the activity of enzymes involved in plant cell redox homeostasis, in particular those of the ASC-GSH cycle, the tolerant variety showed higher activity of monodehydroascorbate reductase (MDHAR), glutathione reductase (GR) and catalases (CAT) in control conditions, but no changes in the activity of these enzymes was observed after salt treatment (Fig.9 A, B and C). On the other hand dehydroascorbate reductase (DHAR) activity showed no significant differences

between the cultivars in control conditions (data not shown). Several data support a key role of cytosolic APX (cAPX) in ROS homeostasis (Locato *et al.*, 2009; de Pinto *et al.*, 2013). Interestingly the activity of cAPX was higher in B cells than in the sensitive line in control conditions and it increased under salt stress more in B than in VN cells (Fig. 9 D).

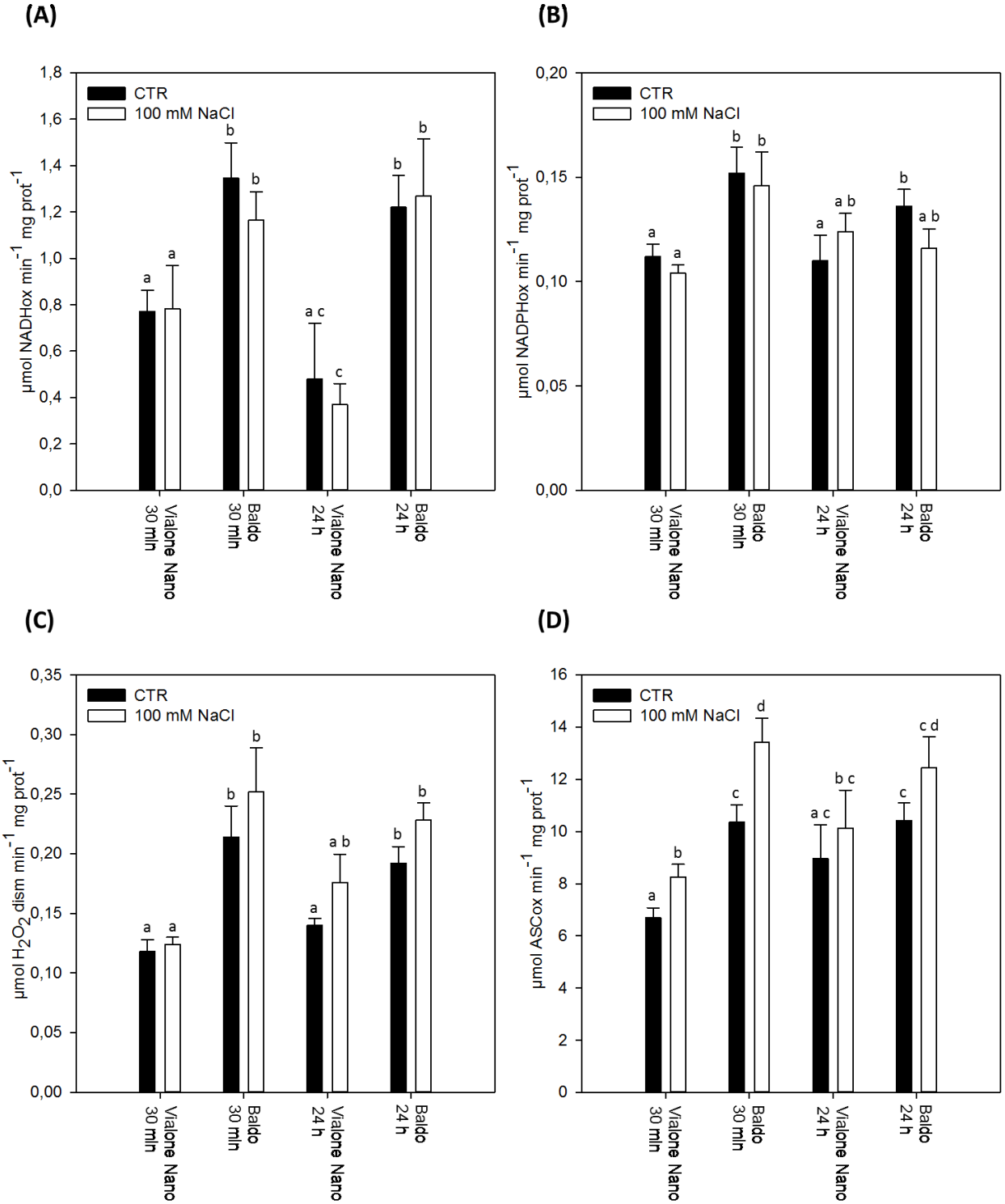

Figure 9. Effects of 100 mM NaCl on (A) MDHAR, (B) GR, (C) CAT and (D) cAPX activity determined at 30 min and 24 h after treatment. Values represent the mean ± SD of three independent experiments. Different letters indicate statistically different activity levels by one-way ANOVA ($p<0.05$).

In addition to the enzymatic system, also non-enzymatic antioxidant systems are present in plants. Therefore, the two major components of the latter system, ascorbate and glutathione, were evaluated. No significant differences in the content of ascorbate was observed in the two cell lines in control and salt stress conditions (Fig.10 A), whereas, glutathione level resulted lower in VN cells than in B ones at 24 h from the treatment in both control and salt stress conditions (Fig.10 B).

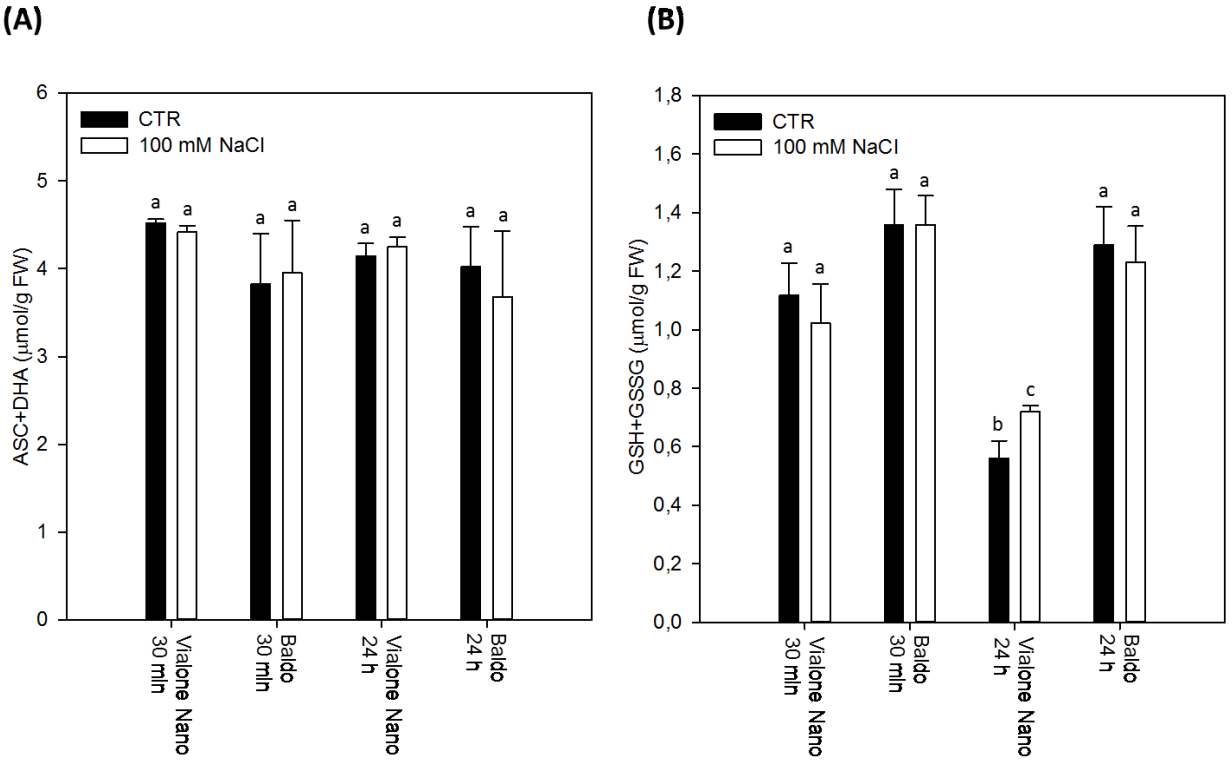

Figure 10. Changes in cytosolic (A) ascorbate and (B) glutathione (reduced plus oxidized forms) pools induced by 100 mM NaCl and determined at 30 min and 24 h after treatment. Values represent the mean ± SD of three independent experiments. Different letters indicate statistically different values by one-way ANOVA ($p<0.05$).

A stronger anti-oxidant system helps B cells to cope with salt stress effects

In order to evaluate more in detail the effectiveness of the stronger anti-oxidant capability of B cells, we treated the two cell cultures with glucose and two concentrations of glucose oxidase (GOX; 1 U/ml and 10 U/ml). This treatment caused an increase in external H_2O_2 levels after 24h into the medium of both cultivars, even in B cell culture where no H_2O_2 could be detected in the medium during salt treatment (Fig. 3B). However, as shown in Fig.11 A, B cells were capable of scavenging H_2O_2 more efficiently with respect to VN cells.

In order to understand whether high levels of H_2O_2 are playing a role in the process of cell death induced by salt stress in VN (Fig.1, 3), this cellular parameter was measured under oxidative stress conditions. Notably, the tolerant variety showed no increase in the percentage of cell death, while in VN cells, cell death reached 100% after 48 h of treatment in presence of the higher concentration of GOX, and 22% and almost 40% after 48 and 96 h respectively, in presence of the

lower concentration (Fig.11 B). This result shows how high levels of H_2O_2 are indeed contributing to the induction of cell death events.

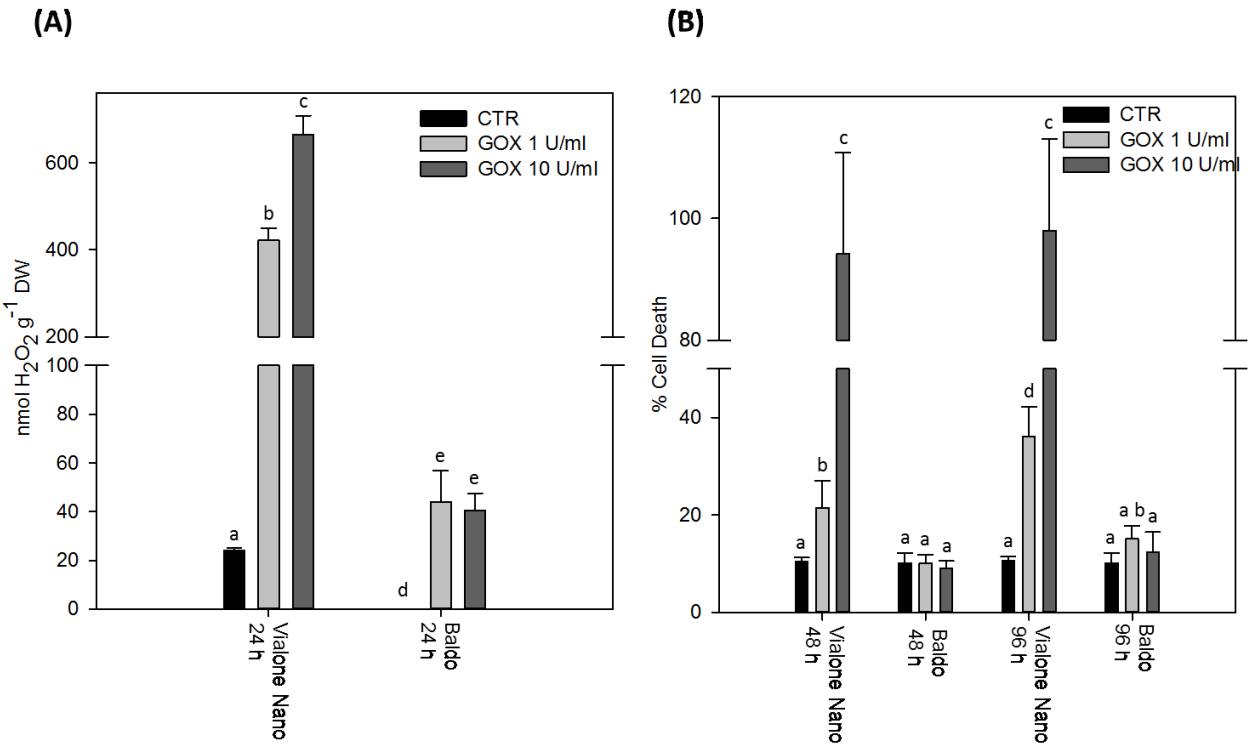

Figure 11. Effects of glucose and GOX on suspension cell cultures. (A) Presence of H_2O_2 in the culture medium of the suspension cell cultures. H_2O_2 concentration was measured after 24 h in the absence (CTR) or after the addition of 14 mM glucose plus 1 or 10 U ml^{-1} glucose oxidase (GOX). (B) Viability of control (CTR) and treated cells after 48h and 96h of treatment with glucose and GOX. Values represent the mean ± SD of two independent experiments at least in duplicate. Different letters indicate statistically different values (Student's *t* test, $p<0.05$).

$[K^+]/[Na^+]$ ratio and regulation of channels/transporter genes can contribute to mitigate salt stress

The maintenance of a high $[K^+]/[Na^+]$ ratio is an important mechanism for salt tolerance. Therefore, this trait was evaluated in B and VN cells.

By performing ionomic analyses, we observed that in both suspension cell cultures, K^+ content dropped while Na^+ content highly increased after salt treatment. However, in the tolerant variety intracellular K^+ concentration started increasing again after 48 h treatment while Na^+ levels decreased after 96 h. By contrast, in VN, the intracellular K^+ content showed constant decrease, while the content of Na^+ did not change (Fig.12 A and B).

Accordingly, the tolerant variety seemed to be able to increase $[K^+]/[Na^+]$ ratio in the days following salt treatment, while in VN this ratio slightly decreased (Fig.12 C).

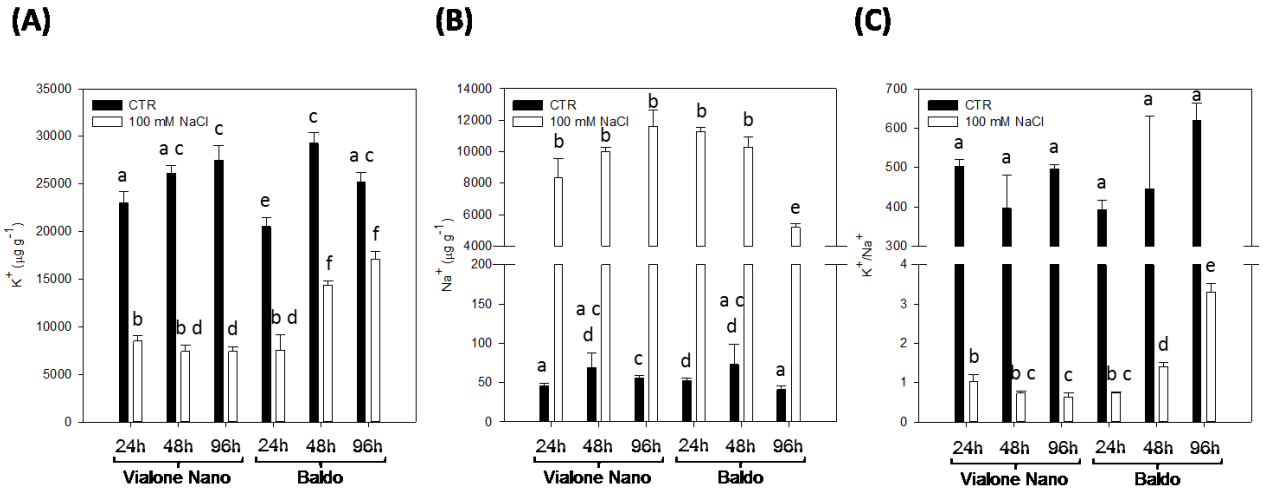

Figure 12. (A) K^+ content, (B) Na^+ content and (C) K^+/Na^+ ratio in VN and B cells after 24 h, 48 h or 96 h of treatment with 100 mM NaCl or H_2O (CTR). Values represent the mean ± SD of three independent experiments. Different letters indicate statistically different values.

Among K^+ transporters analysed, the plasma membrane located high affinity K^+ transporter *HAK5* and the vacuolar localized two-pore K^+ channels, *OsTPKa* and *OsTPKb*, are showing different patterns of expression between the two cell lines (Fig.13). All three genes play a role in modulating $[K^+]$cyt. In fact, HAK5 is involved in potassium uptake, while the vacuolar channels release K^+ from the vacuole into the cytosol. In agreement with the ionomic data, *HAK5* was highly upregulated in the tolerant variety after 6 h of salt treatment, while it was upregulated only at 24 h in the sensitive variety (Fig.13 A). Similarly *OsTPKa* was upregulated at 6 h treatment in B and only at 24 h in VN (Fig.13 B). Almost the same pattern was found for *OsTPKb* (Fig. 13C).

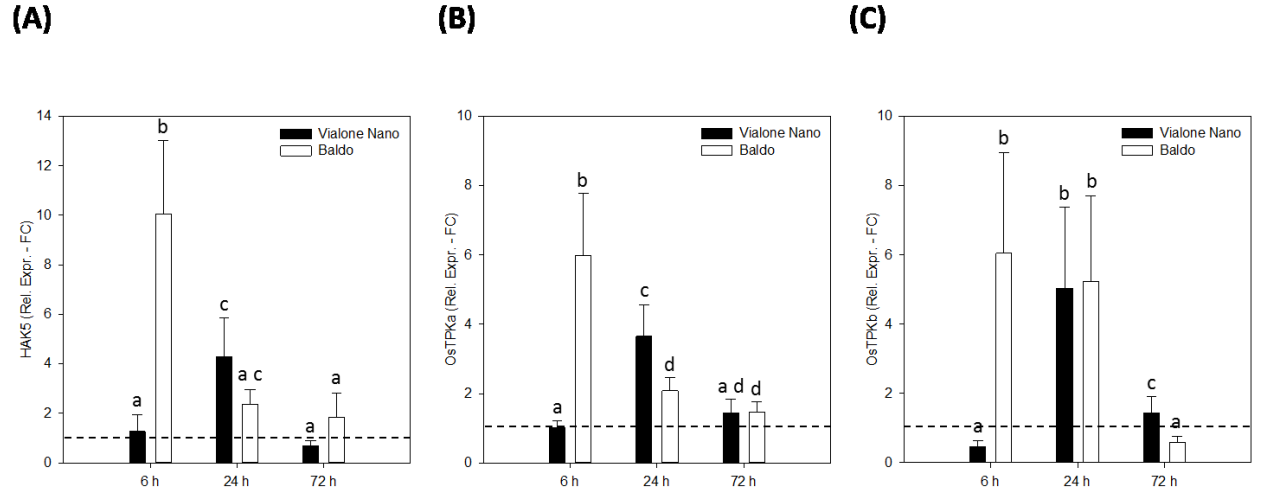

Figure 13. Relative expression (Fold Change) of (A) HAK5, (B) OsTPKa and (C) OsTPKb genes at different times after treatment with 100 mM NaCl. Values represent the mean ± SD of three independent experiments in duplicate. Different letters indicate statistically different expression levels.

The analysis of the expression of *NHX1* (vacuole localized Na^+/H^+ antiporter) and *SOS1* (plasma membrane Na^+/H^+ antiporter) showed no differences between the two cell lines after salt

treatment, while the expression of *HKT1.4* and *HKT1.5* could not be detected, implying that in suspension cultured B cells tolerance may rely more on K^+ cytosolic concentration increase to sustain a high $[K^+]/[Na^+]$ ratio, than in Na^+ compartmentalization or exclusion processes.
The expression of other two potassium channels genes important for salt tolerance, *AKT1* and *KAT1*, was investigated, with the first showing no different expression in both cell lines after treatment while the expression of the second could not be detected.
These results corroborate the hypothesis that a high ratio of $[K^+]/[Na^+]$ might contribute to make B cell line more tolerant to salt stress.

3.3 Discussion

Plants can differ greatly in their tolerance to salt stress, both among species and within species.
The Italian rice varieties VN and B have been demonstrated to own contrasting salt sensitivity, with VN being more sensitive and B more tolerant (see Chapter 2). To investigate salt-stress responses at the cellular level, we generated suspension cell cultures from seeds of both varieties. Notably, VN and B cell cultures showed the same difference in salt sensitivity as in plants. In the present study we demonstrate that, upon stress exposure, B cultured cells are able to set up specific tolerance mechanisms while VN cells undergo cell death. In fact, the presence of genomic DNA fragmentation (DNA laddering, Fig.2), a programmed cell death (PCD) hallmark (Hoeberichts and Woltering, 2003), induced by salt stress in VN cells suggests that PCD is induced in this sensitive variety. Along with DNA laddering, VN cells show up-regulation of *α-DOX2* (Fig.5 A) and of *AOX1a* (Fig.5 B), two genes known for being associated with PCD and induced by H_2O_2 and NO (Koeduka *et al*., 2005; Ponce de León *et al*., 2002; Mlejnek, 2013; Feng *et al*., 2013) in particular at 72 h when the cell death percentage was approximately 40% (Fig.1 C). They both seem indeed following the same trend of expression.
In plants, ROS, normal byproducts of various metabolic pathways, and RNS are dramatically increased under salt stress (Apel and Hirt, 2004, Valderrama *et al*., 2007). By comparing H_2O_2 production in the two cell lines grown in standard conditions, VN cells appear to owning a higher level of extracellular H_2O_2 with respect to B cells (Fig.3 A and B). The two cell cultures also differ in H_2O_2 and NO induction upon salt treatment. In the sensitive variety, salt-stress induces the production of high levels of both extracellular and intracellular H_2O_2 (Fig.3 A and C) together with a stable over time NO production (Fig.4 A). Instead, in B cells exposed to salt stress no extracellular H_2O_2 production can be detected (Fig.3 B) and only a very early and rapid pulse in intracellular H_2O_2 (Fig.3 D) and NO (Fig.4 B) production is observed. These results do explain the increased expression of the two genes mentioned above, *α-DOX2* (Fig.5 A) and *AOX1a* (Fig. 5 B), only in VN cells. Therefore, the larger amounts of H_2O_2 and the continuous production of NO in the sensitive cell line exposed to salt stress may explain the induction of PCD observed in VN variety (Fig.2).
Indeed, it is known that both ROS and RNS must be produced in specific relative amounts for triggering PCD in plant and cultured cells (Delledonne, 2001, de Pinto *et al*., 2002).
Although high levels of ROS can induce cell death, a controlled and transient production of H_2O_2 has been associated to many signalling pathways (Jaspers and Kangasjarvi, 2010). Therefore, the transient increase of H_2O_2 in the tolerant variety identifies this molecule as a possible signalling molecule in B cells. Notably, in B cells *SERF1* (Fig.6 A) and *RBOHA* (Fig.6 B), two genes involved in salt-induced signalling processes (Schmidt *et al*., 2013; Hong *et al*., 2009), appear to increase their level of expression very rapidly after salt stress exposition and much earlier than in VN cells.
The prompt increase of RBOHA transcript in the tolerant line is also coherent with the finding that the *A. thaliana* KO mutant for RBOHA showed decreased salinity tolerance (Jiang *et al*., 2012).
H_2O_2 levels detected in B and VN cells can be explained by a lower H_2O_2 production and/or by a higher H_2O_2 detoxification capacity owned by B more tolerant cells. It is known that plant mitochondria may control ROS generation through energy-dissipating systems (Noctor *et al*., 2007). Notably, we observe that B cells own an *AOX1a* expression level almost 10 times higher than VN cells when grown under standard conditions (Fig. S1). AOX1a has a role in the mitochondrial electron transport chain (mETC) to reduce potentially dangerous excess electrons and by doing so it may prevent dangerous ROS formation (Feng *et al*., 2013). Although the activity of an enzyme is not always correlated to the expression of its gene, we can hypothesize that B

cells, owning a higher expression level of *AOX1a* in control conditions, can be more prone to counteract the excessive electrons formation that usually follows stress conditions.
In addition, the expression analysis of genes encoding for some of ROS detoxifying enzymes show that B cells up-regulate *SODCC2* (Fig.7 A), *GSTU6* (Fig.7 B) and *APX1* (Fig.7 C) more or at earlier times respect to VN cells, suggesting a prompter and a more efficient capacity of the tolerant cells to control its redox state during salt stress. Consistently, exogenous expression of cytosolic APX1 in plum plants has been demonstrated to increase tolerance to salt stress (Diaz-Vivancos *et al*., 2013). A redox control capability higher in B than in VN cells is also suggested by the activities of some of the enzymes involved in ROS scavenging. Notably, the activity levels of MDHAR, GR, CAT and cAPX were already higher in the tolerant variety with respect to the more sensitive one grown in control condition (Fig.9). This further supports the presence in B cells of an innate higher capacity of ROS scavenging, consistent with the observed results reporting low H_2O_2 levels and lower effect on growth and viability upon salt stress exposure in these cells in comparison with the sensitive VN cells (Fig.3 B and D).
The results coming from the exposure of the two cell cultures to an oxidative stress as the Glucose/Glucose Oxidase system represent a further proof of the higher ROS-scavenging capacity owned by B cells. In fact, the tolerant variety was able to scavenge the exogenous production of H_2O_2 more efficiently than the sensitive one (Fig.11 A). Consequently, B cells are able to prevent cell death; while the exogenous H_2O_2 production induces dose-dependent cell death in the sensitive VN line (Fig.11 B).
Another well-known effective strategy to cope with salt stress at cellular level is to keep cytosolic Na^+ levels low while upholding high cytosolic levels of K^+. In fact, the maintenance of a high $[K^+]/[Na^+]$cyt ratio is crucial for salt tolerance (Horie *et al*., 2012). For these reasons, we investigate the ability to maintain K^+ homeostasis in VN and B cells.
The analysis of the expression of some of the genes involved in increasing cytosolic K^+ concentration shows that B cells upregulate *HAK5*, *OsTPK1a* and *OsTPK1b* earlier than VN cells (Fig.13). The overexpression of some K^+ transporters/channels genes has been reported to increase salt tolerance (Obata *et al*., 2007; Horie *et al*., 2011; Isayenkov *et al.*, 2011; Ahmad *et al.*, 2016). Therefore we can hypothesize that a quicker response to salt stress turns in the capacity to maintain more efficiently K^+ homeostasis in salt tolerant B cells.
Consistent with these results, ionomic analyses performed on the two cell lines show that after a first similar drop in K^+ content, B cells are able to increase again K^+ concentration while K^+ content continues to decrease in VN cells (Fig.12 A). Moreover, after a massive increase in Na^+ content in both varieties, only B cells are able to reduce intracellular Na^+ levels (Fig.12 B). This results in a constant increase in $[K^+]/[Na^+]$ ratio in the tolerant variety cells, while this ratio steadily decreases in the sensitive variety (Fig.12 C). As reported by Demidchik *et al*., (2010), GORK channels, that conduct large outwardly rectifying K^+ currents thus increasing K^+ leakage from the tissue, result to be activated by salt stress- increased ROS level. Therefore, we can hypothesize that the higher H_2O_2 level observed in VN treated cells might also be correlated with the decreased $[K^+]/[Na^+]$ ratio.

3.4 Conclusions

In conclusion, in this report we demonstrate that salt-tolerance in B cells depends at least on two different mechanisms: efficient redox homeostasis mediated by high ROS control/scavenging capability and ability to keep high $[K^+]/[Na^+]$ ratio.
The ability to keep low H_2O_2 levels may permit B cells to use H_2O_2 as a signalling molecule to activate tolerance mechanisms. This ability depends on the strong antioxidant system owned by the tolerant cells that allows a fine-tuning of ROS levels under physiological and salt stress conditions.
In B cells the fast initial pulse of H_2O_2 production, probably in synergy with the pulse of NO production, can play the role in activating tolerance mechanisms, as showed by the very early up-regulation of *SERF1* and *RBOHA*.
Conversely, in VN cells H_2O_2 basal levels are already high in normal growth conditions, and salt treatment induces a further increase in H_2O_2 production that is not properly scavenged. These high levels of H_2O_2, combined with the NO increase after salt stress, trigger a cell death program. The presence of DNA fragmentation and of the H_2O_2- and NO-linked upregulation of *α-DOX2* and *AOX1a* show that VN cells are indeed undergoing PCD.
The other key difference in response to salt stress between the two varieties cultured cells is the ability of the tolerant cells to maintain high K^+ concentration. This is due to a rapid increase in the expression of genes encoding for transporters/channels localized to the tonoplast and to the plasma membrane. How and if this behavior is linked to the H_2O_2-dependent signalling pathway induced after salt stress, as suggested by Demidchik *et al*. (2010), will be worth to analyze in future experiments.

3.5 Materials and Methods

Plant Material and Salt Treatment

Experiments were mainly conducted with non-embryogenic cell suspension cultures of two rice (*Oryza sativa* L.) varieties, Baldo and Vialone Nano. Briefly, mature seeds of the two varieties were dehusked and sterilized in 3.5% bleach with the addition of a drop of TWEEN 20 for 20 min in a giratory shaker, followed by 5 min with just 3.5% bleach. After 5 washes in distilled water, seeds were sawn in solid N6 medium (30 g L^{-1} sucrose, Chu (N6) Medium Salt Mixture and vitamins (Duchefa) and 2 mg L^{-1} 2,4-dichlorophenoxyacetic acid (2,4-D), pH = 5.8) in dark conditions and moved to new plates every 2 weeks. After few months the callus was friable, and ready to be transferred in liquid medium. The resulting suspension cell cultures were grown at 25°C under dark conditions on a gyratory shaker in liquid N6 medium. Every week they were filtered to eliminate bigger clumps until quite homogeneous suspension cell cultures were obtained. For the next subculturing, two mL of packed cells were transferred into 50 mL fresh medium every 7 d. Cells at 3 d after subculture were treated with 50, 100 or 150 mM NaCl and used for the next experiments. To determine the growth capabilities of the two suspension cell cultures under salt stress, cells were filtered and the fresh and the dry weight were measured.
For oxidative stress treatment, 14 mM glucose plus glucose oxidase 1 or 10 U ml^{-1} was added to 3 days old cell suspensions.

Cell Viability

Cell death accompanying the loss of membrane integrity was evaluated by a spectrophotometric assay of Evans blue stain retained by cells according to Gaff and Okong'o-Ogola (1971) with minor modifications. Briefly, one mL of cell suspension was sampled from the cultures at desired intervals. Evans blue dye solution was added to the cell suspensions to a final concentration of 0.05% and incubated for 15 min at room temperature, followed by excessive washes with water until the washing showed no significant blue colour. The washed cells were then added to 50% methanol containing 1% (w/v) sodium dodecyl sulfate (SDS) and incubated at 55 °C for 30 min. Absorbance of the supernatant was measured spectrophotometrically at 600 nm. The resulting OD was compared to the absorbance of cells boiled for 45 min, which are considered as 100% dead.

DNA laddering

DNA laddering is tightly associated with PCD both in animals and in plants. Briefly, one g of cells was ground to a fine powder in liquid nitrogen. Hexadecyltrimethyl ammonium bromide (CTAB) isolation buffer (2 % w/v CTAB, 1.4 M NaCl, 20 mM EDTA, 100 mM Tris–HCl, pH 8.0) at 60°C, freshly supplemented with 10 mM mercaptoethanol, was added to broken cells and mixed thoroughly. The mixture was incubated at 60 °C for 40 min. Nucleic acids were extracted with equal volume of phenol and chloroform–isoamyl alcohol (24 : 1 v/v) and centrifuged at 3000 g for 15 min. DNA was incubated with 0.7 volumes of ice-cold isopropanol for 30 min at -20°C and centrifuged at 4000 g for 15 min at 4°C. The nucleic acid pellet was washed with an ice-cold 70 % v/v ethanol and centrifuged for 5 min. The pellet was air dried and dissolved in 300 µL TE buffer (10 mM Tris–HCl, pH 8.0, 1 mM EDTA). DNase-free RNase A (0.1 µg μL^{-1}) was added and the

mixture incubated at 37 °C for 30 min. DNA was separated on 2% agarose gel stained with ethidium bromide with equal amounts of 30 µg DNA per lane.

Hydrogen Peroxide Determination

Extracellular H_2O_2 was measured in culture medium as described by Bellincampi *et al*. (2000), with minor modifications. Briefly, 500 uL of the medium was added to an equal volume of assay reagent (500 µM ferrous ammonium sulfate, 50 mM H_2SO_4, 200 µM xylenol orange, and 200 mM sorbitol) and incubated for 45 min in the dark. The H_2O_2-mediated oxidation of Fe^{2+} to Fe^{3+} was determined by measuring the A560 of the Fe^{3+}-xylenol orange complex. A calibration curve obtained by measuring the A560 of H_2O_2 standards allowed the conversion of the absorbance values into concentration estimates. All reactions were carried out at least in duplicate, and their reproducibility was checked. Values are expressed as µmoles of H_2O_2 per gram of Dry Weight.
Intracellular H_2O_2 production was measured using DHR123 (Sigma-Aldrich Italia, Milan) as a probe. One ml of suspension culture was incubated with 20 µM DHR123 for 15 min in a rotating shaker, and then cells were washed three times with 1 mL of N6 medium. The cells were analyzed under a fluorescence microscope (DM5000) with a I3 filter.

Nitric Oxide Determination

Intracellular NO was detected with the fluorescent dye DAF-FM-DA (Alexis Biochemicals). One ml of suspension culture was incubated with 0.5 mM DAF-FM-DA for 15 min in a rotating shaker, and then cells were washed three times with 1 mL of N6 medium. Fluorescence was estimated using a fluorescence microscope (DM5000) with a GFP filter.

ASC and GSH assay

Cells (0.5 g) were were collected by filtration and homogenized by adding two volumes of cold 5% (w/v) meta-phosphoric acid at 4°C. The homogenates were centrifuged at 14000 g for 15 min at 4°C and the supernatants were collected and used for the analysis of ASC and GSH according to de Pinto *et al*. (1999). These experiments were performed in collaboration with the laboratory of Scienze biochimiche e della nutrizione (Università Campus Bio-Medico of Rome, Italy).

Enzyme assays

Cells (0.5 g) were ground in liquid nitrogen and homogenized at 4°C in an extraction buffer (50 mM Tris-HCl pH 7.5, 0.05 % cysteine, 0.1 % bovine serum albumin). Homogenates were centrifuged at 14000 g for 15 min at 4°C and the supernatants were used for the analyses of enzyme activity according to de Pinto *et al.* (2000) and Paradiso *et al.* (2012) with minor modification. Proteins were determined according to Bradford (1976) using bovine serum albumin (BSA) as a standard.
The activity of SOD (superoxide:superoxide oxidoreductase, EC 1.15.1.1) was performed according to Beauchamp and Fridovich (1971) using the reduction of nitro blue tetrazolium (NBT) as detector of $\bullet O^{2-}$ produced via the riboflavin photoreduction. One SOD unit was defined as the

amount needed to cause half-maximal inhibition of this reaction. Measurements were carried out at 560 nm.
The activity of APX (L-ascorbate: hydrogen peroxide oxidoreductase, EC 1.11.1.11) was measured at 290 nm in a reaction mixture composed of 7 µL of ASC 50 mM, 10 µL of H_20_2 17 mM in 1 mL of 100 mmol/L phosphate buffer, pH 6.4 and using a molar extinction coefficient of 2.7 mM^{-1} cm^{-1}. Glutathione reductase (GR; NADPH: glutathione disulfide oxidoreductase, EC 1.6.4.2) was measured at 340 nm in an reaction mixture composed of 10 µL of NADPH 10 mM, 10 µL of GSSG 100 mM in 1 mL of 100 mmol/L phosphate buffer, pH 7.2 by using a molar extinction coefficient of 6.2 mM^{-1} cm^{-1}. Monodehydroascorbate reductase (MDHAR; NADH: ASC free radical oxidoreductase, EC 1.6.5.4) and dehydroascorbate reductase (DHAR; GSH: dehydroascorbate oxidoreductase, EC 1.8.5.1) were measured respectively at 340 nm with a molar extinction coefficient of 6.2 mM^{-1} cm^{-1} and 265 nm with a molar extinction coefficient of 13.5 mM^{-1} cm^{-1} according to de Pinto *et al*. (2000). CAT (hydrogen-peroxide: hydrogen-peroxide oxidoreductase, EC 1.11.1.6) activity assay was performed at 240 nm with a molar extinction coefficient of 23.5 mM^{-1} cm^{-1} according to Sgobba *et al*. (2014). These experiments were performed in collaboration with the laboratory of “Scienze biochimiche e della nutrizione” (Università Campus Bio-Medico of Rome, Rome, Italy).

Total RNA Isolation and First Strand cDNA Synthesis

Briefly, one g of cells was ground to a fine powder in liquid nitrogen and 1 ml TRIZOL was added. After centrifugation at 5 min 14000 g, the supernatant was added with 200 µl chloroform and centrifuged again. The upper phase with the RNA was transferred to a new tube and chloroform extraction was repeated. The resulting upper phase was incubated with 0.7 volumes of cold isopropanol at -20°C for 20 min and then centrifuged for 10 min at 14000 g. The pellet was washed twice with 500 and 150 µl of 70% ethanol, air-dried and resuspended in 30 µl of water. RNA concentrations were measured using a Nanodrop ND-1000 spectrophotometer (Nanodrop Technologies, Rockland, DE, USA) and 5 µg of RNA was treated with RQ1 DNase (Promega) according to the manufactorer’s protocols. RNA was finally precipitated with 2.2 µl of CH_3COONa 3M pH 5.2 and 60.5 µl of ethanol and incubated for 30 min at -20°C. After centrifugation the pellet was washed with 70% ethanol, air-dried, resuspended in 5 µl of water and used for first-strand cDNA synthesis using the SuperScript II Reverse Transcriptase according to user instructions. In brief, RNA samples were heated to 65°C in the presence of 250 ng random primers (Promega) and dNTPs and then quickly cooled on ice. First-strand buffer and DTT were added and the mix was incubated at 25°C for 2 min. The SuperScript II RT was added and the mix was incubated at 25°C for 10 min, followed by incubation at 42°C for 50 min. The reaction was inactivated by heating at 70°C for 15 min.

qPCR

qPCR for the K^+ and Na^+ channels and transporters encoding genes analysed in this study and for the RBOHA, SODCC2, GSTU6 and CAT A genes was performed using the QuantStudio 12K Flex real-time PCR system and OpenArray technology (Thermo Fisher Scientific, CA, USA), following the manufacturer’s instructions. TaqMan® OpenArray® Real-Time PCR Plate with Custom Gene Expression Assays (Table S1) was designed and purchased from Thermo Fisher Scientific.

qPCR for α-DOX2, AOX1a, SERF1, APX1 and CAT B genes was performed in a 7500 Real-time PCR System (Life Technologies) using the SYBR Green technology of GoTaq qPCR Master Mix (Promega) using specific primers (Table S2).
The results were analysed using the $\Delta\Delta C_T$ method (Livak and Schmittgen, 2001).

Ionomic analysis

Samples were digested with concentrated HNO3 in a microwave system. The elements concentration was determined by inductively-coupled plasma ICP-OES, Ciros Vision EOP (Spectro A. I. GmbH, Kleve, Germany). Elements quantifications were carried out using certified multi-element standards. This experiment was performed in collaboration with the laboratory of Dott. Piergiorgio Stevanato (Department of Agronomy, Food, Natural Resources, Animal and Environment, DAFNAE, University of Padova, Legnaro, Italy).

3.6 Supplementary Material

Table S1. List of Gene Expression Assays used in this work. Two housekeeping genes were used, elongation factor 1-alpha (REFA1) and ubiquitin-40S ribosomal protein S27a-1 (UBQ).

Assay_ID	Gene_ID MSU	Gene_ID RAP	Gene_description
AJ39RWU	LOC_Os07g01810	Os07g0108800	OsTPKb
AJ39RWY	LOC_Os01g70490	Os01g0930400	HAK5
AJ70MFF	LOC_Os04g51830	Os04g0607600	OsHKT1.4
AJAAZRK	LOC_Os07g47100	Os07g0666900	OsNHX1
AJI1MY0	LOC_Os01g20160	Os01g0307500	OsHKT1.5
AJQJB0J	LOC_Os03g54100	Os03g0752300	OsTPKa
AJS08CU	LOC_Os07g46990	Os07g0665200	superoxide dismutase [Cu-Zn] 2 (SODCC2)
AJY9Y72	LOC_Os02g02400	Os02g0115700	catalase isozyme A
Os03472546_m1	LOC_Os01g53294	Os01g0734200	respiratory burst oxidase homolog protein A (rbohA)
Os03503633_m1	LOC_Os01g45990	Os01g0648000	OsAKT1.1
Os03529509_g1	LOC_Os01g55200	Os01g0756700	OsKAT1
Os03619633_g1	LOC_Os12g44360	Os12g0641100	OsSOS1
Os03639305_gH	LOC_Os10g38470	Os10g0528100	glutathione S-transferase (GSTU6)
Os03640561_s1	LOC_Os03g08010	Os03g0177400	elongation factor 1-alpha (REFA1)
AIS09F9	LOC_Os01g22490	Os01g0328400	ubiquitin-40S ribosomal protein S27a-1 (UBQ)

Table S2. List of primers for qPCR used in this work. The housekeeping gene used is the ubiquitin-40S ribosomal protein S27a-1 (UBQ).

Gene_description	Gene_ID	Primers	
AOX1a	Os04g0600200	Primer F	5'-ACTTCGCATCGGACATCCATTA-3'
		Primer R	5'-AAATCCTCGGCAGTAGACAAAC-3'
α-DOX2	Os12g0448900	Primer F	5'-AAATTAAAGGCCCCCTGCCA-3'
		Primer R	5'-TGTGTCGTGCGATGAATCCT-3'
SERF1	Os05g34730	Primer F	5'-GAGTGAGGAGCTCATTGTTTACGA-3'
		Primer R	5'-ACATCAAAATTTCCATGTCATCTA-3'
APX1	Os03g0285700	Primer F	5’-AAGACTACAAGGAGGCCCAC-3'
		Primer R	5’-CAAGAGTACCACGGGCAATG-3'
CATB	Os06g0727200	Primer F	5’-AGAGAGCCTGCACATGTTCT-3'
		Primer R	5’-AAACCCTCCATGTGCCTGTA-3'
UBQ	Os05g0160200	Primer F	5'-TTCTACAAGGTGGACGACGC-3'
		Primer R	5'-AGATCAGAGCAAAGCGAGCA-3'

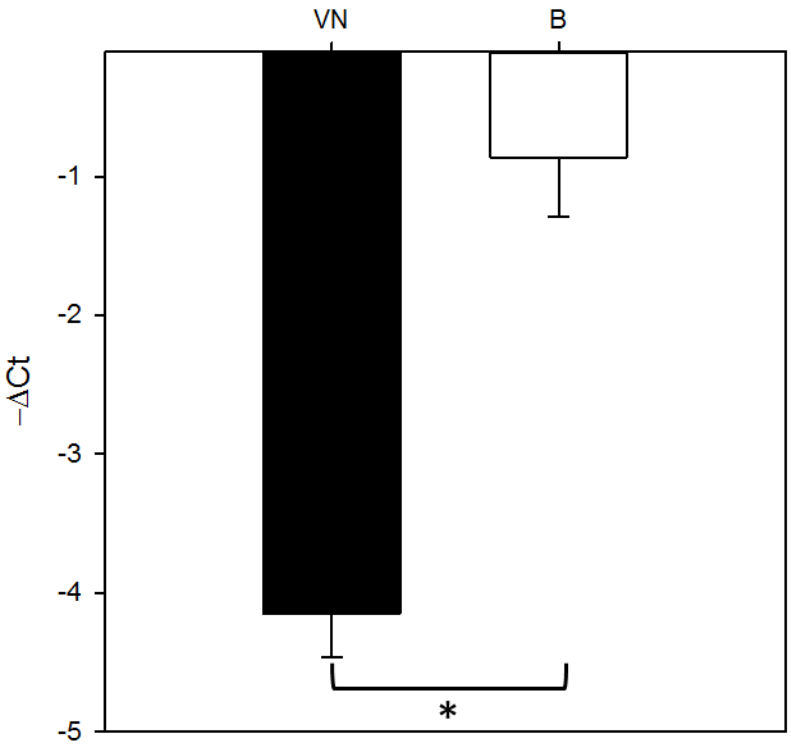

Figure S1. AOX1a expression levels in VN and B cells in control conditions. Data are shown as mean -ΔCt values compared to UBQ as a reference gene. Values represent the mean ± confidence interval ($p<0.05$) of 4 time points of three independent experiments in duplicate. The asterisk indicates significant differences by Student's *t* test (*$p<0.01$).

Chapter 4:

Production of transformed lines of Italian rice varieties

4.1 Introduction

*Agrobacterium tumefaciens*is is the causal agent of crown gall disease (the formation of tumours) in many plants. This is caused by the insertion of a small segment of DNA (known as the T-DNA or transfer DNA), from a plasmid, into the plant cell genome (Ream, 1989). These DNA transmission capabilities of *Agrobacterium* have been vastly explored in biotechnology as a means of inserting foreign genes into plants: the basic mechanism of tumorigenesis was elucidated, and the methods to generate transgenic plants without provoking tumors were developed for many dicotyledons (Fraley *et al*.,1985). The use of *A. tumefaciens* allows efficient insertion with minimal rearrangements of stable, relatively large, single-copy sequences into plant genomes (Nishimura *et al*., 2005), and in fact, nowadays, *A. tumefaciens*-mediated transformation has become the gene transfer method of choice for many plant species.

For a long time, it was generally believed that *A. tumefaciens* could not transform monocotyledons because these plants are not typical hosts of crown gall disease (De Cleene and De Ley, 1976) and, in fact, efficient transformation of monocotyledons was initially difficult to achieve by this method.

Despite this, expression of marker genes in cereals was demonstrated in rice (Raineri *et al*., 1990), maize (Gould *et al*., 1991) and wheat (Mooney *et al*.,1991). The first efficient generation of transgenic cereals was reported in the mid-1990s. Transgenic plants were obtained from calli induced from mature embryos of rice Nipponbare cv of the Japonica group (Hiei *et al*., 1994) after co-cultivation with *A. tumefaciens*. The frequency of independent transformation events obtained per infected explant was around 20%, and the stable integration and inheritance of T-DNA were demonstrated. They also showed that the use of cells which were actively dividing or about to divide and capable of regenerating plants was essential. This is consistent with the observation that induction of cell division by wound responses in dicots is a prerequisite for transformation (Kahl, 1982). Hiei *et al*. (1994) also pointed out that numerous factors were of critical importance as, for instance, the selection of the right strand of *Agrobacterium*, the concentration of the inoculum, etc. The japonica variety Nipponbare is an amenable genotype for *Agrobacterium*-mediated transformation. Nonetheless, it has been demonstrated that transformation abilities are genotype dependent, and thus a specific protocol has to be set up for each rice cultivar of interest (Hiei *et al*., 1997, Hiei and Komari, 2008).

In this study, we set up a transformation protocol for two Italian rice varieties. To our knowledge, transformation experiments of Italian rice varieties have not been reported so far, thus it is not known whether Italian rice varieties may be recalcitrant to transformation or not. To set up this protocol we used the YC3.6 Ca^{2+} sensor gene fused with the UBIQUITIN10 promoter from *Arabidopsis thaliana* (Krebs *et al*., 2012).

The selection of this construct was not casual. In fact, as a final goal, the production of transgenic rice plants and suspension cell cultures harboring the YC3.6 Ca^{2+} sensor will be exploited for the analysis of Ca^{2+} signalling.

In plants, calcium (Ca^{2+}) signalling is fundamental during response to environmental and developmental stimuli. Different cues evokes different [Ca^{2+}]cyt signals in terms of amplitude, frequency and duration of the peak. Because of their stimulus specificity, these signals are also known as Ca^{2+} signatures (Sanders *et al*., 2002) and they are likely to have specific roles in encoding the particular information for plants under stress, activating the downstream response mechanisms either through induction or downregulation of responsive genes. The development of genetically encoded Ca^{2+} indicators has significantly facilitated the study of Ca^{2+} dynamics in plants. Yellow Cameleon (YC) proteins (Batistič and Kudla, 2012) are fluorescence resonance

energy transfer (FRET)-based ratiometric indicator proteins for imaging Ca^{2+} dynamics in vivo. They harbor a cyan fluorescent protein (CFP) and a yellow fluorescent protein (YFP) that are linked together by the Ca^{2+}-binding protein calmodulin and an M13 calmodulin-binding peptide. Binding of Ca^{2+} to the calmodulin moiety induces a conformational change of the indicator protein resulting in enhanced FRET between CFP and YFP. The efficiency of FRET allows quantitative measurements of Ca^{2+} dynamics in plants.

Therefore, the aim of this study was to set up a protocol for the transformation of two Italian rice varieties of the Japonica group, Vialone Nano (VN) and Baldo (B), with the Cameleon-based Ca^{2+} probe YC3.6. VN and B show different salt-sensitivity, thus the availability of YC3.6-expressing lines of these varieties could provide a basis for the study of salt stress-induced Ca^{2+}signalling leading to different outcomes.

4.2 Results and Discussion

In the last part of my Ph.D., the transformation of VN and B variety was performed using a construct harboring the cameleon-based cytosolic Ca^{2+} sensor YC3.6. Different factors have to be taken into account to set up a transformation protocol. Therefore, two different sets of experiments were performed to obtain transformed plants and calli for suspension cell cultures generation. In the I° set of experiments, three *Agrobacterium* strains were tested and the transformed calli were regenerated to give plants. In the II° set of experiments an additional dehydration step was introduced and two concentrations of *Agrobacterium* were tested. The resulting transformed calli were used to generate suspension cell cultures.

I° set of experiments

The choice of the right strain of *A. tumefaciens* is an important factor for the success of transformation (Hiei *et al*., 1994). Therefore, in the first set of experiments, 3 strains of *Agrobacterium* have been tested and used for infection: LBA4404, GV3101 and EHA105.
No transformation events were observed in calli transformed with LBA4404 and GV3101 strains. From the transformation with the EHA105 strain, however, a single VN and a single B hygromycin resistant callus out of almost 200 inoculated calli were recovered after 4 weeks in selection media (Table I).

Table I Effect of different strains of *Agrobacterium* on Transformation efficiency.

	N° exp	N° seeds	N° calli	Strain	Construct	OD	N° clones	% Germination	% Trasformation
VN	1	210	209	LBA4404	UBQ10::YC3.6	1	0	99.5	0
	2	180	168	EHA105	UBQ10::YC3.6	1	1 (α)	93.3	0.6
	3	200	198	GV3101	UBQ10::YC3.6	1	0	99.0	0
B	I	200	188	LBA4404	UBQ10::YC3.6	1	0	94.0	0
	II	200	189	EHA105	UBQ10::YC3.6	1	1 (a0)	94.5	0.53
	III	200	185	GV3101	UBQ10::YC3.6	1	0	92.5	0

The hygromycin resistant calli regenerated two plantlets: VN YC3.6 α and B YC3.6 a0 (Fig. 2A) and both of them showed the presence of the YC3.6 gene (Fig 2B).

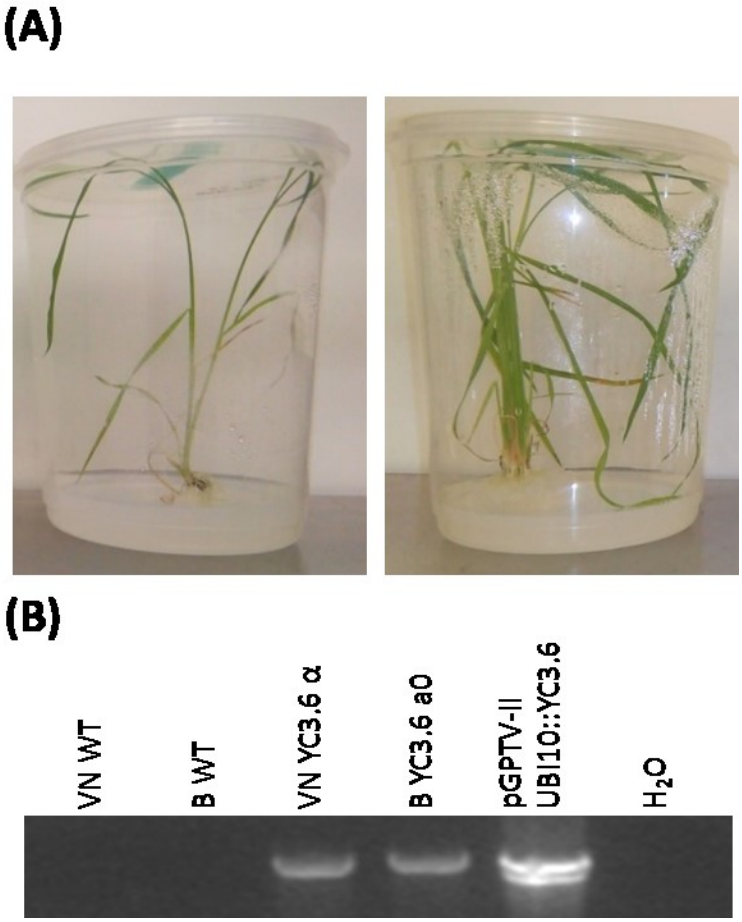

Figure 1. (A) Pictures of the transgenic plants VN YC3.6 α (left panel) and B YC3.6 a0 (right panel). (B) PCR amplification of transgene from genomic DNA of leaves of WT and transgenic plants.

Few roots from the transformed plants were cut and placed on N6 media supplemented with 2,4-D to produce callus. 11 and 3 calli were obtained from different roots of VN YC3.6 α and B YC3.6 a0 respectively. The calli obtained from VN YC3.6 α roots showed a bright fluorescence (Fig.2 A and B), while in the calli recovered from B YC3.6 a0 roots no fluorescence could be detected and were therefore discarded. VN YC3.6 α 4 fluorescent root-derived callus was put in liquid medium to start a suspension cell culture. However it showed to be not suitable for suspension cell culture establishment for its high morphogenetic capabilities (Fig. 2 D).

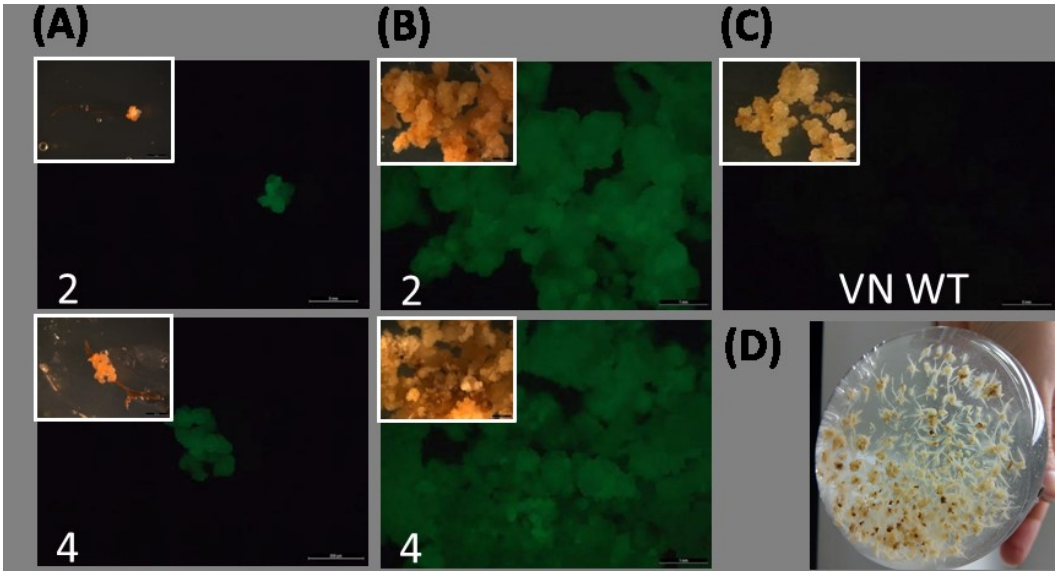

Figure 2. Production of transgenic calli from roots of the transformed plant VN YC3.6 α. (A) Two examples of growing callus from roots of VN YC3.6 α (2 and 4). (B) The same calli after 2 months in N6 medium. (C) VN WT callus (VN WT). (D) Suspension cell culture of VN YC3.6 α 4 showing high morphogenetic capabilities. Bright field images are showed in the insets. Stereo-microscope images were observed using identical parameters (scale bar=2 mm).

The VN YC3.6 α and B YC3.6 a0 plants were transferred in soil pots and grown in greenhouse (laboratory of Prof. Fornara, Department of Bioscience, University of Milan). Mature seeds were collected, and, to evaluate the presence of fluorescence in tissue cultures, few seeds from the transformed plants were sowed on N6 medium. At the same time, to detect fluorescence in roots and shoot, few seeds from the same transformed plants were sowed on MS ½ to obtaining seedlings.
Around 50% of the seeds-derived calli of VN YC3.6 α were fluorescent (positive, Fig.3).

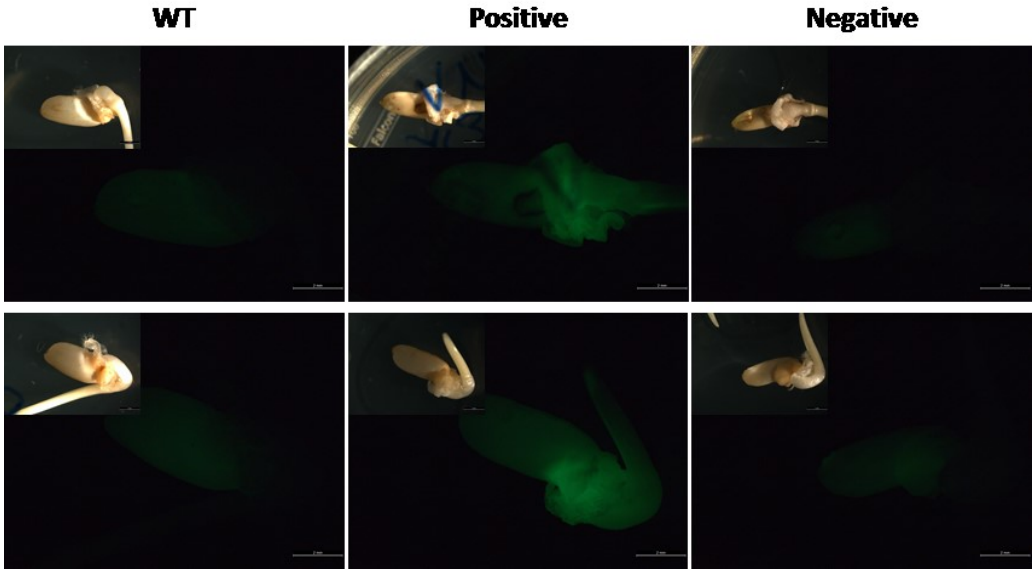

Figure 3. Segregation of GFP-positive and -negative seed-derived calli in the T1 generation of transgenic plants and WT plants. Upper panel: seed-derived calli of VN YC3.6 α; Lower panel: seed-derived calli of B YC3.6 a0. WT: WT seed-derived calli; Positive: fluorescent transgenic seed-derived calli; Negative: non-fluorescent transgenic seed-derived calli. Stereo-microscope images were observed using identical parameters (scale bar=2 mm).

Instead, no fluorescence was observed in the shoots or roots of 3 days old seedlings (Fig.4 A, middle panel), even if almost 50% of the seedlings showed some fluorescence at the level of the coleorhiza (Fig.4 A, upper panel). Similar results were observed for seeds-derived calli (Fig.3) and seedlings of B YC3.6 a0 (Fig.4 B). However, fluorescent roots were observed in 10 days old seedlings from both transformed plants' seeds (Fig.4 A and B lower panel, Fig.5).

Figure 4. Segregation of GFP-positive and -negative seedlings in the T1 generation of transgenic plants and WT plants. Upper panel: coleorhiza (scale bar=1mm); Middle panel: 3 days old seedlings (scale bar=2 mm); Lower panel: 10 days old seedlings' roots (scale bar=2 mm) (A) VN WT: seeds from WT VN plants; VN YC3.6 α positive: seeds from VN YC3.6 α plant showing fluorescent coleorhiza; VN YC3.6 α negative: seeds from VN YC3.6 α plant showing non-fluorescent coleorhiza. (B) B WT: seeds from WT B plants; B YC3.6 positive: seeds from B YC3.6 a0 plant showing fluorescent coleorhiza; B YC3.6 negative: seeds from B YC3.6 a0 plant showing non-fluorescent coleorhiza. Bright field images are showed in the insets. Stereo-microscope images were observed using identical parameters, unless otherwise specified.

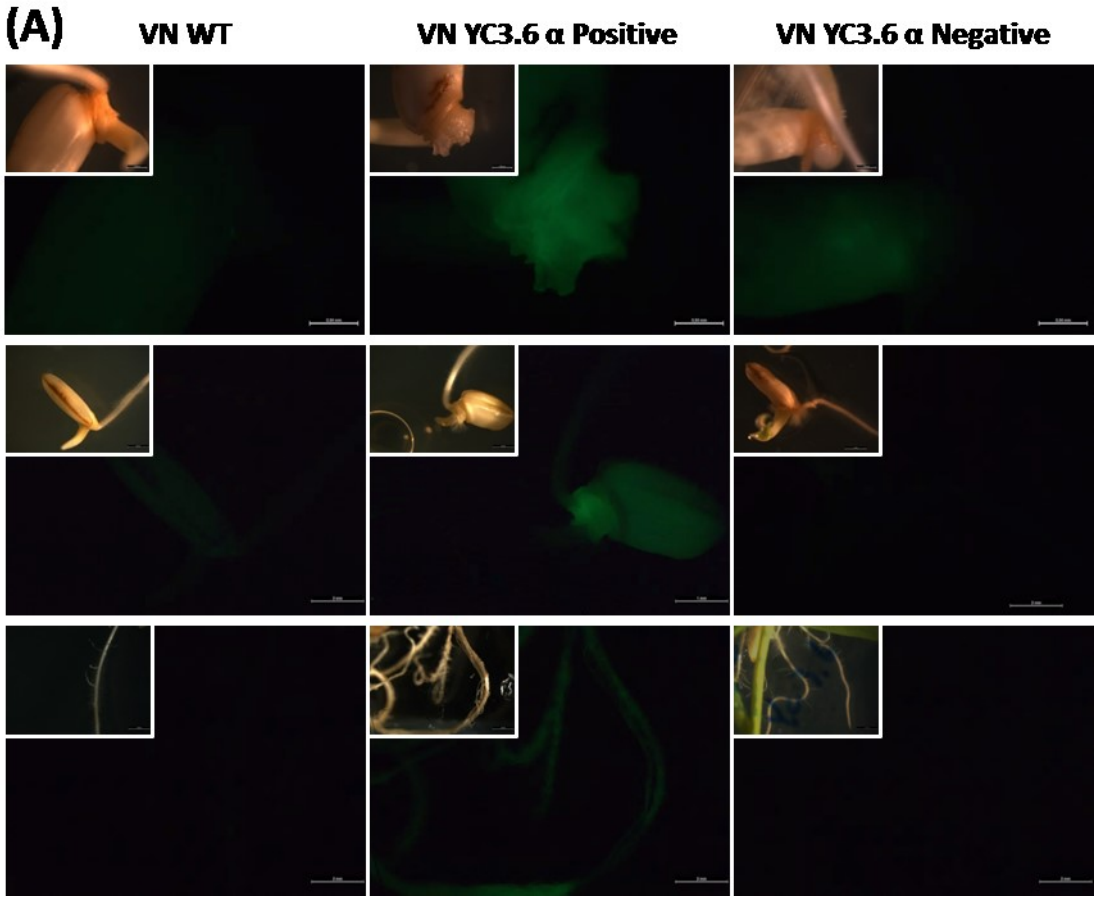
(A)
VN WT
VN YC3.6 α Positive
VN YC3.6 α Negative

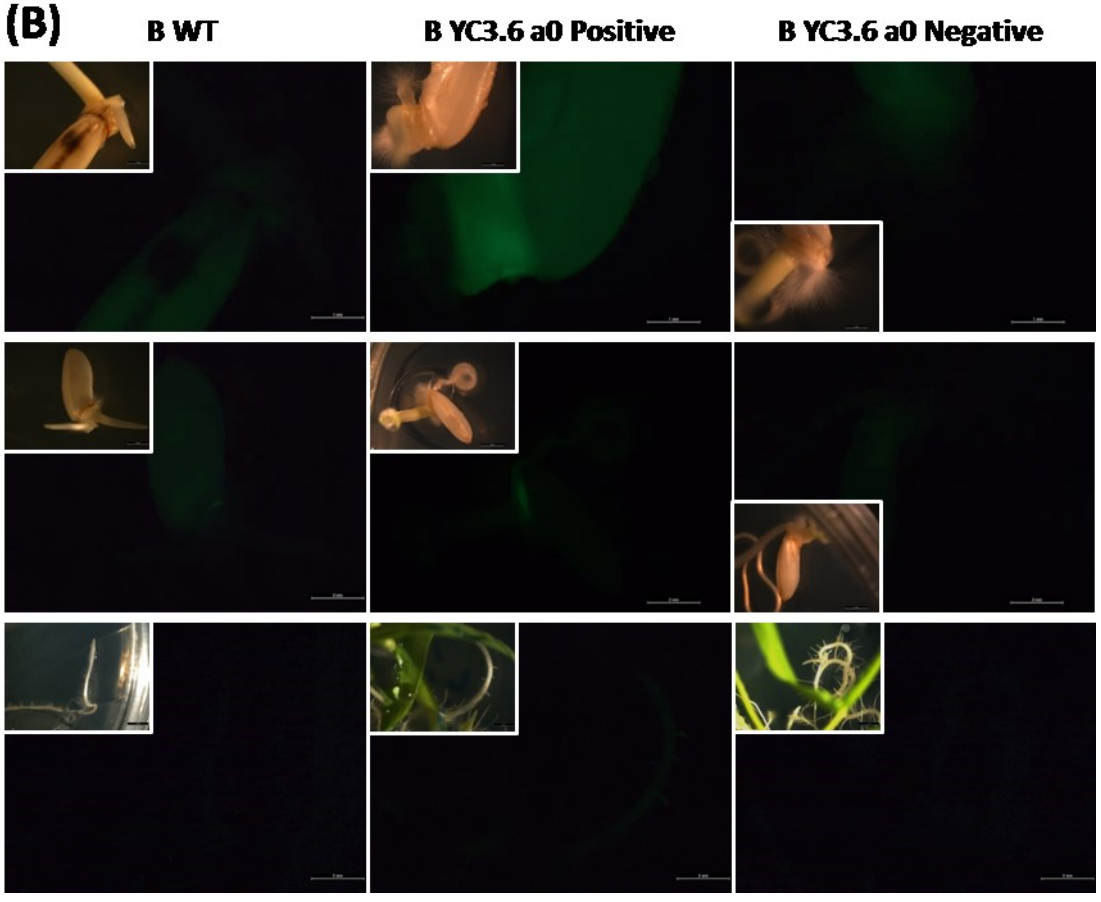
(B)
B WT
B YC3.6 a0 Positive
B YC3.6 a0 Negative

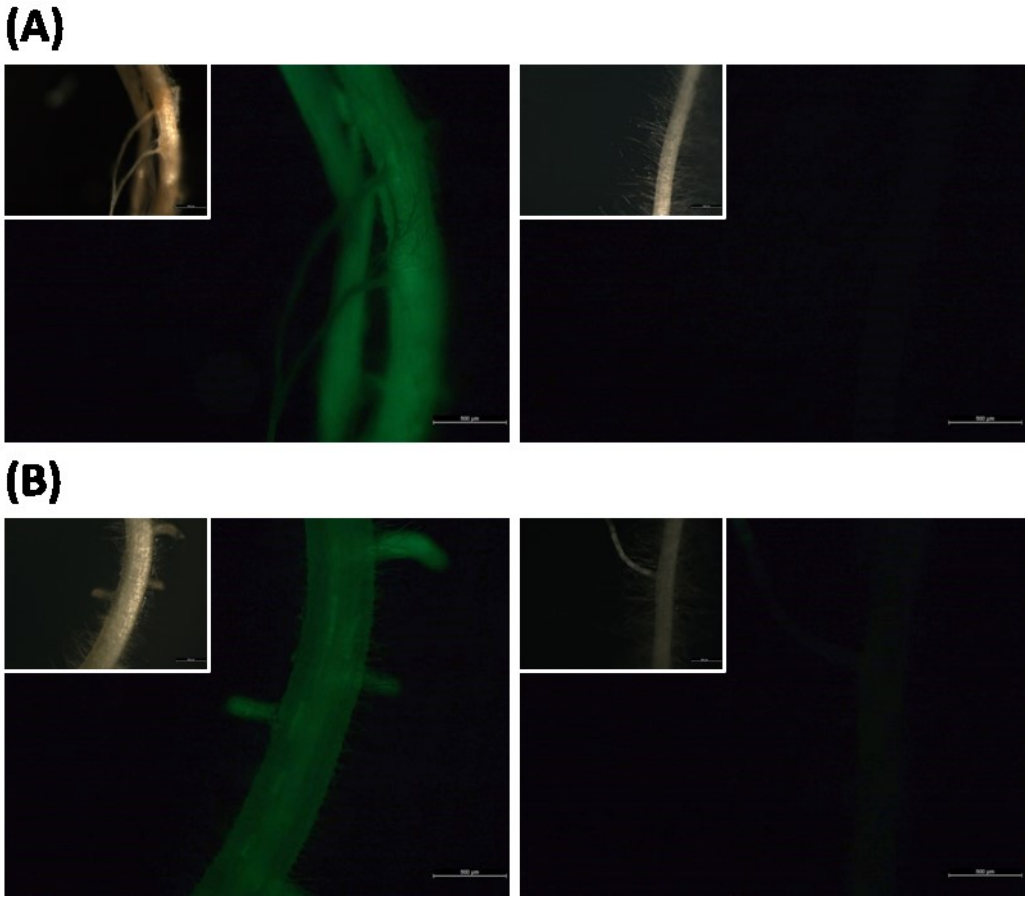

Figure 5. Roots of positive seedlings at higher magnification (scale bar=500 µm). (A) VN YC3.6 α seedlings (left panel), VN WT seedlings (right panel); (B) B YC3.6 a0 seedlings (left panel), B WT seedlings (right panel). Bright field images are showed in the insets. Stereo-microscope images were observed using identical parameters (scale bar=500 µm).

The number of seedlings with fluorescent coleorhiza and/or fluorescent roots are presented in Table II. Given the low number of seeds analyzed so far, this percentage must be taken with caution. More seedlings will be analyzed in the future.

Table II. Number of 3 and 10 days old seedlings with fluorescent/non-fluorescent (positive,+/negative,-) coleorhiza and/or roots.

		3 d seedlings	10 d seedlings		
	N° seeds	+ coleorhiza	+ coleorhiza + roots	+ coleorhiza - roots	- coleorhiza - roots
B YC3.6 a0	20	9	4	5	11
VN YC3.6 α	9	5	5	0	4

The absence of fluorescence in roots and shoots of the 3 days old seedlings derived from the transgenic plants may be due to developmental-dependent silencing problems or to the architecture of the roots at that stage. The primary root, which is the one present at 3 days post germination, is, in fact, thicker and thus maybe more difficult to analyze under a fluorescent

stereomicroscope. However, since none of the seedlings presenting a non-fluorescent coleorhiza showed fluorescent root at later stages, the analysis of coleorhiza fluorescence under the stereo-microscope may be used as an early selection of seedlings to use for Ca^{2+} analysis.
In conclusion of this first part, we selected the only strain among the three analyzed that gave positive results (EHA105), and we obtained transgenic plants. The seeds from these transgenic plants are suitable for Ca^{2+} analysis on seedlings, and may be also exploited as a source of YC3.6-expressing cells (calli).

II° set of experiments

The transformation efficiency for this first set of experiments was very low (around 0.5%) for both varieties, and positive results were obtained only with the *Agrobacterium* strain EHA105. To further optimize this protocol we decided to use EHA105 as *Agrobacterium* strain and adjusted other variables.
Since applying a drought stress to calli has been shown to facilitate the bacterial infection (Arenciba *et al*., 1998), a brief dehydration was imposed on the calli. This pre-treatment slightly increased the transformation efficiency that, in fact, reached the level of 1% (Table III).
Agrobacterium cell concentration prior to infection is an important factor for stable and efficient transformation. High concentrations of bacteria, in fact, can kill the cells or cause overgrowth of *Agrobacterium* on the medium while less numbers of bacteria can reduce the transformation efficiency. Therefore, bacterial concentration (OD_{600}) was adjusted to 0.6 or to 1 in AAM medium. The transformation efficiency with the lower concentration of *Agrobacteria* was far lower than when OD_{600} was 1. Higher bacterial concentration (OD_{600} 1) will therefore be selected for further optimization of the transformation experiments (Table III).

Table III. Effect of different *Agrobacterium* concentrations on Transformation efficiency.

	N° exp	N° seeds	N° calli	Strain	Construct	OD	N° clones	% Germination	% Trasformation
VN	4	200	195 $\frac{100}{95}$	EHA105	UBQ10::YC3.6	1	1 (β)	97.5	1
						0.6	0		0
	5	200	187 $\frac{90}{97}$	EHA105	UBQ10::YC3.6	1	2 (γ, θ)	93.5	2.22
						0.6	0		0
B	IV	210	207 $\frac{100}{107}$	EHA105	UBQ10::YC3.6	1	1 (a)	98.6	1
						0.6	0		0
	V	218	205 $\frac{100}{105}$	EHA105	UBQ10::YC3.6	1	1 (b)	94.0	1
						0.6	1 (c)		1
	VI	220	211 $\frac{100}{111}$	EHA105	UBQ10::YC3.6	1	1 (d)	95.9	1
						0.6	0		0
	VII	196	176 $\frac{100}{76}$	EHA105	UBQ10::YC3.6	1	1 (e)	89.8	1
						0.6	0		0

All calli were initially selected for hygromycin tolerance and then microscopically inspected for GFP fluorescence. 3 and 5 hygromycin-resistant calli of VN (VN YC3.6 β, γ, θ) and B (B YC3.6 a, b, c, d, e) respectively were obtained and they were all fluorescent (Fig.6).

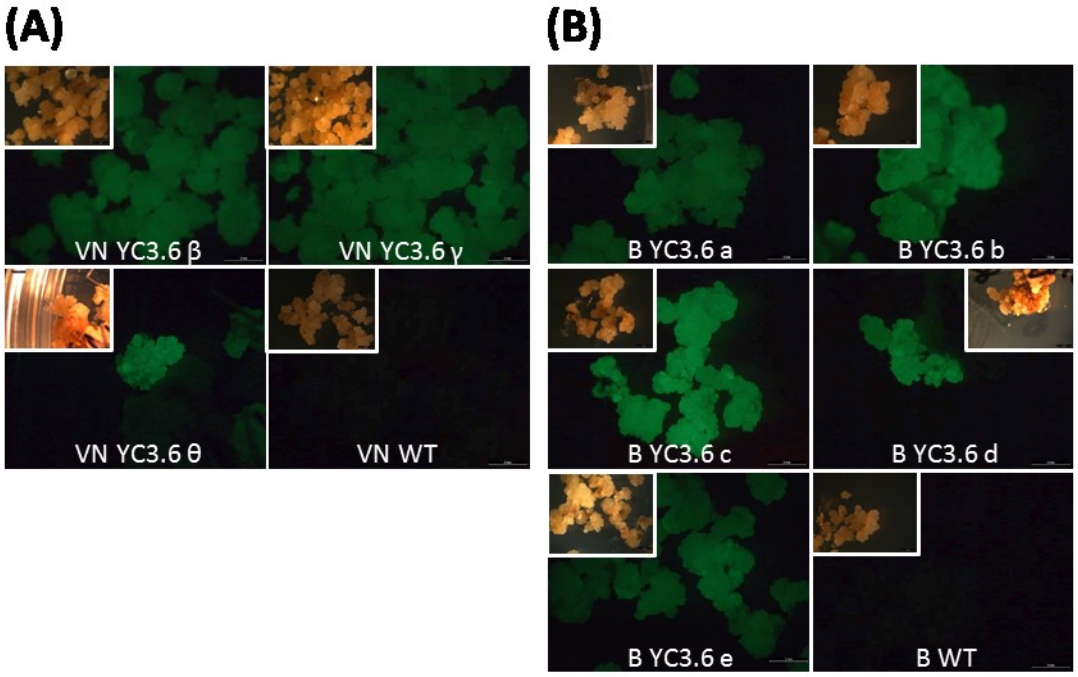

Figure 6. Production of transgenic calli after *Agrobacterium*-mediated transformation. After 1 month of selection vigorously growing calli with strong GFP signals were observed. Left panel: VN YC3.6 lines and VN control line (VN CTR); right panel: B YC3.6 lines and B control line (B CTR). Bright field images are showed in the insets.

Since VN YC3.6γ and B YC3.6a calli were producing friable callus, they were used to generate suspension cell cultures. After some time in liquid N6 medium, they were tested for YC3.6 calcium indicator functionality. In collaboration with the laboratory of Prof. Alex Costa (Department of Bioscience, University of Milan), we performed live cell imaging by applying an Imaging Buffer (IB) containing 500 mM NaCl for 8 min, and following FRET signal after the exchange to the same buffer without NaCl (hypo-osmotic stress). The cameleon probe resulted to be functional in both genotypes. In fact, a clear calcium transient following the stimulus could be recorded in our suspension cell cultures (Fig.7 A). Interestingly, initial experiments show B inducing a more intense Ca^{2+} transient with respect to VN following the stress (Fig.7 B). Therefore, these suspension cell cultures will be a useful tool to study salt stress-induced Ca^{2+} signalling.

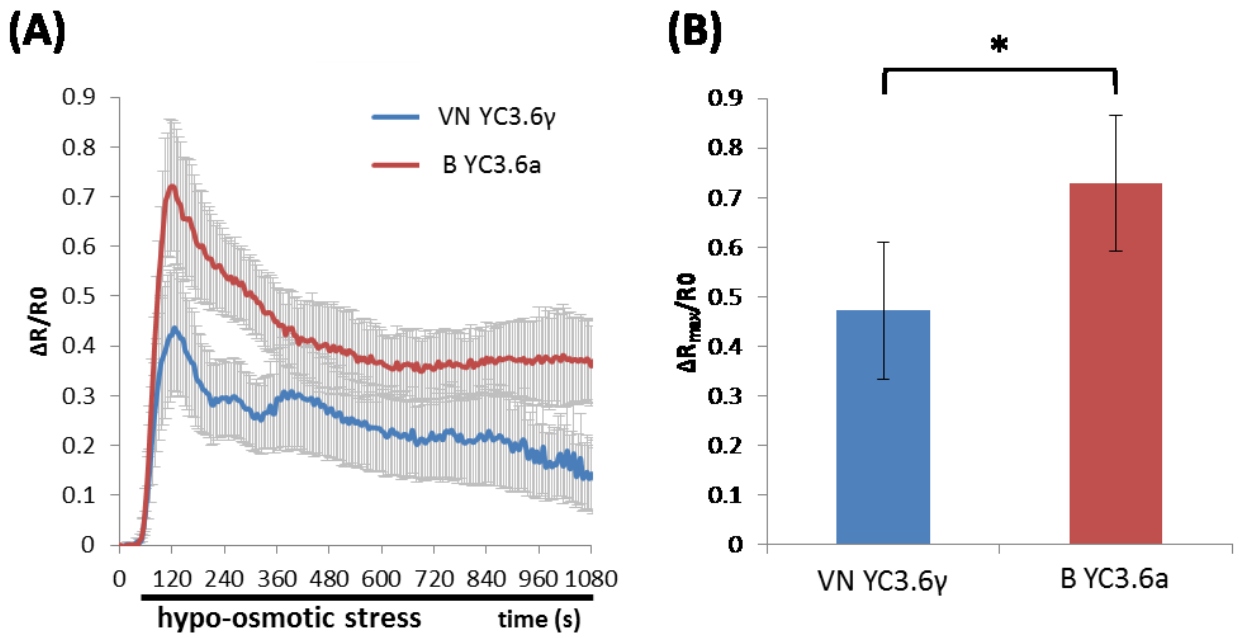

Figure 7. Ca^{2+} dynamics in transgenic suspension cell cultures treated with osmotic stress. (A) Presentation of normalized change in ratio values (ΔR/R0) corresponding to changes in Ca^{2+} concentration upon treatment with hypo-osmotic stress in VN YC3.6γ and B YC3.6a suspension cell cultures. (B) Maximal relative amplitude of FRET ratio ($\Delta R_{max}/R0$). The ratio graphs represent the mean +/- confidence interval ($p<0.05$), $n \geq 7$. *$p<0.05$ (*t* test).

4.3 Conclusions

In this work we set up a transformation protocol for the recalcitrant Italian rice varieties VN and B. We selected EHA105 and OD_{600} 1 as the more suitable strand and bacterial concentration for transformation, respectively. The additional dehydration step may have played a role in increasing the transformation efficiency. We should underline that the selection in the I° set of experiments was performed on regeneration plantlets that may have underestimated the real transformation efficiency. Seeds from the regenerated plants obtained in the I° set of experiments developed seedlings showing fluorescence in roots 10 days after sowing. Notably, both seed derived-calli produced in the I° set of experiments and calli obtained in the II° set of experiments were highly fluorescent. Moreover, the cameleon sensor was functional in the two suspension cell cultures established from transgenic calli of both variety. Therefore, both seedlings and calli of VN and B transgenic lines will be used to study salt-induced Ca^{2+} signalling at different levels of complexity.

4.4 Materials and Methods

Culture media

The Supplementary Table I lists all the culture media used in the present study.

Plant material and callus induction

Mature dry seeds of VN and B varieties were used in this study. Scutellar calli were used as the target material for transformation and regeneration. For this purpose, seeds were surface-sterilized with 70% ethanol (v/v) for 1 min, 20 min in 3.5% (v/v) bleach and a drop of TWEEN-20 with shaking at 90 rpm, followed by 5 min in 3.5% (v/v) bleach. Seeds were then washed 5 times with sterile distilled water, inoculated on N6 medium and incubated at 25°C in dark. After 14 days in dark, seeds and shoots were removed from calli. The calli were subcultured again onto fresh N6 and kept for 4 days in the same conditions before transformation with *Agrobacterium tumefaciens*.

Agrobacterium strains and construct used for transformation

The construct used in this study is the pGPTVII.Kan vector harbouring the UBQ10::YC3.6-Hyg transgene (Krebs *et al*., 2012), which was kindly provided by Professor Alex Costa (Department of Bioscience, University of Milan, Italy). This plasmid was amplified in DH5α *Escherichia coli* and transformed into three commonly used strains of *A. tumefaciens*; LBA4404, EHA105 and GV3101. Briefly, 1 µg of plasmid was added to an aliquot of competent *Agrobacterium*. The aliquot was frozen in liquid nitrogen and incubated at 37°C for 5 min before adding 1 ml of YEP medium. After 2 h on a rotatory shaker at 28°C, bacteria were spread on LB media plus antibiotics for selection of transformed colonies (100 mg/l rifampicin, 25 mg/l of streptomycin and 50 mg/l kanamycin for LBA4404, 100 mg/l rifampicin and 50 mg/l kanamycin for EHA105 and 100 mg/l rifampicin, 5 mg/l of tetracyclin, 50 mg/l gentanamycin and 50 mg/l kanamycin for GV3101).

Preparation of Agrobacterium culture

Primary *Agrobacterium* culture was prepared by inoculating a single colony in 5 ml of YEP medium supplemented with the proper antibiotics. The culture was incubated for 16-20 h on a rotatory incubator shaker at 180 rpm in the dark at 28°C. Secondary culture was prepared in a 500 ml flask containing 150 ml YEP medium (supplemented with same antibiotics as used for primary culture) by adding 5 ml of the primary culture and grown under similar conditions overnight. The day of transformation, *Agrobacterium* cells were pelleted by centrifugation at 4000 × g for 15 min. The cells were resuspended in AAM medium containing 150µM acetosyringone to adjust the OD_{600} of the bacterial suspension to 0.6 or 1.

Co-cultivation and selection of transformed calli

The 4 day subcultured calli were collected: for part of the transformation experiments they were dried for 10 min under the laminar flow before *Agrobacterium* inoculation, for the other part calli were directly Agro-infected. Agro-infection was performed by immersing the calli in the *Agrobacterium* culture for 20-25 min on a rotatory shaker. After that, calli were dried on sterile filter paper for 10 min, transferred to plates containing filter paper moistened with AAM medium + 150 µM acetosyringone and incubated at 25°C in the dark. After 3 days in co-coltivation, calli were rinsed 4 times with sterile distilled water and 20 min with 250 mg/l cefotaxime and 0.1% PPM in sterile distilled water, dried on sterile filter paper and transferred onto Selection Medium I. After 14 days in I selection, calli were shifted to the Selection Medium II and maintained at 25°C in the dark. After II selection for 14 days, the calli that were not dried before Agro-infection were moved to Pre-Regeneration Medium, while the others were transferred to fresh Selection Medium II and allowed to proliferate in the dark.

Regeneration of calli after transformation

After 7 days in Pre-Regeneration Medium in the dark, calli were shifted to Regeneration Medium and incubated in light until shoot started to grow. For development of roots, the regenerated shoots were shifted to sterile plastic containers with Rooting medium and maintained in light until a fully regenerated plantlet was formed. Plants were then transferred to soil pots and maintained in a growth chamber until seeds developed in collaboration with Professor Fabio Fornara (Department of Bioscience, University of Milan, Italy).

Molecular analysis of putative transgenic plants

To confirm the presence of transgene in the regenerated plants, we analyzed these plants along with wild type (WT) lines through PCR analysis. Total genomic DNA was extracted and was used for PCR. Briefly one leaf was grounded in liquid nitrogen and homogenized in 500 µl of Extraction Buffer (100 mMTris/HCl pH 8, 500 mM NaCl and 50 mM EDTA). 35 µl of SDS 20% were added and the mixture was put at 60°C for 5 min. 130 µl of KO-Ac 5 M were added and the mixture was centrifuged to eliminate the cellular debris. The precipitation of DNA was achieved by adding 500 µl of isopropanol to the supernatant and by putting it at -20°C for 20 min. After centrifugation, the pellet was washed twice with 70% ethanol and air-dried before resuspension in sterile distilled water. PCR was performed using specific primers binding to the ubiquitin promoter and to the cameleon moiety:

forward 5'-CATGGGTACCGTCGACGAGTCAGTAATAAACG-3'
reverse 5'-GTCATCATTTGTACAAACTCTTCA-3'.

The PCR products were analyzed on 0.8% agarose gel containing GelRed and visualized under gel documentation unit.

Microscopic selection of transformed seedlings and calli

Growing calli were analyzed for fluorescence. Calli were observed under a fluorescent stereomicroscope (Leica MZ16 F Fluorescence Stereomicroscope) using a GFP filter. Fluorescent (positive) calli were kept and subcultured every 3 weeks in N6 media. Seeds from the regenerated plant were sown in N6 media for callus induction and in half strength MS media for seedling growth. Both calli and seedling were observed at the stereo-microscope, and divided as positive if fluorescent and negative if no fluorescence could be detected.

Suspension cell culture establishment

Some of the transformed calli were put in liquid N6 media to give suspension cell cultures. After stabilization, 2 ml of packed cells were subcultured in 50 ml of fresh N6 liquid media every 10 days.

Ca^{2+} imaging

To investigate whether the cameleon sensor was functional, transgenic suspension cell cultures were analyzed according to Behera and Kudla (2013). Some cells aggregates from the suspension cell cultures were placed inside a perfusion chamber containing Imaging Buffer (IB; 5 mM KCl, 10 mM MES and 10 mM $CaCl_2$, pH 5.8, adjusted with TRIS). The samples were perfused in the IB (continuous flow-through) for 2 min before replacing the buffer with IB containing 500 mM NaCl for 8 min. The samples were monitored after the buffer was exchanged back to the IB without NaCl.

Ca^{2+} imaging data analysis

Fluorescence intensity was determined over the regions of interest (ROIs) using the software FIJI (Schindelin J. *et al*., 2012). Background subtraction was performed independently for both channels. YFP and CFP emissions of the analyzed ROIs were used for the ratio (Rt) calculation (YFP/CFP). We calculated the change in ratio Rt - R0 (ΔR), where R0 is the basal ratio before the application of the stimulus and then normalized to the basal ratio (ΔR/R0) and plotted versus time.

4.5 Supplementary Material

Table S1 Culture media used for transformation

Media for cell cultures

Abbreviations: 2,4-D, 2,4-Dichlorophenoxyacetic acid; PPM, Plant Preservative Mixture; ABA, Abscissic Acid; 6-BAP, 6-Benzylaminopurine; NAA, Naphthaleneacetic Acid.

Basal N6-medium (pH 5.8)

Components	Concentration (mg/l)
$(NH_4)_2SO_4$	463
KNO_3	2830
$MgSO_4$	90.27
KH_2PO_4	400
$CaCl_2$	125.33
FeNaEDTA x 2 H_2O	36.7
H_3BO_3	1.6
$MnSO_4$ x H_2O	3.33
$ZnSO_4$ x 7 H_2O	1.5
KI	0.8
Glycine	2
Nicotinic Acid	0.5
Thiamine Hydrocloride	1
Pyridoxal Hydrocloride	0.5

N6 Medium (pH 5.8)

Components	Concentration (mg/l)
Basal N6-medium	
Sucrose	30000
2,4-D	2
Plant Agar	8000

Selection Medium I (pH 5.8)

Components	Concentration (mg/l)
N6 medium	
Casamino Acid	300
Glutamine	500
Cefotaxime	400
Vancomycin	100
Hygromycin	25
Plant Agar	8000

PPM	0.1%

Selection Medium II (pH 5.8)

Components	Concentration (mg/l)
N6 medium	
Casamino Acid	300
Glutamine	500
Cefotaxime	400
Vancomycin	100
Hygromycin	50
Plant Agar	8000

PPM	0.1%

Pre-Regeneration Medium (pH 5.8)

Components	Concentration (mg/l)
Basal N6-medium	
Sucrose	30000
Casamino Acid	300
Glutamine	500
Cefotaxime	100
Vancomycin	100
Hygromycin	50
ABA	5
6-BAP	2
NAA	1
Plant Agar	8000

PPM	0.05%

Regeneration Medium (pH 5.8)

Components	Concentration (mg/l)
Basal N6-medium	
Sucrose	30000
BAP	3
NAA	0.5
Plant Agar	8000
Hygromycin	25

PPM	0.05%

Media for *Agrobacterium*

LB medium

Components	Concentration (mg/l)
Yeast extract	5000
Tryptone	10000
NaCl	5000
Agar	8000

YEP medium

Components	Concentration (mg/l)
Yeast extract	10000
Tryptone	10000
NaCl	5000

AAM (pH 5.2)

Components	Concentration (mg/l)
$MgSO_{4\ x}$	250
CaCl2	150
NaH_2PO_4	150
fe-EDTA	40
$MnSO_{4\ x}$	10
$ZnSO_4$	2.0
$CuSO_{4\ H}$	0.025
$COCl_2$	0.025
KI	0.75
H_3BO_3	3.0
Na_2MoO_4	0.25
Casamino Acid	500
Glycine	7.5
L-Arginine	176.7
L-Glutamine	900
L-Aspartic Acid	300
Myo-Inositol	100
Nicotinic Acid	1.0
Pyridoxine HCl	1.0
Thiamine HCl	10
Sucrose	68.5
Glucose	36
KCl	3

Chapter 5:

Main Conclusions

Salt tolerance is a complex trait varying between and within species. The strategies adopted by plants to cope with salt-stress are numerous, but while a tolerant variety may present some of these traits, not all of them are present simultaneously in the same variety. Therefore, a comprehensive understanding on how plants respond to salt stress at different levels is mandatory for the development of salt-tolerant varieties.

My Ph.D. project fits in the frame of the analysis of salt tolerance mechanisms in two Italian rice varieties differing in salt-sensitivity, the tolerant Baldo (B) and the sensitive Vialone Nano (VN). Morpho-physiological, biochemical and molecular analyses were combined together to explain their different sensitivity. Interestingly, B plants proved to be able to respond rapidly to salt stress, by setting up an adaptation program. In VN plants, instead, the chaotic regulation of genes expression led to the inability to set up a specific response, and thus early senescence was induced. Among the salt tolerance mechanisms adopted by B plants, key traits were the maintenance of a high $[K^+]/[Na^+]$ ratio, confirmed by the fast upregulation of K^+ channels and transporters genes, and the preferential Na^+ allocation in the roots. A fast and proper response to a stimulus, as the one showed by B plants, is the result of a fast and proper sensing and signalling. Molecular analyses performed in plants show differences in salt-induced signalling pathways, either as in timing or as in signalling transduction components involved that could cause the different outcome in the two varieties when exposed to salt stress conditions.

The main objective of my project was therefore to analyse the role of different signalling molecules in salt stress response in the two varieties. To achieve this goal, suspension cell cultures from both varieties were produced and characterized. Notably, the two cell lines showed the same difference in salt sensitivity as in plant, with B cells being more salt-tolerant and VN cells more sensitive, meaning that differences in salt sensitivity were present at cellular level too, and were not only related to intrinsic tissue or organ characteristics. Consistently, VN cells undergo cell death, while in B cells an adaptation response is induced. In VN cells, salt stress induced high levels of H_2O_2 and NO, that likely represent signals for Programmed Cell Death (PCD) induction instead of specific salt stress response, as also demonstrated by the upregulation of H_2O_2- and NO-dependent PCD associated genes in this sensitive line. Conversely, in B cells the basal stronger antioxidant system can explain the maintenance of a low basal level of H_2O_2, allowing the production of fine-tuned H_2O_2 signatures that can set up salt-tolerance mechanisms. In fact, only a very early and transient peak in H_2O_2 production is observed in the tolerant cell line that may play the role of an early signal to induce a prompt tolerance response. Consistent with this, B cells upregulates genes involved in H_2O_2 signalling, known for being involved in salt tolerance, earlier than VN cells.

Moreover, the ability to maintain a high $[K^+]/[Na^+]$ ratio seems to be an important trait for B cells. Interestingly, also in cell cultures timing seems to be an important factor for salt-stress tolerance, in fact, mirroring the behavior of plants, B cells upregulate K^+ channels and transporters genes earlier than the sensitive line.

Although we did not yet investigate the possible involvement of ROS in K^+ homeostasis under salt stress, ROS have previously been suggested to activate outwardly-rectifying K^+ channels, in particular during the initial phases of salt stress, increasing K^+ leakage from the cell. We can therefore hypothesize that the higher H_2O_2 level in VN treated cells might be correlated with the observed decrease in $[K^+]/[Na^+]$ ratio. Further investigation will be needed to confirm this hypothesis.

Therefore, the analysis in cell cultures showed that timing and intensity of salt stress-induced signals are indeed important to discriminate between the induction of an adaptive response or of PCD. In this regard, the stronger antioxidant system owned by B cells maintains low the H_2O_2 level

and, by doing so, let H_2O_2 playing the role of a signalling molecule in activating tolerance mechanisms.
In addition, the ability of B to maintain high the K^+ content, thanks to a rapid upregulation of K^+ channels and transporters genes, represent another key trait required for salt stress tolerance. Notably, this strategy is present both at cellular and at whole-plant level in this tolerant variety.
In conclusion, the results obtained during my project highlight that salt tolerance in B variety rely mainly in a prompt and fine-tuned response. Early induced genes were found involved in such tolerance that can be exploited as molecular markers for the selection of new Italian rice varieties more tolerant to high salinity.
Lastly, in the final part of my project, transgenic plants encoding the calcium sensor Cameleon were obtained. They will be used in next experiments for the analysis of Ca^{2+} early signalling upon salt stress superimposition.

References

Abogadallah G. M. (2010) Antioxidative defense under salt stress. *Plant Signaling and Behavior* **5,** 369–374.

Agarwal P.K., Agarwal P., Reddy M.K. and Sopory S.K. (2006) Role of DREB transcription factors in abiotic and biotic stress tolerance in plants. *Plant Cell Reports* **25,** 1263–1274.

Ahmad I., Devonshire J., Mohamed R., Schultze M. and Maathuis F.J. (2016) Overexpression of the potassium channel TPKb in small vacuoles confers osmotic and drought tolerance to rice. *New Phytologist* **209,** 1040-1048.

Akbar M., Yabuno T. and Nakao S. (1972) Breeding for saline-resistant varieties of rice. I. Variability for salt tolerance among some rice varieties. *Japanese Journal of Breeding* **22,** 277–284.

Amin U.S.M., Biswas S., Elias S.M., Razzaque S., Haque T., Malo R. and Seraj Z.I. (2016) Enhanced salt tolerance conferred by the complete 2.3 kb cDNA of the rice vacuolar Na^+/H^+ antiporter gene compared to 1.9kb coding region with 5'UTR in transgenic lines of rice. *Frontiers in Plant Science* **7,** 14.

Anders S., McCarthy D.J., Chen Y., Okoniewski M., Smyth G.K., Huber W. and Robinson M.D. (2013) Count-based differential expression analysis of RNA sequencing data using R and Bioconductor. *Nature Protocols* **8**, 1765–1786.

Andrés Z., Pérez-Hormaeche J., Leidi E.O., Schlücking K., Steinhorst L., McLachlan D.H., Schumacher K., Hetherington A.M., Kudla J., Cubero B. and Pardo J.M. (2014) Control of vacuolar dynamics and regulation of stomatal aperture by tonoplast potassium uptake. *Proceedings of the National Academy of Sciences U S A* **111,** E1806-1814.

Apel K. and Hirt H. (2004) Reactive oxygen species: metabolism, oxidative stress, and signal transduction. *Annual Reviews of Plant Biology* **55**, 373–399.

Apse M.P., Aharon G.S., Snedden W.A. and Blumwald, E. (1999) Salt tolerance conferred by overexpression of a vacuolar Na^+/H^+ antiport in Arabidopsis. *Science* **285,** 1256-1258.

Arencibia A.D., Carmona E.R., Tellez P., Chan M.T., Yu S.M., Trujillo L.E. and Oramas, P. (1998) An efficient protocol for sugarcane (*Saccharum* spp. L.) transformation mediated by *Agrobacterium tumefaciens*. *Transgenic Research* **7,** 213–222.

Asada K. (1999) The water-water cycle in chloroplasts: scavenging of active oxygens and dissipation of excess photons. *Annual Reviews of Plant Physiology* **50,** 601–639.

Azzabi G., Pinnola A., Betterle N., Bassi R. and Alboresi A. (2012) Enhancement of non-photochemical quenching in the Bryophyte *Physcomitrella patens* during acclimation to salt and osmotic stress. *Plant Cell Physiology* **53,** 1815–1825.

Bagdi D.L., Shaw B.P., Sahu B.B. and Purohit G.K. (2015) Real time PCR expression analysis of gene encoding p5cs enzyme and proline metabolism under NaCl salinity in rice. *Journal of Environmental Biology* **36,** 955–961.

Bánfi B., Tirone F., Durussel I., Knisz J., Moskwa P., Molnár G.Z., Krause K.H. and Cox J.A. (2004) Mechanism of Ca^{2+} activation of the NADPH oxidase 5 (NOX5). *Journal of Biological Chem*istry **279,** 18583-18591.

Banuelos M.A., Garcia de blas B., Cubero B. and Rodriguez-Navarro A. (2002) Inventory and functional characterization of the HAK potassium transporters of rice. *Plant Physiology* **130,** 784–795.

Barr H.D. and Weatherley P.E. (1962) A re-examination of the relative turgidity technique for estimating water deficit in leaves. *Australian Journal of Biological Science* **15,** 413-428.

Barragán V., Leidi E.O., Andrés Z., Rubio L., De Luca A., Fernández J.A., Cubero B. and Pardo J.M. (2012) Ion exchangers NHX1 and NHX2 mediate active potassium uptake into vacuoles to regulate cell turgor and stomatal function in Arabidopsis. *Plant Cell* **24,** 1127-1142.

Bassil E., Coku A. and Blumwald E. (2012) Cellular ion homeostasis: emerging roles of intracellular NHX Na^+/H^+ antiporters in plant growth and development. *Journal of Experimental Botany* **63:** 5727-5740.

Batistič O. and Kudla J. (2012) Analysis of calcium signaling pathways in plants. *Biochimica et Biophysica Acta* **1820,** 1283–1293

Baxter A., Mittler R. and Suzuki N. (2013) ROS as key players in plant stress signalling. *Journal of Experimental Botany* doi:10.1093/jxb/ert375.

Beauchamp C.O., Fridovich I. (1971): Superoxide dismutase: improved assays and an assay applicable to acrylamide gels. *Analytical Biochemistry* **44,** 276–287.

Behera S. and Kudla J. (2013) High-resolution imaging of cytoplasmic Ca^{2+} dynamics in Arabidopsis roots. *Cold Spring Harb Protocols* **2013,** 665–669.

Bellincampi D., Dipierro N., Salvi G., Cervone F. and De Lorenzo G. (2000) Extracellular H_2O_2 induced by oligogalacturonides is not involved in the inhibition of the auxin-regulated rolB gene expression in tobacco leaf explants. *Plant Physiology* **122,** 1379-1385.

Benjamini Y. and Hochberg Y. (1995) controlling the false discovery rate: a practical and powerful approach to multiple testing. *Journal of the Royal Statistical Society Series B* **57,** 289–300.

Bertazzini M. and Forlani G. (2011) Differential sensitivity of Italian rice cultivars to salt stress conditions. *Proceedings of the AGI-SIBV-SIGA Joint Meeting*, Assisi, September 19-22, 3A.11, ISBN: 978-88-904570-2-9.

Bertl A., Reid J. D., Sentenac H. and Slayman C. L. (1997) Functional comparison of plant inward-rectifier channels expressed in yeast. *Journal of Experimental Botany* **48,** 405–413

Blumwald E. (2000) Sodium transport and salt tolerance in plants *Current Opinion in Cell Biology* **12,** 431–434.

Bohnert H.J. and Shen B. (1999) Transformation and compatible solutes. *Scientia horticulturae* **78,** 237-260.

Boursiac Y., Chen S., Luu D-T., Sorieul M., van den Dries N. and Maurel C. (2005) Early effects of salinity on water transport in *Arabidopsis* roots: Molecular and cellular features of aquaporin expression. *Plant Physiology* **139**, 790–805.

Bray E.A., Bailey-Serres J. and Weretilnyk E. (2000) Responses to abiotic stresses. *Biochemistry and Molecular Biology of Plants*, B. Buchanan, W. Gruissem and R. Jones (eds), p 1160, *American Society of Plant Physiologists*.

Bradford M.M. (1976) A rapid and sensitive method for the quantitation of microgram quantities of protein utilizing the principle of protein-dye binding. *Analytical Biochemistry* **72,** 248-254.

Carraretto L., Formentin E., Teardo E., Checchetto V., Tomizioli M., Morosinotto T., Giacometti G.M., Finazzi G. and Szabó I. (2013) A Thylakoid-Located Two-Pore Potassium Channel Controls Photosynthetic Light Utilization in Plants. *Science* **342(6154),**114-118.

Chen Z., Cuin T.A., Zhou M., Twomey A., Naidu B.P. and Shabala S. (2007) Compatible solute accumulation and stress-mitigating effects in barley genotypes contrasting in their salt tolerance. *Journal of Experimental Botany* **58(15-16),** 4245-4255.

Cotsaftis O., Plett D., Shirley N., Tester M. and Hrmova M. (2012) A two-staged model of Na^+ exclusion in rice explained by 3D modeling of HKT transporters and alternative splicing. *PLoS One* **7,** e39865.

Counce P.A., Keisling T.C. and Mitchell A.J. (2000) A uniform, objective, and adaptive system for expressing rice development. *Crop Science* **40,** 436–443.

Cuin T.A. and Shabala S. (2008) Compatible solutes mitigate damaging effects of salt stress by reducing the impact of stress-induced reactive oxygen species. *Plant Signaling and Behavior* **3,** 207–208.

De Gara L., Locato V., Dipierro S. and de Pinto M.C. (2010) Redox homeostasis in plants. The challange of living with endogenous oxygen production. *Respiratory Physiology and Neurobiology* **173S,** 13-19.

Delledonne M., Zeier J., Marocco A. and Lamb C. (2001) Signal interactions between nitric oxide and reactive oxygen intermediates in the plant hypersensitive disease resistance. *Proceedings of the National Academy of Sciences USA* **98,** 13454–13459

Demidchik V., Cuin T.A., Svistunenko D., Smith S.J., Miller A.J., Shabala S., Sokolik A. and Yurin V. (2010) Arabidopsis root K^+-efflux conductance activated by hydroxyl radicals: Single-channel properties, genetic basis and involvement in stress-induced cell death. *Jounal of Cell Science* **123,** 1468–1479.

de Pinto M.C., Locato V., Sgobba A., Romero-Puertas M. del C., Gadaleta C., Delledonne M. and De Gara L. (2013) S-nitrosylation of ascorbate peroxidase is part of programmed cell death signaling in tobacco bright yellow-2 cells. *Plant Physiology* **163,** 1766-75.

de Pinto M.C., Locato V. and De Gara L. (2012) Redox regulation in plant programmed cell death. *Plant, Cell and Environment* **35(2),** 234-244.

de Pinto M.C., Paradiso A., Leonetti P. and De Gara L. (2006) Hydrogen peroxide, nitric oxide and cytosolic ascorbate peroxidase at the crossroad between defence and cell death. *Plant Journal* **48,** 784–795.

de Pinto M.C., Tommasi F. and De Gara L. (2002) Changes in the antioxidant systems as part of the signaling pathway responsible for the programmed cell death activated by nitric oxide and reactive oxygen species in tobacco Bright-Yellow 2 cells. *Plant Physiology* **130,** 698-708.

de Pinto M.C., Tommasi F. and De Gara L. (2000) Enzymes of the ascorbate biosynthesis and ascorbate-glutathione cycle in cultured cells of tabacco Bright Yellow 2. *Plant Physiology and Biochemistry* **38,** 541-550

de Pinto M.C., Francis D. and De Gara L. (1999) The redox state of the ascorbate-dehydroascorbate pair as a specific sensor of cell division in tobacco BY-2 cells. *Protoplasma* **209,** 90-97.

Diaz-Vivancos P., Faize M., Barba-Espin G., Faize L., Petri C., Hernández J.A. and Burgos L. (2013) Ectopic expression of cytosolic superoxide dismutase and ascorbate peroxidase leads to salt stress tolerance in transgenic plums. *Plant Biotechnology Journal* **11,** 976–985.

Dionisio-Sese M.L. and Tobita S. (1998) Antioxidant responses of rice seedlings to salinity stress. *Plant Science* **135,**1-9.

Donaldson L., Ludidi N., Knight M.R., Gehring C. and Denby K. (2004) Salt and osmotic stress cause rapid increases in *Arabidopsis thaliana* cGMP levels. *FEBS Letters* **569,** 317–320.

Dubiella U., Seybold H., Durian G., Komander E., Lassig R., Witte C.P., Schulze W.X. and Romeis T. (2013) Calcium-dependent protein kinase/NADPH oxidase activation circuit is required for rapid defence signal propagation. *Proceedings of the National Academy of Sciences USA* **110,** 8744-8749.

Du H., Wang N., Cui F., Li X., Xiao J. and Xiong L. (2010) Characterization of the beta-carotene hydroxylase gene DSM2 conferring drought and oxidative stress resistance by increasing xanthophylls and abscisic acid synthesis in rice. *Plant Physiology* **154,** 1304–1318.

Erickson E., Wakao S. and Niyogi K.K. (2015). Light stress and photoprotection in *Chlamydomonas reinhardtii*. *Plant Journal* **82,** 449-465.

Evans M.J., Choi W.G, Gilroy S. and Morris R.J. (2016) A ROS-assisted calcium wave dependent on AtRBOHD and TPC1 4 propagates the systemic response to salt stress in Arabidopsis roots. *Plant Physiology* DOI:10.1104/pp.16.00215

Faiyue B., Vijayalakshmi C., Nawaz S., Nagato Y., Taketa S., Ichii M., Al-Azzawi M.J. and Flowers T.J. (2010) Studies on sodium bypass flow in lateral rootless mutants lrt1 and lrt2, and crown rootless mutant crl1 of rice (*Oryza sativa* L.). *Plant Cell and Environment* **33,** 687–701.

Falda M., Toppo S., Pescarolo A., Lavezzo E., Di Camillo B., Facchinetti A., Cilia E., Velasco R. and Fontana P. (2012) Argot2: a large scale function prediction tool relying on semantic similarity of weighted Gene Ontology terms. *BMC Bioinformatics* **13** Suppl 4:S14.

Falda M., Lavezzo E., Fontana P., Bianco L., Berselli M., Formentin E. and Toppo S. (2016) Eliciting the Functional Taxonomy from protein annotations and taxa. *Scientific Reports* **6,** 31971.

Feng H., Guan D., Sun K., Wang Y., Zhang T. and Wang R. (2013) Expression and signal regulation of the alternative oxidase genes under abiotic stresses. *Acta Biochimica et Biophysica Sinica (Shanghai)* **45(12),** 985-994.

Finotello F., Lavezzo E., Bianco L., Barzon L., Mazzon P., Fontana P., Toppo S. and Di Camillo B. (2014) Reducing bias in RNA sequencing data: a novel approach to compute counts. *BMC Bioinformatics* **15** Suppl 1:S7.

Fitter A.H. and Stickland T.R. (1991) Architectural analysis of plant root systems. 2. Influence of nutrient supply on architecture in contrasting plant species. *New Phytologist* **118,** 383-389.

Fitter A.H. (1996) Characteristics and functions of root system. In: Waisel, Y., Eshel, A., Kafkafi, U. (Eds.), Plant Roots, the Hidden Half. *Marcel Dekker*, New York, pp. 1-20.

Flowers TJ and Flowers SA (2005) Why does salinity pose such a difficult problem for plant breeders? *Agriculture and Water Management* **78,**15-24.

Flowers T.J. and Yeo A.R. (1995) Breeding for salinity resistance in crop plants: Where next? *Australian Journal of Plant Physiology* **22,** 875–884.

Flowers T,J. and Yeo A.R.(1988) Ion relation of salt tolerance. In: Baker DA, Hall JL, eds. Solute transport in plant cells and tissues. *Harlow: Longman Scientific and Technical*, 392–413.

Foyer C.H. and Halliwell B. (1977) Purification and properties of dehydroascorbate reductase from spinach leaves. *Phytochemistry* **16,** 1347-1350.

Foyer C.H. and Noctor G. (2011) Ascorbate and glutathione: the heart of the redox hub. *Plant Physiology* **155(1),** 2-18.

Fraley R.T., Rogers S.G., Horsch R.B., Eichholtz D.A., Flick J.S., Fink C.L., Hoffmann N.L. and Sanders P.R. (1985) The SEV system: a new disarmed Ti plasmid vector system for plant transformation. *Biotechnology* **3,** 629–635

Fuchs I., Stolzle S., Ivashikina N. and Hedrich R. (2005) Rice K(+) uptake channel OsAKT1 is sensitive to salt stress. *Planta* **221,** 212-121.

Fukuda A., Nakamura A., Hara N., Toki S. and Tanaka Y. (2011) Molecular and functional analyses of rice NHX-type Na^+/H^+ antiporter genes. *Planta* **233,** 175-188.

Fukuda A., Nakamura A., Tagiri A., Tanaka H., Miyao A., Hirochika H. and Tanaka Y. (2004) Function, intracellular localization and the importance in salt tolerance of a vacuolar Na(+)/H(+) antiporter from rice. *Plant Cell Physiology* **45,** 146-159.

Gaff D.F. and Okong'O-Ogola O (1971) The Use of Non-permeating Pigments for Testing the Survival of Cells. *Journal of Experimental Botany* **22,** 756–758.

Galvan-Ampudia C.S. and Testerink C. (2011) Salt stress signals shape the plant root. *Current Opinion in Plant Biology* **14,** 296-302.

Gaxiola R.A., Li J., Undurraga S., Dang L.M., Allen G.J., Alper S.L. and Fink G.R. (2001) Drought- and salt-tolerant plants result from overexpression of the AVP1 H^+-pump. *Proceedings of National Academy of Sciences U.S.A* **98**, 11444–11449.

Gechev T.S. and Hille J. (2005) Hydrogen peroxide as a signal controlling plant programmed cell death. *Journal of Cell Biology* **168(1),** 17–20.

Gechev T., Gadjev I., Van Breusegem F., Inze ´ D., Dukiandjiev S., Toneva V. and Minkov I. (2002) Hydrogen peroxide protects tobacco from oxidative stress by inducing a set of antioxidant enzymes. *Cellular and Molecular Life Sciences* **59,** 708–714.

Gill S.S. and Tuteja N. (2010) Reactive oxygen species and antioxidant machinery in abiotic stress tolerance in crop plants. *Plant Physiology and Biochemistry* **48,** 909-930.

Goeman J.J. and Buhlmann P. (2007) Analyzing gene expression data in terms of gene sets: methodological issues. *Bioinformatics* **23,** 980–987.

Golldack D., Quigley F., Michalowsky C.B., Kamasani U.R. and Bohnert H.J. (2003) Salinity stress-tolerant and -sensitive rice (*Oryza sativa* L.) regulate AKT1-type potassium channel differently. *Plant molecular biology* **51,** 71-81.

Gong H.J., Randall D.P. and Flowers T.J. (2006) Silicon deposition in the root reduces sodium uptake in rice (*Oryza sativa* L.) seedlings by reducing bypass flow. *Plant Cell and Environment* **29,**1970–1979.

Gould J., Devery M., Heeegawa O., Ulian, E.C., Peterson G. and Smith R.H. (1991) Transformation of *Zea mays* L. using *Agrobacterium tumefaciens* and the shoot apex. *Plant Physiology* **95,** 426-434.

Gould K. S., Lamotte O., Klinguer A., Pugin A. and Wendehenne D. (2003) Nitric oxide production in tobacco leaf cells: a generalized stress response? *Plant, Cell and Environment* **26,** 1851–1862.

Gregorio G.B., Senadhira D., Mendoza R.D., Manigbas N.L., Roxas J.P. and Guerta C. Q. (2002) Progress in breeding for salinity tolerance and associated abiotic stresses in rice. *Field Crops Research* **76,** 91–101.

Guo L., Wang Z.Y., Lin H., Cui W.E., Chen J., Liu M., Chen Z.L., Qu L.J. and Gu H. (2006) Expression and functional analysis of the rice plasma-membrane intrinsic protein gene family. *Cell Research* **16,** 277–86.

Gupta B. and Huang B. (2014) Mechanism of salinity tolerance in plants: Physiological, biochemical, and molecular characterization. *International Journal of Genomics*, 701596.

Hare P.D., Cress W.A. and Van Staden J. (1988) Dissecting the roles of osmolyte accumulation during stress. *Plant, Cell and Environment* **21,** 535–553.

Hasegawa P.M., Bressan R.A., Zhu J-K. and Bohnert H.J. (2000) Plant cellular and molecular responses to high salinity. *Annuual Review of Plant Physiology Plant Molecular Biology* **51**, 463–99.

Hauser F. and Horie T. (2010) A conserved primary salt tolerance mechanism mediated by HKT transporters: a mechanism for sodium exclusion and maintenance of high K(+)/Na(+) ratio in leaves during salinity stress. *Plant, Cell and Environment* **33,** 552-565.

Haynes W.A., Higdon R., Stanberry L., Collins D. and Kolker E. (2013) Differential expression analysis for pathways. *PLoS Computational Biol*ogy **9,** e1002967.

Hernández J.A., Corpas F.J., Gómez M., del Río L.A. and Sevilla F. (1993) Salt-induced oxidative stress mediated by activated oxygen species in pea leaf mitochondria. *Physiologia Plantarum* **89,** 103–110.

Hiei Y., Komari T. and Kumashiro T. (1994) Efficient transformation of rice (*Oryza sativa* L.) mediated by *Agrobacterium* and sequence analysis of the boundaries of the T-DNA. *Plant Journal* **6,** 271–282.

Hiei Y., Komari T. and Kubo T. (1997) Transformation of rice mediated by *Agrobacterium tumefaciens*. *Plant Molecular Biology* **35,** 205–218.

Hiei Y. and Komari T. (2008). *Agrobacterium*-mediated transformation of rice using immature embryos or calli induced from mature seed. *Nature Protocols* **3,** 824–834.

Hirayama T. and Shinozaki K. (2010) Research on plant abiotic stress responses in the postgenome era: Past, present and future. *Plant Journal* **61,** 1041–1052.

Hoagland D.R. and Arnon D.I. (1938) The water-culture method for growing plants without soil. *University of California Collections Agriculture Experimental Station Berkley* **Circ,** 347-353.

Hoeberichts F.A. and Woltering E.J. (2003). Multiple mediators of plant programmed cell death: interplay of conserved cell death mechanisms and plant-specific regulators. *Bioessays* **25,** 47–57.

Hong C.Y., Chao Y.Y., Yang M.Y., Cheng S.Y., Cho S.C. and Kao C.H. (2009) NaCl-induced expression of glutathione reductase in roots of rice (*Oryza sativa* L.) seedlings is mediated through hydrogen peroxide but not abscisic acid. *Plant Soil* **320,** 103–115.

Horie T., Karahara I. and Katsuhara M. (2012) Salinity tolerance mechanisms in glycophytes: An overview with the central focus on rice plants. *Rice* (N Y). **5,** 11.

Horie T., Sugawara M., Okada T., Taira K., Kaothien-Nakayama P., Katsuhara M., Shinmyo A. and Nakayama H. (2011) Rice sodium-insensitive potassium transporter, OsHAK5, confers increased salt tolerance in tobacco BY2 cells. *Journal of Bioscience and Bioengineering* **111,** 346-356.

Horie T., Kaneko T., Sugimoto G., Sasano S., Panda S. K., Shibasaka M. and Katsuhara M. (2011b) Mechanisms of water transport mediated by PIP aquaporins and their regulation via phosphorylation events under salinity stress in barley roots. *Plant and Cell Physiology* **52(4),** 663-675.

Hur J., Jung K.H., Lee G.H. and An G.H. (2004) Stress-inducible OsP5CS2 gene is essential for salt and cold tolerance in rice. *Plant Science* **167,** 417–426.

Isayenkov S., Isner J.C. and Maathuis F.J. (2011) Membrane localisation diversity of TPK channels and their physiological role. *Plant Signaling and Behavior* **6,** 1201-1204.

Isayenkov S. and Maathuis F.J. (2015) The expression of rice vacuolar TPK channels genes restores potassium uptake in *E. coli* mutant strain LB2003. *Cytology and Genetics* **49(1),** 1–5.

Ismail A., Takeda S. and Nick P. (2014) Life and death under salt stress: same players, different timing? *Journal of Experimental Botany* **65,** 2963-2979.

Ismail A.M., Heuer S., Thomson M.J. and Wissuwa M. (2007) Genetic and genomic approaches to develop rice germplasm for problem soils. *Plant Molecular Biology* **65,** 547–570.

Jaspers P. and Kangasjarvi J. (2010). Reactive oxygen species in abiotic stress signaling. *Physiologia Plantarum* **138,** 405–413.

Ji H., Pardo J.M., Batelli G., Oosten M.J.V., Bressan R.A. and Li X. (2013) The salt overly sensitive (SOS) pathway: established and emerging roles. *Molecular Plant* **6,** 275–286.

Jiang C., Belfield E.J., Mithani A., Visscher A., Ragoussis J., Mott R., Smith J.A. and Harberd N.P. (2012) ROS-mediated vascular homeostatic control of root-to-shoot soil Na delivery in Arabidopsis. *EMBO Journal* **31,** 4359–4370.

Kader M.A. and Lindberg S. 2010. Cytosolic calcium and pH signaling in plants under salinity stress. *Plant Signaling and Behavior* **5,** 233–238.

Kahl G. (1982) Molecular biology of wound healing: the conditioning phenomenon. *Molecular Biology of Plant Tumors*, 211–267.

Kanehisa M., Sato Y. and Morishima K. (2016) BlastKOALA and GhostKOALA: KEGG tools for functional characterization of genome and metagenome sequences. *Journal of Molecular Biology* **428,** 726-731.

Katsuhara M. and Kawasaki T. (1996) Salt stress induced nuclear and DNA degradation in meristematic cells of barley roots. *Plant and Cell Physiology* **37,**169-173.

Kawahara Y., de la Bastide M., Hamilton J.P., Kanamori H., McCombie W.R., Ouyang S., Schwartz D.C., Tanaka T., Wu J., Zhou S., Childs K.L., Davidson R.M., Lin H., Quesada-Ocampo L., Vaillancourt B., Sakai H., Lee S.S., Kim J., Numa H., Itoh T., Buell C.R. and Matsumoto T. (2013) Improvement of the *Oryza sativa* Nipponbare reference genome using next generation sequence and optical map data. *Rice* **6,** 4.

Kim D., Pertea G., Trapnell C., Pimentel H., Kelley R. and Salzberg S.L. (2013) TopHat2: accurate alignment of transcriptomes in the presence of insertions, deletions and gene fusions. *Genome Biology* **14,** R36.

Knight H., Trewavas A.J. and Knight M.R. (1997) Calcium signalling in Arabidopsis thaliana responding to drought and salinity. *Plant Journal* **12,** 1067–1078.

Koeduka T., Matsui K., Hasegawa M., Akakabe Y. and Kajiwara T. (2005) Rice fatty acid *α*-dioxygenase is induced by pathogen attack and heavy metal stress: activation through jasmonate signaling. Journal of Plant Physiology **162,** 912–920.

Kurusu T., Kuchitsu K. and Tada Y. (2015) Plant signaling networks involving Ca(2+) and Rboh/Nox-mediated ROS production under salinity stress. *Frontiers in Plant Science* **6,** 427.

Khush G.S and P.S. Virk. (2000) Rice breeding : Achievements and future strategies. *Crop Improvement* **27(2),** 115-144.

Krebs M., Held K., Binder A., Hashimoto K., Den Herder G., Parniske M., Kudla J and Schumacher K. (2012) FRET-based genetically encoded sensors allow high-resolution live cell imaging of Ca^{2+} dynamics. *Plant Journal* **69,** 181–192.

Langsrud Ø (2005) Rotation tests. *Statistics and Computing* **15,** 53–60.

Lavezzo E., Falda M., Fontana P., Bianco L. and Toppo S. (2016) Enhancing protein function prediction with taxonomic constraints--The Argot2.5 web server. *Methods* **93,** 15-23.

Law C.W., Chen Y., Shi W. and Smyth G.K. (2014) voom: Precision weights unlock linear model analysis tools for RNA-seq read counts. *Genome Biology* **15,:** R29.

Li G. W., Peng Y.H., Yu X., Zhang M.H., Cai W.M., Sun W.N. and Su W.A. (2008) Transport functions and expression analysis of vacuolar membrane aquaporins in response to various stresses in rice. *Journal of Plant Physiology* **165,** 1879–88.

Li Y., Yuan F., Wen Z., Li Y., Wang F., Zhu T., Zhu T., Zhuo W., Jin X., Wang Y., Zhao H., Pei Z.M. and Han S. (2015) Genome-wide survey and expression analysis of the OSCA gene family in rice. *BMC Plant Biology* **15,** 261.

Livak K.J. and Schmittgen T.D. (2001) Analysis of relative gene expression data using real-time quantitative PCR and the 2(-Delta Delta C(T)). *Methods* **25,** 402-408.

Locato V., de Pinto M.C. and De Gara L. (2009) Different involvement of the mitochondrial, plastidial and cytosolic ascorbate-glutathione redox enzymes in heat shock responses. *Physiologia Plantarum* **135(3),** 296-306.

Ma L., Zhang H., Sun L., Jiao Y., Zhang G., Miao C. and Hao F. (2012) NADPH oxidase AtrbohD and AtrbohF function in ROS-dependent regulation of Na^+/K^+homeostasis in Arabidopsis under salt stress. *Journal of Experimental Bota*ny **63,** 305-317.

Maathuis F.J. (2011) Vacuolar two-pore K^+ channels act as vacuolar osmosensors. *New Phytologist* **191,** 84-91.

Maathuis F.J. and Amtmann A. (1999) K^+ nutrition and Na^+ toxicity: The basis of cellular K^+/Na^+ ratios. *Annals of Botany* **84,**123–133

Mallikarjuna G., Mallikarjuna K., Reddy M.K. and Kaul T. (2011). Expression of OsDREB2A transcription factor confers enhanced dehydration and salt stress tolerance in rice (*Oryza sativa* L.). *Biotechnology Letters* **33,** 1689–1697.

Martínez-Atienza J., Jiang X., Garciadeblas B., Mendoza I., Zhu J. K., Pardo J. M. and Quintero F.J. (2007) Conservation of the salt overly sensitive pathway in rice. *Plant Physiology* **143,** 1001–1012.

Maurel C., Verdoucq L., Luu D. T. and Santoni V. (2008) Plant aquaporins: membrane channels with multiple integrated functions. *Annual Reviews of Plant Biolology* **59,** 595-624.

Maxwell K. and Johnson G.N. (2000). Chlorophyll fluorescence - A practical guide. *Journal of Experimental Botany* **51,** 659–668.

Miller G., Suzuki N., Ciftci-Yilmaz S. and Mittler R. (2010) Reactive oxygen species homeostasis and signalling during drought and salinity stresses. *Plant, Cell and Environment* **33,** 453-467.

Mittler R. (2002) Oxidative stress, antioxidants and stress tolerance. *Trends in Plant Science* **7,** 405–410.

Mittler R and Blumwald E. (2010) Genetic engineering for modern agriculture: challenges and perspectives. *Annual Review of Plant Biology* **61,** 443-462.

Mittler R., Vanderauwera S., Gollery M. and Van Breusegem F. (2004) Reactive oxygen gene network of plants. *Trends in Plant Science* **9,** 490–498.

Mittler R., Vanderauwera S., Suzuki N., Miller G., Tognetti V.B., Vandepoele K., Gollery M., Shulaev V. and Van Breusegem F. (2011) ROS signaling: the new wave? *Trends in Plant Science* **16,** 300-309.

Mlejnek P. (2013) Cytokinin-induced cell death is associated with elevated expression of alternative oxidase in tobacco BY-2 cells. *Protoplasma* **250(5),**1195-202.

Mohammadi-Nejad G., Singh R.K., Arzani A., Rezaie A.M., Sabouri H. and Gregorio G.B. (2010) Evaluation of salinity tolerance in rice genotypes. *International Journal of Plant Production* **4,** 199–207.

Mooney P.A., Goodwin P.B., Dennis E.S. and Llewellyn D.J. (1991) *Agrobacterium tumefaciens*-gene transfer into wheat tissues. *Plant Cell, Tissue and Organ Culture* 25, 209-218.

Munns R. and Tester M. (2008) Mechanisms of salinity tolerance. *Annual Review of Plant Biology* **59,** 651-681.

Nakamura R.L., McKendree W.L., Hirsch R.E., Sedbrook J.C., Gaber R.F. and Sussman M.R. (1995) Expression of an *Arabidopsis* potassium channel gene in guard cells. *Plant Physiology* **109,** 371–374.

Nieves-Cordones M., Aleman F., Martinez V. and Rubio F. (2010) The *Arabidopsis thaliana* HAK5 K^+ transporter is required for plant growth and K^+ acquisition from low K^+ solutions under saline conditions. *Molecular Plant* **3,** 326–333.

Nishimura A., Ashikari M., Lin S., Takashi T., Angeles E. R., Yamamoto T. and Makoto Matsuoka (2005) Isolation of a rice regeneration quantitative trait loci gene and its application to transformation systems. *Proceedings of National Academy of Sciences U.S.A* **102,** 11940–11944

Noctor G., Mhamdi A. and Foyer C. H. (2014) The roles of reactive oxygen metabolism in drought: not so cut and dried. *Plant Physiology* **164,** 1636–1648.

Nounjan N., Nghia P. T. and Theerakulpisut P. (2012) Exogenous proline and trehalose promote recovery of rice seedlings from salt-stress and differentially modulate antioxidant enzymes and expression of related genes. *Journal of Plant Physiology* **169,** 596–604.

Obata T., Kitamoto H.K., Nakamura A., Fukuda A. and Tanaka Y. (2007) Rice Shaker potassium channel OsKAT1 confers tolerance to salinity stress on yeast and rice cells. *Plant Physiology* **144,** 1978-1985.

Pandey P., Ramegowda V. and Senthil-Kumar M. (2015) Shared and unique responses of plants to multiple individual stresses and stress combinations: physiological and molecular mechanisms. *Frontiers in Plant Science* **6,** 723.

Pang C. H. and Wang B. (2008) Oxidative stress and salt tolerance in plants. *Progress in Botany* 231–245.

Paradiso A., de Pinto M. C., Locato V. and De Gara L. (2012) Galactonoγ-lactone-dependent ascorbate biosynthesis alters wheat kernel maturation. *Plant Biology (Stuttg)* **14,** 652–658.

Parida AK and Das AB (2005) Salt tolerance and salinity effects on plants: a review. *Ecotoxicology and Environmental Safety* **60**, 324–349.

Ponce de León I., Sanz A., Hamberg M. and Castresana C. (2002) Involvement of the *Arabidopsis* α-DOX1 fatty acid dioxygenase in protection against oxidative stress and cell death. *Plant Journal* **29,** 61–62.

Qi Z., Hampton C.R., Shin R., Barkla B.J., White P.J. and Schachtman D.P. (2008) The high affinity K^+ transporter AtHAK5 plays a physiological role in planta at very low K^+ concentrations and provides a caesium uptake pathway in *Arabidopsis*. *Journal of Experimental Bot*any **59,** 595–607.

Quinlan A.R. and Hall I.M. (2010) BEDTools: a flexible suite of utilities for comparing genomic features. *Bioinformatics* **26,** 841-842.

Raineri D. M., Bottino P., Gordon M.P. and Nester E.W. (1990) *Agrobacterium*-mediated transformation of rice (*Oryza sativa* L.). *Biotechnology*, **8,** 33-38.

Ream W. (1989) *Agrobacterium tumefaciens* and Interkingdom Genetic Exchange. *Annual Reviews of Phytopathology* **27,** 586-618

Robinson M.D., McCarthy D.J. and Smyth G.K. (2010) edgeR: a Bioconductor package for differential expression analysis of digital gene expression data. *Bioinformatics* **26,** 139–140.

Rocchetti E., Sharma T., Wulfetange C., Scholtz-Starke J., Gripps A., Carpaneto A., Dreyer I., Vitale A., Czempinski K. and Pedrazzini E. (2013) The putative K^+ channel subunit AtKCO3 forms stable dimers in Arabidopsis. *Frontiers in Plant Science* Volume 3, Article 251.

Rodriguez-Navarro A. and Rubio F. (2006) High-affinity potassium and sodium transport systems in plants. *Journal of Experimental Botany* **57,** 1149–1160

Roy S.J., Negrão S. and Tester M. (2014) Salt resistant crop plants. *Current Opinion in Biotechnology* **26,** 115-124.

Sales G., Calura E., Cavalieri D. and Romualdi C. (2012) graphite - a Bioconductor package to convert pathway topology to gene network. *BMC Bioinformatics* **13,** 20.

Sanders D., Pelloux J., Brownlee C. and Harper J.F. (2002) Calcium at the crossroads of signaling. *Plant Cell (Suppl)* **14,** S401–S417.

Santa-María G.E., Rubio F., Dubcovsky J. and Rodríguez-Navarro A. (1997) The HAK1 gene of barley belongs to a large gene family and encodes a high-affinity potassium transporter. *The Plant Cell* **9(12),** 2281–2289.

Sakamoto A., Alia and Murata N. (1998) Metabolic engineering of rice leading to biosynthesis of glycine betaine and tolerance to salt and cold. *Plant Molecular Biology* **38,** 1011–1019.

Schindelin J., Arganda-Carreras I. and Frise, E., Kaynig V., Longair M., Pietzsch T., Preibisch S., Rueden C., Saalfeld S., Schmid B., Tinevez J.Y., White D.J., Hartenstein V., Eliceiri K., Tomancak P. and Cardona A. (2012) Fiji: an open-source platform for biological-image analysis. *Nature methods* **9(7),** 676-682.

Schmidt R., Mieulet D., Hubberten H.M., Obata T., Hoefgen R., Fernie A.R., Fisahn J., San Segundo B., Guiderdoni E., Schippers J.H. and Mueller-Roeber B. (2013) Salt-responsive ERF1 regulates reactive oxygen species-dependent signaling during the initial response to salt stress in rice. *Plant Cell* **25,** 2115-2131.

Schneider C. A., Rasband W. S. and Eliceiri K. W. (2012) NIH Image to ImageJ: 25 years of image analysis. *Nature methods* **9,** 671-675.

Schroeder J., Delhaize E., Frommer W. B., Guerinot M. L., Harrison M. J., Herrera-Estrella L., Horie T., Kochian L. V., Munns R., Nishizawa N. K., Tsay Y-F. and Sanders D. (2013) Using membrane transporters to improve crops for sustainable food production. *Nature* Vol. 497.

Sgobba A., Paradiso A., Dipierro S., De Gara L. and de Pinto M.C. (2014) Changes in antioxidants are critical in determining cell responses to short- and long-term heat stress. *Physiologia Plantarum* **153,** 68–78.

Shabala S. and Pottosin I. (2014) Regulation of potassium transport in plants under hostile conditions: implications for abiotic and biotic stress tolerance. *Physiologia Plantarum* **151,** 257-279.

Shabala S. and Cuin T. A. (2007) Potassium transport and plant salt tolerance. *Physiologia Plantarum* **133,** 651–669.

Shabala L., Cuin T.A., Newman I.A. and Shabala S. (2005) Salinity induced ion flux patterns from the excised roots of Arabidopsis sos mutants. *Planta* **222,** 1041–1050.

Sharma T., Dreyer I. and Riedelsberger J. (2013) The role of K^+ channels in uptake and redistribution of potassium in the model plant Arabidopsis thaliana. *Frontiers in Plant Science* **4,** 224

Skopelitis D.S., Paranychianakis N.V., Paschalidis K.A., Pliakonis E.D., Delis I.D., Yakoumakis D.I., Kouvarakis A., Papadakis A.K., Stephanou E.G. and Roubelakis-Anfelakis K.A. (2006) Abiotic stress generates ROS that signal expression of anionic glutamate dehydrogenases to form glutamate for proline synthesis in tobacco and grapevine. *The Plant Cell* **18,** 2767– 2781.

Suzuki N., Koussevitzky S., Mittler R. and Miller G. (2012) ROS and redox signalling in the response of plants to abiotic stress. *Plant, Cell and Environment* **35(2),** 259-70.

Suzuki N., Miller G., Morales J., Shulaev V., Torres M. A. and Mittler R. (2011) Respiratory burst oxidases: the engines of ROS signaling. *Current Opinion in Plant Biology* **14,** 691–699.

Suzuki K., Yamaji N., Costa A., Okuma E., Kobayashi N.I., Kashiwagi T., Katsuhara M., Wang C., Tanoi K., Murata Y., Schroeder J.I., Ma J.F. and Horie T. (2016) OsHKT1;4-mediated Na(+) transport in stems contributes to Na(+) exclusion from leaf blades of rice at the reproductive growth stage upon salt stress. *BMC Plant Biology* **19,** 16-22.

Suzuki-Yamamoto, M., Mimura, T. and Ashihara, H. (2006), Effect of short-term salt stress on the metabolic profiles of pyrimidine, purine and pyridine nucleotides in cultured cells of the mangrove tree, *Bruguiera sexangula*. *Physiologia Plantarum* **128,** 405–414.

Tester M. and Davenport R. (2003) Na^+ tolerance and Na^+ transport in higher plants. *Annals of Botany* **91,** 503-527.

Torres M.A. and Dangl J.L. (2005) Functions of the respiratory burst oxidase in biotic interactions, abiotic stress and development. *Current Opinion in Plant Biology* **8,** 397–403.

Tóth G., Montanarella L. and Rusco E. (2008) Threats to Soil Quality in Europe. EUR 23438 – Scientific and Technical Research series Luxembourg: Office for Official Publications of the European Communities p.61-74.

Tracy F. E., Gilliham M., Dodd A.N., Webb A.A.R. and Tester M. (2008) NaCl-induced changes in cytosolic free Ca^{2+} in *Arabidopsis thaliana* are heterogeneous and modified by external ionic composition. *Plant Cell and Environment* **31,** 1063–1073.

Valderrama R., Corpas F.J., Carreras A., Fernandez-Ocana A., Chaki M., Luque F., Gomez-Rodriguez M.V., Colmenero-Varea P., del Rio L.A. and Barroso J.B. (2007) Nitrosative stress in plants. *FEBS Letters* **581,** 453–461

Van Breusegem F. and Dat J. (2006) Reactive oxygen species in plant cell death. *Plant Physiology* **141,** 384–390.

Véry A. and Sentenac H. (2003) Molecular mechanisms and regulation of K^+ transport in higher plants. *Annual Reviews of Plant Biology* **54,** 575-603.

Wang X., Zhang M.M., Wang Y.J., Gao Y.T., Li R., Wang G.F., Li W.Q., Liu W.T. and Chen K.M. (2016) The plasma membrane NADPH oxidase OsRbohA plays a crucial role in developmental regulation and drought-stress response in rice. *Physiologia Plantarum* **156,** 421-443.

Wassmann R., Jagadish S.V.K., Sumfleth K., Pathak H., Howell G., Ismail A., Serraj R., Redona E., Singh R.K. and Heuer S. (2009) Chapter 3 Regional vulnerability of climate change impacts on Asian rice production and scope for adaptation. *Advanced Agronomy* **102,** 91–133.

Yang T., Zhang S., Hu Y., Wu F., Hu Q., Chen G., Cai J., Wu T., Moran N., Yu L. and Xu G. (2014) The role of a potassium transporter OsHAK5 in potassium acquisition and transport from roots to shoots in rice at low potassium supply levels. *Plant Physiology* **166,** 945–959.

Yeo A.R., Yeo M.E. and Flowers T.J. (1987) The contribution of an apoplastic pathway to sodium uptake by rice roots in saline conditions. *Journal of Experimental Botany* **38,** 1141–1153.

Yeo A.R., Yeo M.E., Flowers S.A. and Flowers T.J. (1990). Screening of rice (*Oryza sativa* L) genotypes for physiological characters contributing to salinity resistance, and their relationship to overall performance. *Theoretical and Applied Genetics* **79,** 377–384.

Yuan F., Yang H., Xue Y., Kong D., Ye R., Li C., Zhang J., Theprungsirikul L., Shrift T., Krichilsky B., Johnson D.M., Swift G.B., He Y., Siedow J.N. and Pei Z.M. (2014) OSCA1 mediates osmotic-stress-evoked Ca increases vital for osmosensing in Arabidopsis. *Nature* **514,** 367-371.

Zhang J., Li J., Wang X. and Chen J. (2011) OVP1, a vacuolar H^+-translocating inorganic pyrophosphatase (V-PPase), overexpression improved rice cold tolerance. *Plant Physiology and Biochemistry* **49,** 33-38.

Zhu J.K. (2001) Plant salt tolerance. *Trends in Plant Science* **6,** 66-71.

Zhu J.K. (2002) Salt and drought stress signal transduction in plants. *Annual Reviews in Plant Biology* **53,** 247–273.

Zhu J.K. (2003) Regulation of ion homeostasis under salt stress. *Current Opinion in Plant Biology* **6,** 441–445.

Zhu S.Q., Chen M.W., Ji B.H., Jiao D.M. and Liang J.S. (2011) Roles of xanthophylls and exogenous ABA in protection against NaCl-induced photodamage in rice (*Oryza sativa* L) and cabbage (*Brassica campestris*). *Journal of Experimental Botany* **62,** 4617–4625.

Zulfugarov I.S., Tovuu A., Eu Y.J., Dogsom B., Poudyal R.S., Nath K., Banerjee M., Yoon U.C., Moon Y.H., An G., Jansson S. and Lee C.H. (2014) Production of superoxide from Photosystem II in a rice (*Oryza sativa* L.) mutant lacking PsbS. *BMC Plant Biology* **14,** 242.